A naturally ventilated office building through solar chimneys and ‘venturi’ exhausts

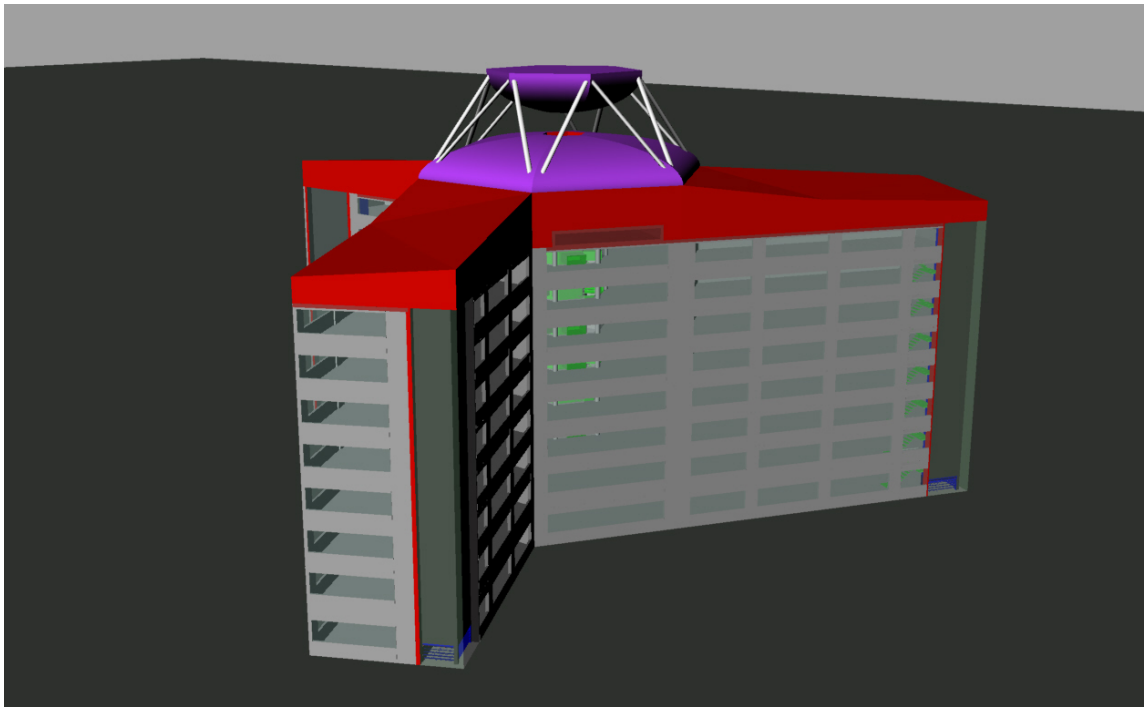

Remco Kemperman

Graduation report
Faculty of Architecture, Urbanism & Building sciences
MSc-track: Building Technology
Graduation lab: Green Building Innovation

TU Delft
Delft University of Technology

A naturally ventilated office building through solar chimneys and ‘venturi’ exhausts

R. A.M. Kemperman
student number: 1211323

Graduation report
Delft University of Technology
Faculty of Architecture, Urbanism & Building sciences
MSc-track: Building Technology
Graduation lab: Green Building Innovation

1st tutor: dr.ir. P.J.W. van den Engel
2nd tutor: ing. T. Klein

1 February 2012

Abstract

Ventilation of office buildings through the natural driving forces of sun and wind
Natural ventilation of office buildings is a growing field of practice and research. At the Faculty of Architecture, Urbanism & Building sciences of the Technical University in Delft, research is being executed on the specific characteristics and performance of the driving ventilation components : solar chimneys and wind-induced exhausts. Along with this development the performance of a natural ventilated office building model with use of solar chimneys and wind-induced exhausts is investigated. The focus in this graduation project was on the integration of the two driving ventilation components in the office building, fan energy saving and the influence on other building characteristics such as thermal comfort. With fan energy saving in mind the regarded building models are equipped with low pressure drop ventilation systems to decrease the amount of driving pressure needed in the system. With solar chimneys and wind-induced exhausts, the driving force provided by nature is used to force fresh air through the building for ventilation.

Fan energy saving in the building is the main evaluation criterion in the research. Energy saving in general is treated in this project by reducing other energy demands in the building such as energy consumption for heating and demand for cooling.

Finally, an overview is given of the important characteristics of the solar chimneys and wind-induced exhausts which have to be taken into account in the integration into the building ventilation system. As well, a short summary of the possibilities on architectural integration of the two systems in buildings is given.

Contents

Introduction – “a modern office building without fans”

The modern office building often has an air conditioning system based on mechanical appliances to provide the user in the building with fresh air and a comfortable temperature. These appliances use energy to control the temperature of the air flow and fans to drive the fresh air through the building. In former times the architect would design a building in such a way that fresh air was provided to the building on natural driving forces such as wind and thermal buoyancy in the building. As the modern age provided us with all kinds of mechanical equipment to provide a comfortable climate in almost any circumstance, the need for smart use of natural driving forces faded. This resulted in HVAC systems in modern building which use large amounts of fan energy to drive fresh air through the building.
Nowadays climate problems such as global warming and energy problems such as the diminishing fossil fuel stock motivate architects and engineers to come up with solutions in the built environment to reduce the energy consumption of buildings and to make use of renewable energy sources in order to reduce green house gas emission and carbon footprint. Reduction of the energy demand is practiced in the form of good insulation of buildings, heat recovery systems in the exhaust flows of the building. As the total energy demand decreases with these measures, the relative part fan energy takes in the total energy demand increases.
This research project focuses on the reduction of fan energy consumption in the built environment by making use of the natural driving forces the physical environment provides. As in former times, the regarded office building is ventilated by the natural driving forces of the sun and the wind. The driving force of the sun is used to drive the exhaust air out of the building through solar chimneys. The driving force of the wind is used to create under pressure on the exhaust of the chimneys through venturi-shaped exhausts. Together all these measures are applied to see if the underlying goal of this project is achievable: “a modern office building without fans”.

This project focuses on the integration of the regarded ‘driving ventilation components’: the solar chimney and venturi-shaped exhaust into the building system by simulating the behavior of the total building. While the energy reduction of the buildings ventilation system is the focus of the research, the user comfort of the building can’t be discarded as our buildings are first and foremost meant to create a comfortable environment to live and work in.

During the research project which was done during my graduate internship at Deerns consulting engineers in Rijswijk, Heleen Doolaard from the faculty of Applied Physics at the TU Delft executed the necessary wind studies during her internship at Deerns. The wind studies on the building cases where done by her with the CFD-software package Phoenics.

Furthermore this project is closely related to the topics in the PhD research project at the TU Delft by B. Bronsema: ’Earth, Wind & Fire – Air conditioning without fans’ which focuses deeply on the characteristics of the solar chimney and venturi-shaped exhaust. As mentioned my research focuses on the integration of these systems into the building in order to get an understanding of the do’s and don’ts of natural ventilation in general and the regarded ‘driving ventilation components’ specifically.

Part 1: Context of research and Research questions

In the history of sustainable building design the energy demand and carbon footprint of the built environment has been gradually reduced by decreasing energy demand due to measures such as better insulation, heat recovery and efficient artificial lighting. With all other elements of the total energy demand in the built environment decreasing, fan energy consumption becomes a relatively large part of energy demand in buildings. Especially in mechanically ventilated buildings fan energy consumption can be high due to the large number of appliances in air conditioning which produce resistance in the ventilation system.
This project is meant to make a contribution to the decrease of fan energy demand in the built environment. Specifically, the project focuses on ventilation through natural driving forces or 'natural ventilation'

Chapter 1: Natural ventilation

The definition of natural ventilation in building practice is not entirely unambiguous. While in this research project the term 'natural ventilation' will be used in the sense of 'fresh air supply through natural driving forces'; in building practice 'natural ventilation' is often linked with personal control on the indoor climate for building occupants. In sustainability assessment methods such as BREEAM, operable windows are inseparable from the definition of 'natural ventilation' as used in that method.

In the Netherlands since 2003, a new type of thermal comfort assessment was introduced with the ATG-method which is based on the adaptive thermal comfort limits of people with altering conditions. This method describes a separate category of buildings in which people are likely to have a greater range of indoor climate conditions in which they find themselves comfortable. This is largely found to be linked to personal control in which operable windows are a hard requirement to fall in to this separate assessment category.

While this project focuses on fan energy reduction, the definition of 'natural ventilation' in this project applies to fresh air supply by the natural driving forces of the wind and the sun.

Chapter 2: Research question

The research question which the project is based on and which is to be answered in order to finalize to project is given in this chapter and divided into sub questions.

2.1. Main research question

How much fan energy can be saved in an office building ventilated by solar chimneys and venturi-shaped exhausts during occupation time?

2.2. Sub questions

1) For which configuration of shunt duct(s) and solar chimneys at the end of each office wing does the complex induce the largest resulting stack pressures?
2) What configuration of the venturi shaped exhaust in the given roof shape delivers the largest negative wind pressure coefficient at the exhaust

2.3. Latitude hypothesis

A characteristic of chimneys in general is that stack pressure is related to the difference between the chimney air temperature and the external air temperature. A characteristic of solar chimneys in this project in particular is that the solar chimney and the absorber plane in

the chimney are vertically orientated. A hypothesis resulting from these characteristics is that a vertically orientated solar chimney will produce more stack pressure on a location on the globe with higher latitude, hence further from the equator.
This hypothesis for chimneys in general is based on the fact that the difference between the indoor air temperature of a building and the external air temperature is larger for locations further from the equator where the climate is colder hence having lower external temperatures with roughly the same indoor temperature resulting in a larger temperature difference.
For vertically orientated solar chimneys the hypothesis states that for locations with higher latitude the zenith, or sun angle, is lower which results in a more perpendicular solar radiation on the absorber plane which in turn cancels out the decreasing mean solar power with higher latitude resulting in even solar power in the solar chimney.

The latitude hypothesis is shown schematically in Figure 1.1

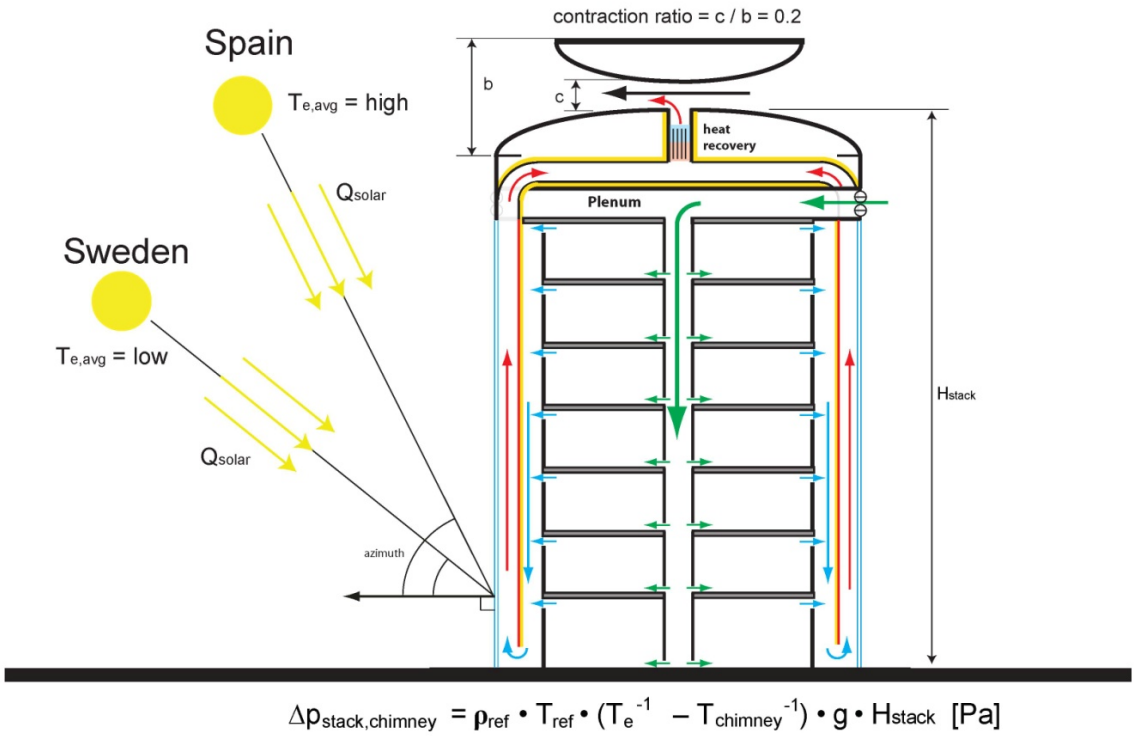

Figure 1.1: Latitude hypothesis; Climate influence on the performance of vertically orientated solar chimneys

Part 2: Relevant theory

Frequently used symbols:

Symbol:	Basic quantity or derived quantity:	Unit	SI-unit:
A	cross sectional area of a duct	-	m^2
C_{di}	coefficient of discharge	-	-
C_p	Wind pressure coefficient	-	-
Clo	clothing factor	clo	$(m^2•K)/W$
D	depth of solar chimney	-	m
D_h	hydraulic diameter of a duct	-	m
p	pressure	Pa	N/m^2
g	gravitational acceleration	-	m/s^2
GFA	Gross Floor Area	-	m^2
GTO	weighted temperature exceedance hours	h	-
H	height of solar chimney	-	m
l	length of a duct	-	m
M	metabolic rate of a person	met	W/m^2
O	cross sectional perimeter of a duct	-	m
PMV	Predicted Mean Vote of thermal comfort	-	-
PPD	Predicted Percentage Dissatisfied	-	-
Q_v	volume flow of air	-	m^3/s
r	thermal resistance	-	$(m^2•K)/W$
Re	Reynolds number in air flow resistance	-	-
SWM	specific accessible thermal mass	kg/m^2 GFA	-
T	air temperature	°C	K
T_0	reference temperature	°C	K
T_{chim}	average air temperature in a chimney	°C	K
T_e	external air temperature	°C	K
T_i	internal air temperature	°C	K
T_{op}	operative temperature	°C	K
U	thermal flux coefficient	-	$W/(m^2•K)$
U_0	reference wind velocity at building site	-	m/s
U_m	wind velocity at meteo station	-	m/s
U_w	Wind velocity	-	m/s
v	air velocity in a duct	-	m/s
W	width of solar chimney	-	m
ZTA	g-value or SHGC of glass	-	-
λ	friction factor in air flow	-	-
ρ	mass density	-	kg/m^3
ρ_0	mass density of air at reference temperature	-	kg/m^3
ζ	aerodynamic loss factor in ducts	-	-
η_{fan}	fan efficiency	-	-

Chapter 3: Buoyancy

An important driving force in natural ventilation is buoyancy, also known as stack effect in a chimney. It is caused by a difference in mass density of air in two columns of air and the height difference of the air links between these columns of air. The mass density of air in a zone can be expressed by the temperature of the air in the zone.

$\rho = \rho_0 \cdot (T_0) / (T)$ (3.1)
ρ_0 is the reference density of air (normally 1,2041 [kg/m^3] at T_0)
T_0 is the reference air temperature [K] (normally 293K, 20˚C)
T is the temperature of the air in the zone [K]
Note that this is an approximation of the density of air which is valid at sea level in the range of -25˚C $<$T $<$ 50˚C hence useable for ventilation calculations in buildings.

According to the law of Gay-Lussac, with rising temperature of a body of air the volume of this body increases and the density decreases:

V/T = constant or $V_0/T_0 = V_1/T_1 = V_2/T_2$ (3.2)
V is volume [m^3]
T is air temperature [K]

While $V = 1 / \rho$, (3.2) can be written as:
$\rho_0 \bullet T_0 = \rho_1 \bullet T_1 = \rho_1 \bullet T_1$ (3.3)

With the height of a stack or chimney taken into account and the temperatures in- and outside the chimney, the stack pressure is expressed as:

$\Delta p_{stack} = \rho_0 \bullet T_0 \bullet (T_e^{-1} - T_{chim}^{-1}) \bullet g \bullet (h_2 - h_1)$ (3.4a)
ρ_0 is reference pressure at T_0 [kg/m^3]
T_0 is reference temperature [K]
T_{chim} is the average air temperature inside the stack [K]
T_e is the temperature of the air outside the stack or of the zone to which the air flows [K]
h_1 is the height of the lower opening where stale air enters the chimney [m]
h_2 is the height of the opening where air exits the chimney to the exterior [m]

When temperatures are expressed in mass densities through (3.1), (3.4a) can be written as:

$p_s = g \bullet (h_2 - h_1) \bullet (\rho_{chim} - \rho_e)$ (3.4b)
ρ_{chim} is the mass density of air inside the chimney [kg/m^3]
ρ_e is the mass density the external air [kg/m^3]
Note that this is indirectly derived from the static pressure term in Bernoulli's law ($g \bullet z \bullet \rho$)

Bernoulli's law with the static pressure term highlighted:
$p_1 + 0{,}5 \bullet \rho_1 \bullet v_1^2 + \mathbf{g \bullet z_1 \bullet \rho_1} = p_2 + 0{,}5 \bullet \rho_2 \bullet v_2^2 + \mathbf{g \bullet z_2 \bullet \rho_2} + \Delta p_f$ (3.5)
Δp_f is pressure drop due to friction

3.1: Neutral pressure plane

In natural ventilation of a building the buoyancy component is based on the difference between pressures on the inlet and outlet of a window, a room or a whole building. In a

properly functioning system the inlet is in over pressure [Δp>0Pa] and the outlet is in under pressure [Δp<0Pa]. Between the in- and outlet, a fictional horizontal plane, the neutral pressure plane, is the turning point between under- and overpressure. The neutral pressure plane occurs in large openings such as windows at zones with single sided ventilation. It also occurs on the scale of the total building and in chimneys. In this specific project the neutral pressure plane in the chimneys determines where exhaust openings to the chimney can be placed.

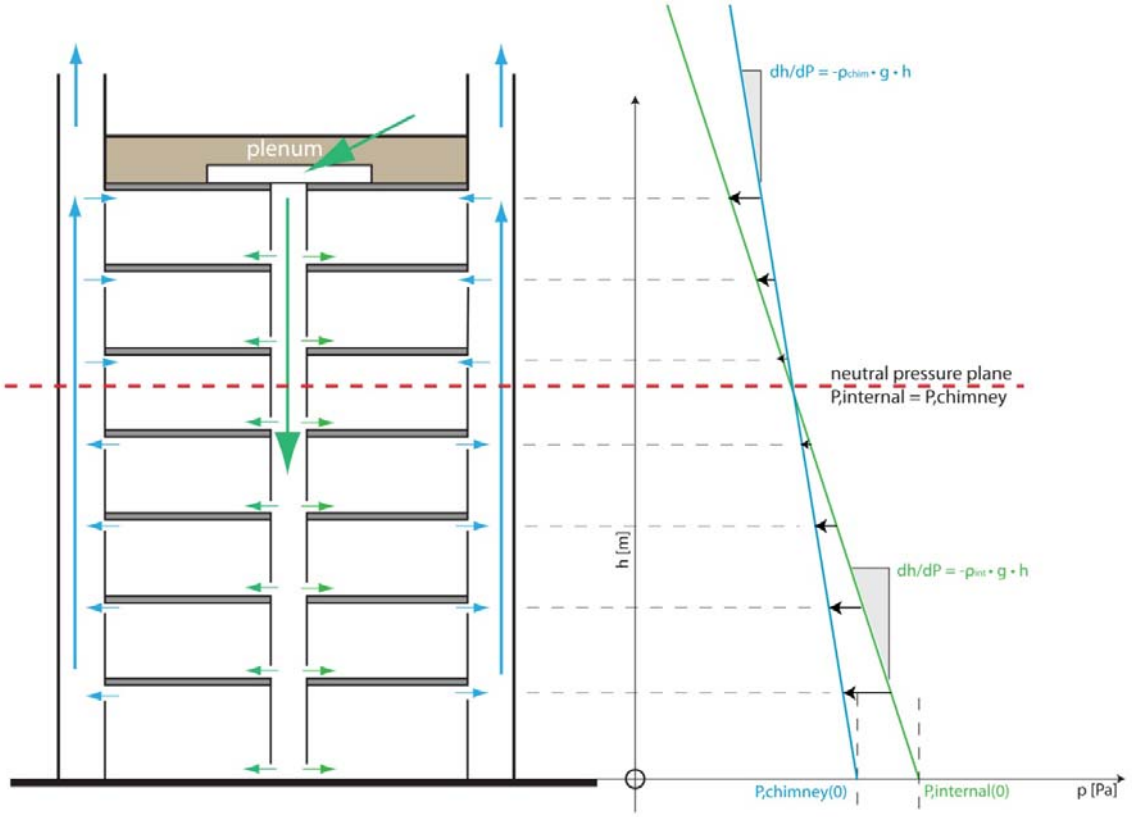

Figure 3.1: Neutral pressure plane in the chimney of the reference building case [case-0]

Chapter 4: 'venturi' effect

In order to take advantage of the driving force of the wind, the exhaust of the building ventilation system is in a venturi-shaped profile to induce under pressure on the exhaust. This profile consist of two curved scales around the exhaust (figure 4.2) which force the air flow over the exhaust to contract and therefore to accelerate. According to Bernoulli's law (3.5) a contracted flow of a gas or liquid accelerates to keep the same volume flow through a smaller cross sectional area. The dynamic pressure term in Bernoulli's law and the law of conservation of energy state that the pressure in the contraction decreases as the flow velocity increases in order to keep kinetic energy constant.Bernoulli's law with the dynamic pressure term highlighted:

$$p_1 + \mathbf{0{,}5 \bullet \rho_1 \bullet v_1^2} + g \bullet z_1 \bullet \rho_1 = p_2 + \mathbf{0{,}5 \bullet \rho_2 \bullet v_2^2} + g \bullet z_2 \bullet \rho_2 + \Delta p_f \qquad (4.1)$$

Δp_f ➔ pressure loss due to friction

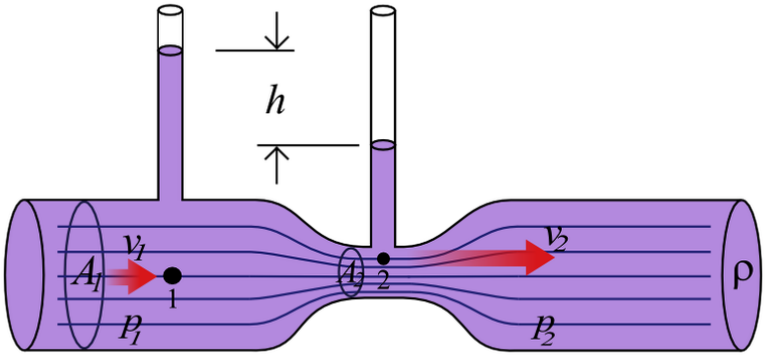

Figure 4.1: Bernoulli principal in confined flow

Bernoulli's law is true for the assumption that mass density of the flow is constant and that the flow is confined. In case of the venturi-shaped exhaust, external air with constant temperature and mass density is forced through the contraction. However, the flow in the contraction is not confined. The wind can flow around and over the venturi-shaped roof which will result in a smaller pressure decrease then theoretically possible in confined flow.

Theoretical maximum pressure difference in the venturi-shaped roof

$$\Delta P = 0{,}5 \bullet \rho \bullet (v_2^2 - v_1^2) \qquad (4.2)$$

This phenomenon is called 'wind-blocking' by Blocken in 'a venturi-shaped roof for wind induced ventilation' (Blocken et. al, April 2011). As the contraction of the venturi-shaped roof becomes too narrow the air flow will be deflected around and over the roof.
As the phenomenon described by Venturi in Bernoulli's law is strictly applicable to a confined flow, the unconfined contracted flow in the venturi-shaped roof will be referred to as the 'venturi' effect and the construction as 'venturi' roof.

The possible increase in flow velocity and decrease in pressure in the 'venturi' roof is influenced by the contraction ratio of the roof.

$$R_c = c / b \qquad (4.3)$$

c ➔ horizontal cross section of the contraction at the exhaust (figure 4.2)
b ➔ horizontal cross section of the roof (figure 4.2)

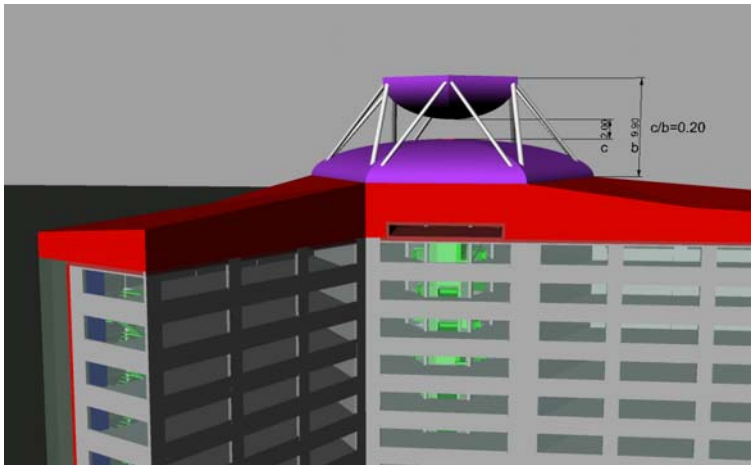

Figure 4.2: contraction ratio (c/b) in the 'venturi' roof of the final design – solar & 'venturi'

4.1: 'Wind blocking; versus 'venturi' effect

In the 'venturi' roof a balance between 'wind blocking' and 'venturi' effect can be found which is expected to result in an ideal contraction ratio, R_c.

The air which is supposed to flow through the contraction undergoes a flow resistance at the inflow at the windward side of the roof construction due to the pressure built up at the roof edges (figure 11.1) and in practice also due to structural elements for the upper roof. In the contraction the air flow is accelerated which causes a pressure drop, however this pressure drop is relative to the pressure at the airflow at the inflow entrance between the edges of the ellipsoids. While the wind pressure coefficient at the exhaust, $C_{p,e}$, is determined relative to the unobstructed air flow in front of the building, the theoretical pressure drop is not reached.

When the ellipsoids are too close together the pressure built up at the inflow creates and area of overpressure which will deflect the oncoming air around the 'venturi' contraction which will from now on be called 'wind blocking'.

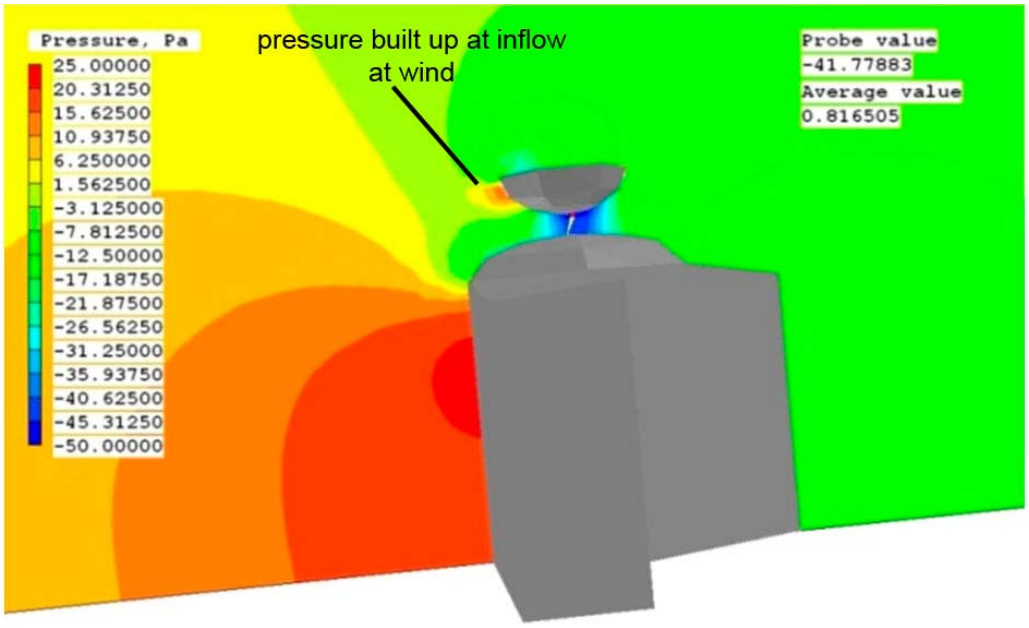

Figure 4.3: pressure built up at the windward side of the contraction at frontal area of roof edges and structural elements.

Blocken described the relation between 'venturi' effect and 'wind blocking' in the article "*Computational analysis of the performance of a venturi-shaped roof for natural ventilation: venturi-effect versus wind-blocking effect* (April, 2011). Figure 4.3, 4.4 and 4.5 are taken from this article and show 'wind blocking' at the building scale (figure 4.3), and at the 'venturi' roof scale (figure 4.4a and 4.5a). They also show the 'venturi' effect in the roof contraction (figure 4.4b and 4.5b).

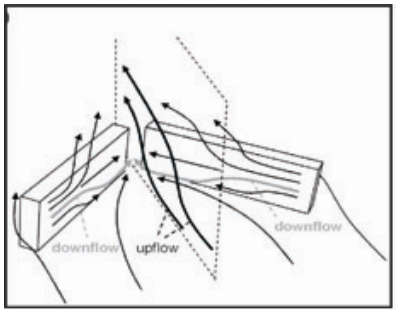

Figure 4.3: Wind blocking at building scale

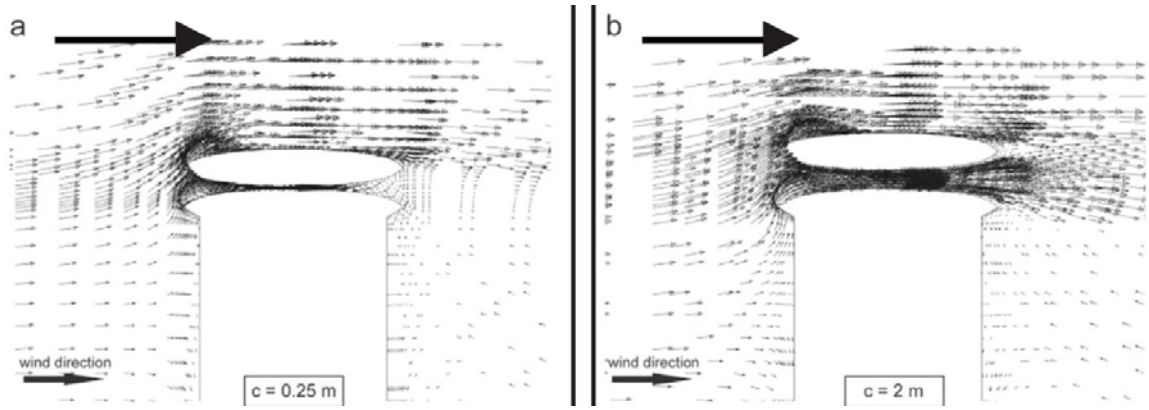

Figure 4.4: Wind blocking and 'venturi' effect in 'venturi' roof in section (Blocken et. al, April 2011), a) contraction is too small ➔ wind blocking, b) contraction is large enough ➔venturi effect

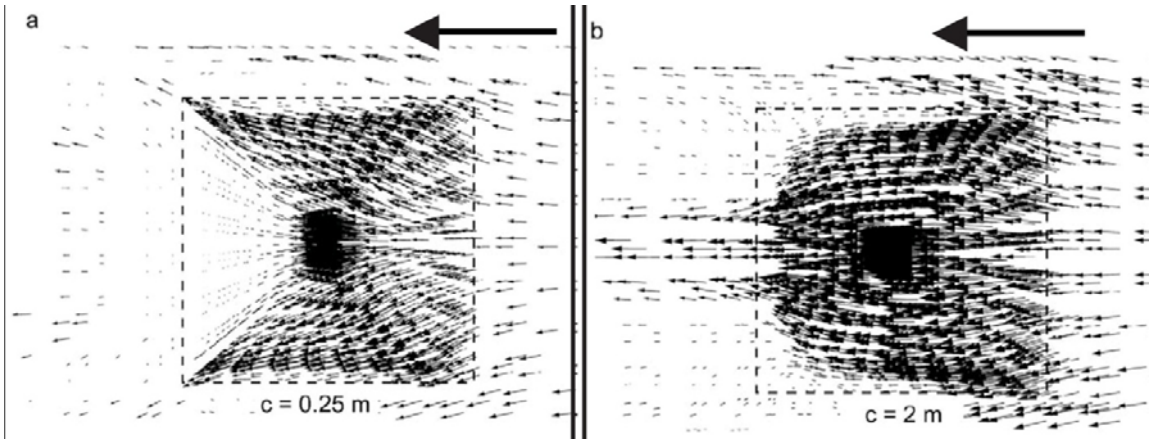

Figure 4.5: Wind blocking and 'venturi' effect in 'venturi' roof in the horizontal plane between the upper and lower roof (Blocken et. al, April 2011), a) contraction is too small ➔ wind blocking – the air flow is directed away from the contraction, b) contraction is large enough ➔venturi effect – air flow is drawn into the contraction and accelerated

4.2: Wind pressure coefficient

The resulting under pressure in the 'venturi' roof contraction at the exhaust is dependent on the wind velocity at the building site. As this is a dynamic variable, the resulting pressure is expressed as a function of the wind velocity by the wind pressure coefficient [C_p]. This is determined in the CFD-analyses:

$\Delta p = C_p \bullet 0{,}5 \bullet \rho \bullet U_0^2$
U_0 ➔ wind velocity at the building site

$U_0 = U_m \bullet [\, h_b / h_m]^{\wedge}\alpha_m \bullet [\, h_0 / h_b \,]^{\wedge}\alpha_0$
U_m ➔ wind velocity at the meteo station at pylon height
h_m ➔ pylon height at meteo station
h_0 ➔ reference height at the building site, usually height of the roof edge
h_b ➔ height of boundary layer, 60m for $\alpha_0 < 0.34$
α_0 ➔ wind velocity profile exponent at the building site
α_m ➔ wind velocity profile exponent at the meteo station

Figure 4.6: wind velocity exponent in TRNFLOW manual		
Class	Terrain description	α
1	Sea, flat terrain without obstacles	0,1 – 0,15
2	Open terrain with isolated obstacles	0,15 – 0,25
3	Wood, small city, suburb	0,25 – 0,35
4	City centre	0,35 – 0,45

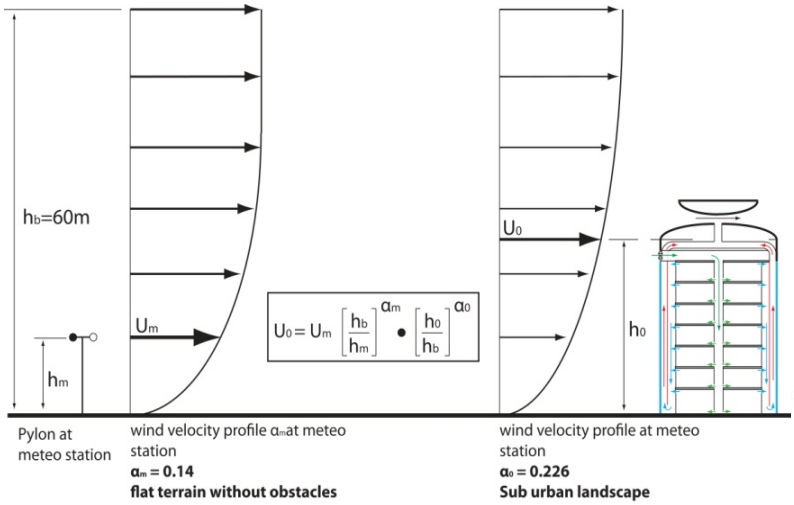

Figure 4.7: Determination of U_0 at the building site from U_{met} at the meteo station

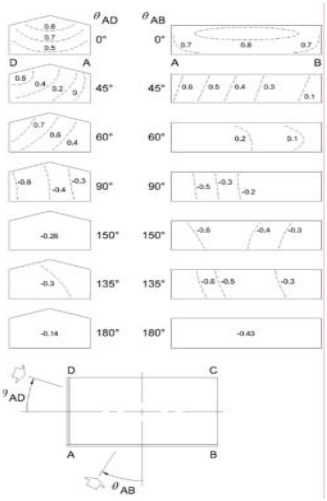

Figure 4.8: ASHRAE C_p-values

For standard building shapes like rectangular blocks and housing blocks with sloped roofs C_p-values are known and given in literature (Figure 4.8).
For complex building forms, such as the building case in this project, C_p-values can't be described by general models. For these cases testing in an atmospheric boundary layer tunnel or numerical analysis with CFD-software is needed to determine the wind pressure coefficients on the facades and ventilation openings. Such CFD-analyses are done for the 'venturi' roof at the building case in this project in which the inlet openings are taken into account as well.

Chapter 5: Aerodynamic flow resistance

A medium flowing along a surface experiences friction which results in pressure loss. In case of air flowing through ducts and chimney this is described as aerodynamic flow resistance.
The kinetic energy needed for a volume of air to flow with a certain velocity is of similar form as the general kinetic energy formula and is expressed in the dynamic pressure term in the Bernoulli equation:

$\Delta p_{dyn} = 0{,}5 \bullet \rho \bullet v^2$ (5.1)
Δp_{dyn} ➔ dynamic pressure loss [Pa]
v ➔ mean flow velocity in a ventilation component like a duct or chimney

Pressure loss due to friction along duct walls, in bends in ducts or appliances such as heat exchangers can be expressed in loss factors [ζ] of the separate components of the ventilation system:

$\Delta p_{static} = \zeta \bullet 0{,}5 \bullet \rho \bullet v^2$ (5.2)
Δp_{static} ➔ static pressure loss [Pa]

The loss factors for bends and conduits and appliances can be found in literature on hydraulic resistance (Recknagel, 2011) (ISSO, 2010), (Idelchik, 2005). For flow resistance in straight elements with constant rectangular cross section, pressure loss can be calculated through:

$\Delta p = \lambda \bullet (l/D_h) \bullet 0{,}5 \bullet \rho \bullet v^2$ (5.3)
λ ➔ friction factor
l ➔ length of duct element
D_h ➔ hydraulic diameter
Note that [ζ] in (5.2) is the same term as [$\lambda \bullet (l/D_h)$] in (5.3). The loss factor in a duct is therefore [$\lambda \bullet (l/D_h)$].

$D_h = (4 \bullet A) / O$ [m] (5.4)
A ➔ cross sectional area of the duct
O ➔ cross sectional perimeter of the duct

The friction factor [λ] is described by the implicit Colebrooke-White equation:

$\lambda^{-0,5} = -2\log[(k/ D_h \bullet 3{,}72) + (2{,}51 / Re \bullet \lambda^{-0,5})]$ [-] (5.5)
k ➔ wall roughness of the duct walls [m]
Re ➔ Reynolds number

The Reynolds number for rectangular ducts of constant cross sectional area is described by:

$Re = \rho \bullet v \bullet D_h / \mu$ [-] (5.6)
μ ➔ dynamic viscosity of air [$1{,}8 \bullet 10^5$ m^2/s at T =293K]

The static pressure loss in a duct is the sum of wall friction loss and pressure losses due to local resistances such as bends and appliances. The dynamic pressure loss is the kinetic energy needed to propel the volume of air through the duct (5.1). The static and dynamic pressure loss sum up to the total pressure drop in a duct at a given air velocity. This pressure loss has to be overcome by the driving pressures of wind and buoyancy in order to get to the desired volume flow designed in the duct.

$$\Delta p_{total} = \Delta p_{static} + \Delta p_{dyn} \quad (5.7)$$

The loss factor over a ventilation component can also be described in the coefficient of discharge [C_{di}]. The coefficient originates from the orifice flow meter as the ratio between the area of the opening in an orifice plate and the smallest cross sectional area of the airflow behind it, the 'vena contracta'. This ratio describes the Nett passing flow and gives the coefficient of discharge in:

$$C_{di} = A_{vc} / A \quad [-] \quad (5.8)$$

A_{vc} ➔ Area of 'vena contracta' the narrowest part of the stream after the opening
A ➔ area of the orifice opening

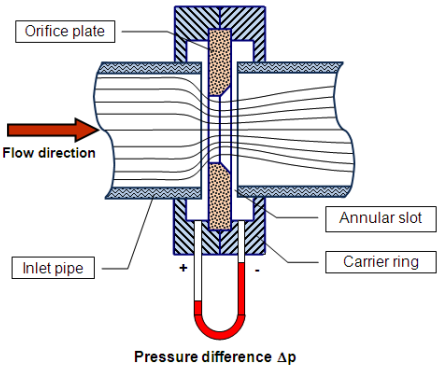

Figure 5.1: Orifice flow meter

The coefficient of discharge and loss factor of ventilation components are interchangeable by the equation:

$$C_{di} = \zeta^{-0.5} \quad (5.9)$$

This relation is used in the building simulations in TNSYS-TrnFlow to derive the C_{di} of ventilation components needed as input in the building models.

Chapter 6: Fan energy calculation

When the driving forces of wind and buoyancy are not sufficient to provide the desired volume flow, auxiliary fans have to be used to provide the remaining driving pressure. The power needed to drive these fans is described by:

$$P_e = Q_v \bullet \Delta p \bullet (\eta_{fan} \bullet \eta_{e)}^{-1} \quad (6.1)$$

P_e ➔ electrical power [W]
Qv ➔ desired volume flow [m^3/s]
η_{fan} ➔ efficiency of fan [-]
η_e ➔ efficiency of electro engine [-]

Primary energy

The fan energy consumption of the building cases in this project is the energy demand of the auxiliary fans in the system. The energy cost of the system is first discounted in output energy consumption. The energy cost can also be discounted in primary energy. Primary energy is the energy equivalent used in a power plant to produce 1unit of electrical energy used in the building. As the power grid and power plants have a combined efficiency of 40%, 2,5kWh of primary energy [kWh_{pr}] is used to provide 1kWh of electrical energy to end users such as buildings.

Chapter 7: Thermal comfort

The building envelope and the climate system of the building are meant to provide the user with a comfortable indoor climate. There are several ways to express thermal comfort based on indoor temperature.

7.1: Thermo physiological approach of thermal comfort

To qualify the indoor climate in a building the PPD or Predicted Percentage of Dissatisfied people is defined for a population in the building with a uniform metabolic rate [met] and uniform clothing insulation [clo].
In calculation and simulation a PPD lower than a theoretic minimum of 5 is not possible, which is due to the uniform population assumed in the method. In reality someone with a lower metabolic rate will adapt to the indoor climate by putting more clothes on or taking on a more active posture to keep warm. In practice a thermal comfort corresponding to a PPD of 0 is certainly possible due to the adaptive nature of people.

In the thermo physiological approach of the thermal comfort the PPD is used to define the thermal quality of an indoor climate. The PPD is obtained from the Predicted Mean Vote or PMV (Kurvers, 2011). PMV is the mean vote over the population on the indoor climate:

Figure 7.1: Thermal sensation- or ASHRAE-scale	
+3	Hot
+2	Warm
+1	Slightly warm
0	Neutral
-1	Slightly cool
-2	Cool
-3	Cold

PPD is related to PMV by:

$$PPD = 100 - 95 \cdot \exp(-0{,}03353 \cdot PMV^4 - 0{,}2179 \cdot PMV^2) \quad (7.1)$$

Equation (7.1) is described in standard (NEN-EN-ISO 7730)

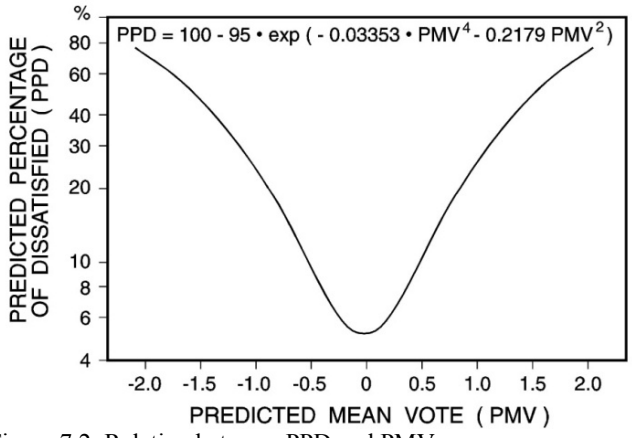

Figure 7.2: Relation between PPD and PMV

In simulation of the building cases in this project the PPD and PMV can be obtained from TRNSYS-TrnFlow as output variables. In these simulations the clothing insulation and the metabolic rate of the uniform population are needed as input as well as the relative air velocity in the room. The relative air velocity in this case is the average air velocity in the office zones due to the displacement ventilation.

7.2: GTO-method

The GTO-method, or weighted temperature exceedance method, is one method to express the quality of the indoor climate based on operative indoor temperature and the metabolic rate of the users of the building.
The exceedance of given temperature boundaries in winter and summer are multiplied, weighted, by PPD and the temperature exceedance of the boundaries. The temperature boundaries in GTO are:

$20°C < T_{op} < 25,5°C$
T_{op} ➔ operative temperature in the occupied building zones
Heating season ➔ September 29th - April 28th

- Relative air velocity = 0,15m/s
- Metabolism = 1,2 met
- Clothing insulation = 0,7 clo

Cooling season ➔ April 29th – September 28th

- Relative air velocity = 0,20m/s
- Metabolism = 1,2 met
- Clothing insulation = 0,9 clo

These boundaries are found in Dutch building regulation (NEN-EN-ISO 7730)
When the temperature boundaries set in winter and summer time are exceeded, the excess is multiplied by PPD resulting in GTO hours:

$$GTO = \Sigma (|\Delta T_{exceedance}| \bullet PPD/10) \quad (7.2)$$

GTO ➔ weighted exceedance hours [h]
$\Delta T_{exceedance}$ ➔ exceedance of the temperature boundary [°C]

An indoor climate is considered acceptable when GTO over a year is less than 5% of occupation time multiplied by 1,5 for the weight factor:

$GTO_{max} = 3132 \times 5\% \times 1,5 = 235$ [h]
(specific for the building models in this project)

7.3: ATG-method

The ATG-method or Adaptive Temperature G…, is developed as a different way to express the quality of indoor climate which takes into account the difference of outdoor temperature over time. Whereas the GTO-method uses set indoor temperature boundaries, in the ATG-method the temperature boundaries fluctuate with the mean outdoor temperature over the last few days. Different temperature boundaries are set for different comfort classes: A, B and C, whereas GTO has fixed boundaries and counts the number over weighted hours these boundaries are exceeded.
Two types of buildings are described for the ATG-method with different types of temperature boundaries:

Alpha-buildings: typical naturally ventilated or 'free running' buildings with decentral heating and cooling in which the user has individual control of the indoor climate by operable windows or ventilation openings and local thermostats.

Beta-buildings: typically mechanically ventilated buildings with central heating and cooling and closed facades.

7.4: Choice of thermal comfort assessment method

For this project the GTO-method is chosen to qualify the indoor climate of the building in the simulations. Due to the large number of criteria on which the decision is taken if a building is in the alpha or beta category the ATG-method, the category of the building case in this project is uncertain. This is mainly due to the fact that the influence of operable windows or ventilation openings is not taken into account in the simulations while this is one of the main criteria on which the evaluation category of the building is decided.

7.5: Robustness of natural ventilation in combination with operable windows

For further research the influence of operable windows or ventilation openings in the office zones is recommended in order to investigate to robustness of the natural ventilation system combined with operable windows. In current building practice the application of operable windows or ventilation openings is recommended to improve comfort in the building. Apart from the individual control of the indoor climate that is provided by operable windows, these are also used to provide the possibility to create higher ventilation rates to remove short term odors or prevent summertime overheating.

Part 3: Building cases for simulation

In this project a variety of building cases is examined in order to answer the research questions. These cases are examined to evaluate the integration of the three 'driving ventilation components': the solar chimney, the 'venturi' roof and buoyancy. At the same time the different cases provide the possibility to evaluate the individual contribution to the fan energy savings of the final case.

The evaluated cases include:

[test-case]:

A building model with simple non-partitioned, internal chimneys a free running ventilation system to investigate the natural flows occurring in the building and assess the robustness of the simulation model.

[case-0]:

A building model with partitioned internal chimneys and conventional exhausts

[case-1A]:

A building model with solar chimneys combined with shunt ducts and conventional exhausts

[case-1B]:

A building model with partitioned solar chimney and conventional exhausts

[case-2A] – Final design

The final building design model with solar chimneys combined with shunt ducts and a central 'venturi' roof.

Chapter 8: [case-2A] - Final design

The final building case is based on a design made for the new office complex of the French Ministry of Defense in Paris which will have mechanical supply ventilation and internal chimneys. Deerns advising engineers is involved in the design of the exhaust system which includes the chimney and the exhaust shape at the roof. Because of safety issues the exhaust has to be covered hence the architect came up with a roof design which had a roof shape with a yet undefined void over the internal chimneys (Figure 8.1).

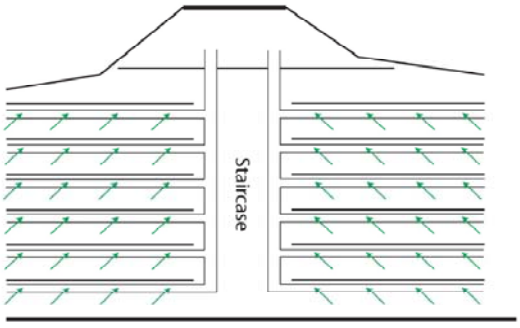

Figure 8.1: Schematic representation of internal ducting and undefined void under the roof

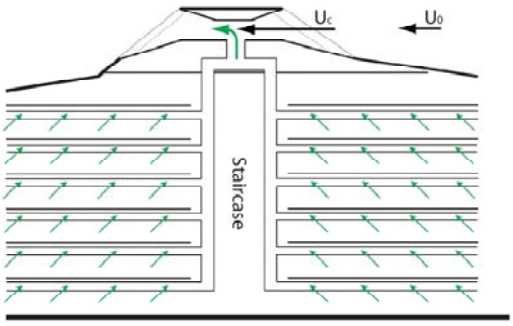

Figure 8.2: Schematic representation of the venturi-shape in the roof design

In the formerly undefined void over the internal chimney a venturi-shaped contraction is constructed to induce additional power to the natural exhaust to decrease the energy demand of the fans at the mechanical supply.

The final design case in this project is based on a cut out of the complex of one set of internal chimneys with the adjacent office wings. It contains three office wings and has eight office floors. (figure 8.3 and 8.4)

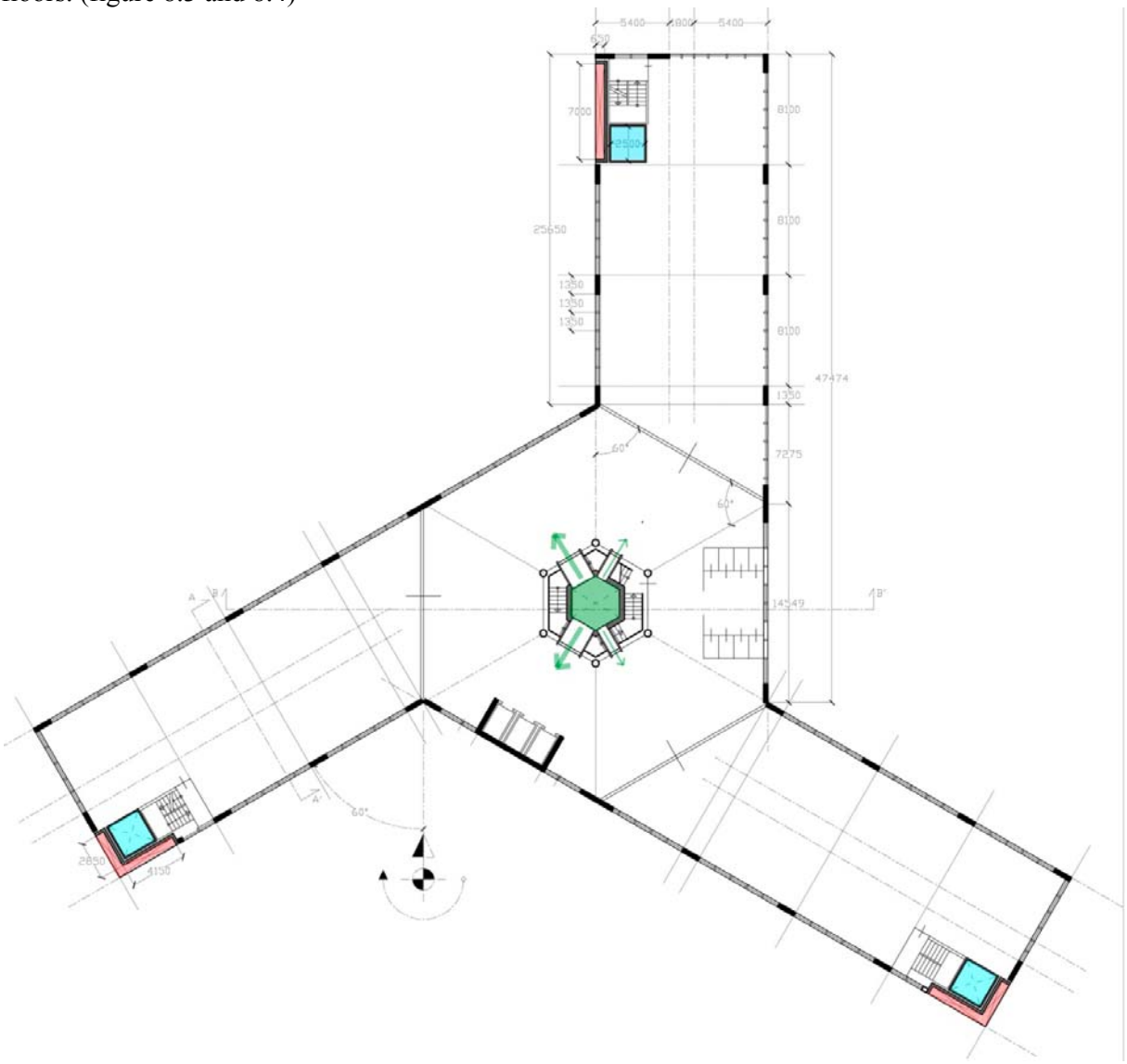

Figure 8.3: Plan of a typical floor of the final design case

[case-2A], the final design, has solar chimneys which are combined with shunt ducts which are meant to provide the same stack pressure in the chimney configuration for every office floor.

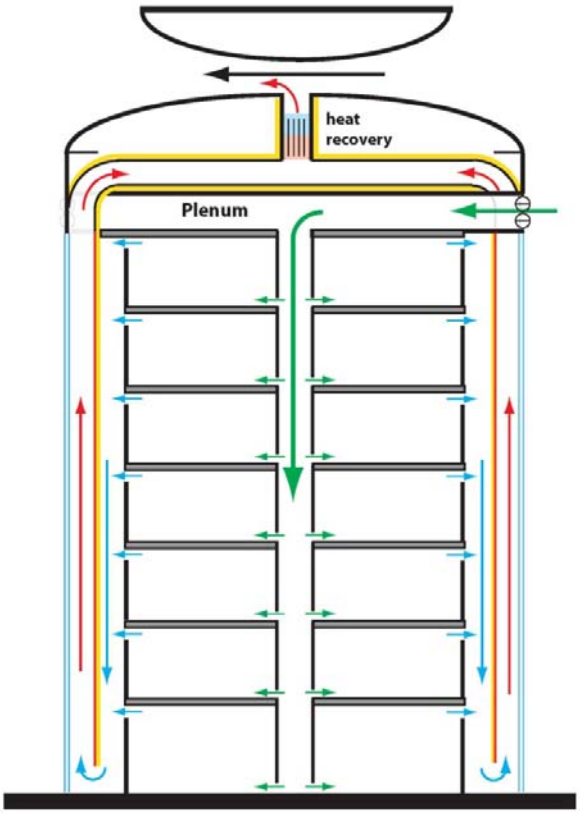

Figure 8.4: Schematic representation of the ducting system in the final design case

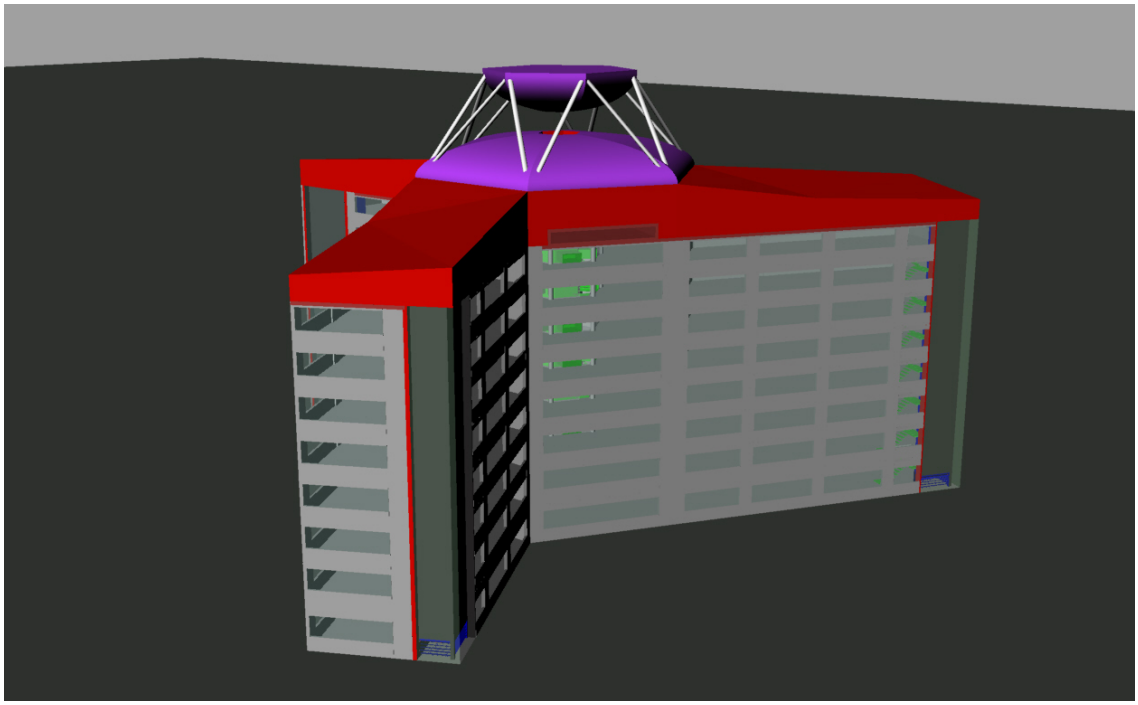

Figure 8.5: The final design with solar chimneys and central ‘venturi’ roof

Chapter 9: Research cases

In this chapter the building cases aside the final case used in the simulations to evaluate the performance of the individual driving ventilation components are introduced.

[test-case] – 'free running' behavior

The test case model has the same office floor layout as the final case but is not equipped with valves, or pre heating and cooling systems of the supply air and opening and closing regulations based on occupation. It also has unpartitioned 'simple' internal chimneys. This must result in a clear view of the natural behavior of the air flows in the building after which systems such as control valves can be added to control the air flow in the building according to the results of this test case.

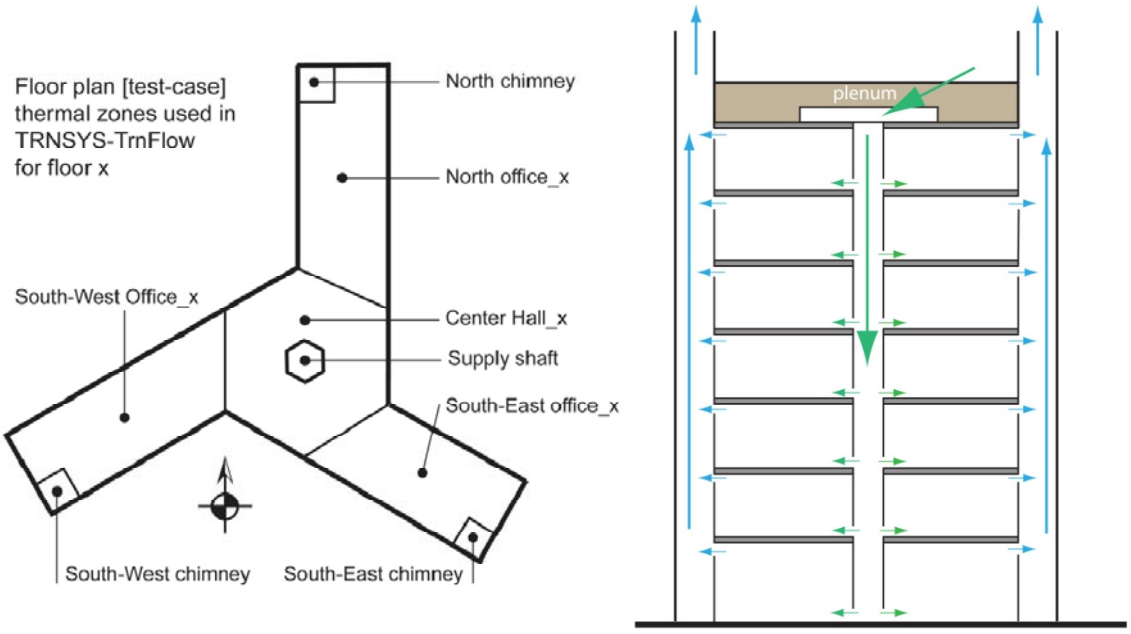

Figure 9.1: schematic plan and section of the [test-case] model

[case-0] – the reference case with internal chimneys

The reference case model includes partitioned internal chimneys which creates a bypass for the fifth to seventh floor. This is done to prevent backflow of stale air from the lower floors into the upper floors. The bypassed chimneys are based on several university library designs in the UK and US including the library of the School for Slavonic and East-European studies [SEESS] in Bloomsbury, London. (Short et. al, February 2007)

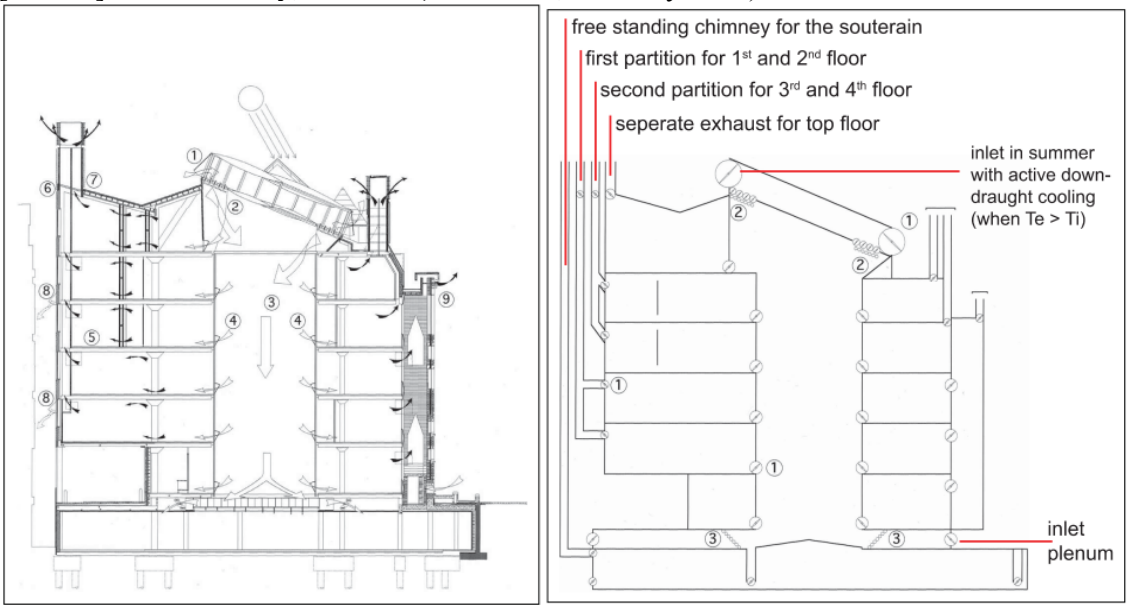

Figure 9.2: Natural ventilation system for the SEESS building – Bloomsbury, London (Short et. al, February, 2007)

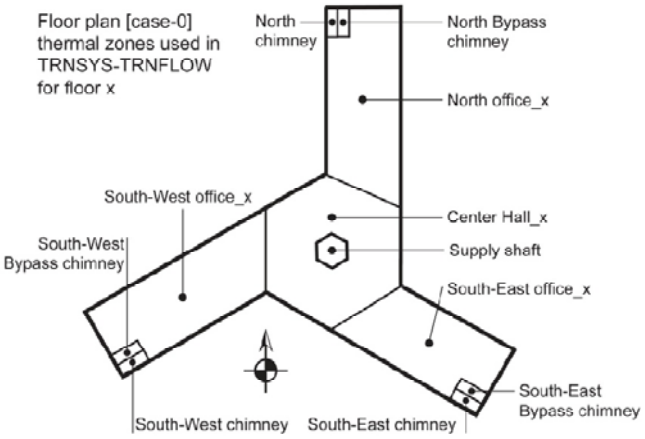

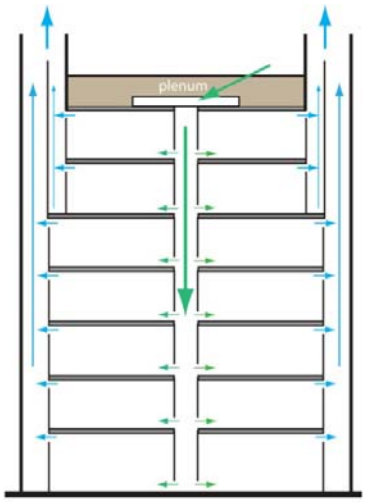

Figure 9.2: schematic plan and section of the [case-0] reference model

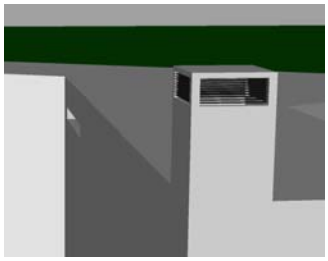

Figure 9.3: conventional exhaust at the internal chimneys at the outer corners of the office wings and inlet plenum with air intakes at three sides at the center in [case-0].

[case-1A] – solar chimneys in combination with shunt ducts and conventional exhaust

[case-1] is meant to investigate the contribution of solar chimneys to natural ventilation and to energy savings on fan energy. Two configurations of solar chimneys are investigated.

In [case-1A] a solar chimney with shunt duct is tested. As mentioned in chapter 8 the shunt duct is meant to provide each floor with the same driving pressure from the solar chimney as every floor uses the full height of the chimney.

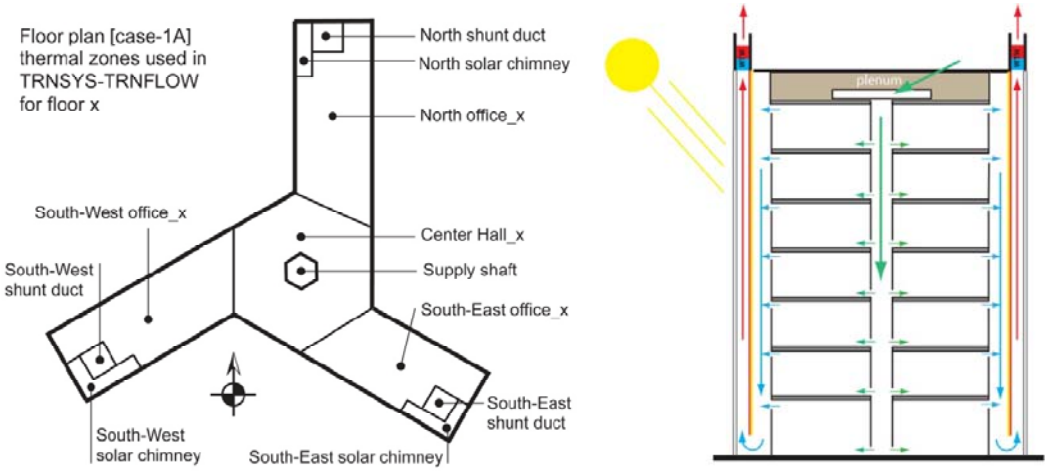

Figure 9.4: schematic plan and section of the [case-1A] model

[case-1B] – partitioned solar chimneys with conventional exhausts

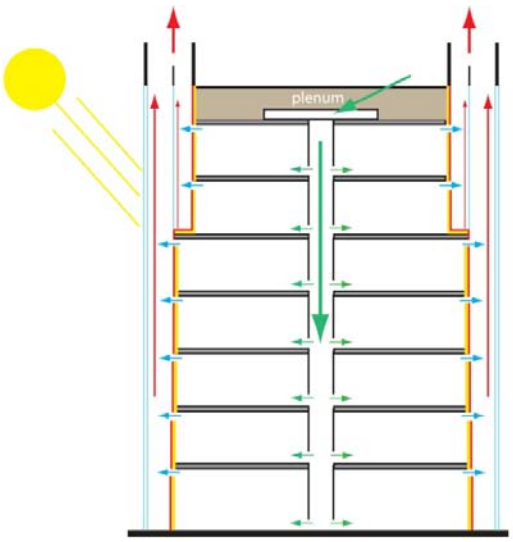

Figure 9.5: section of the [case-1B] model

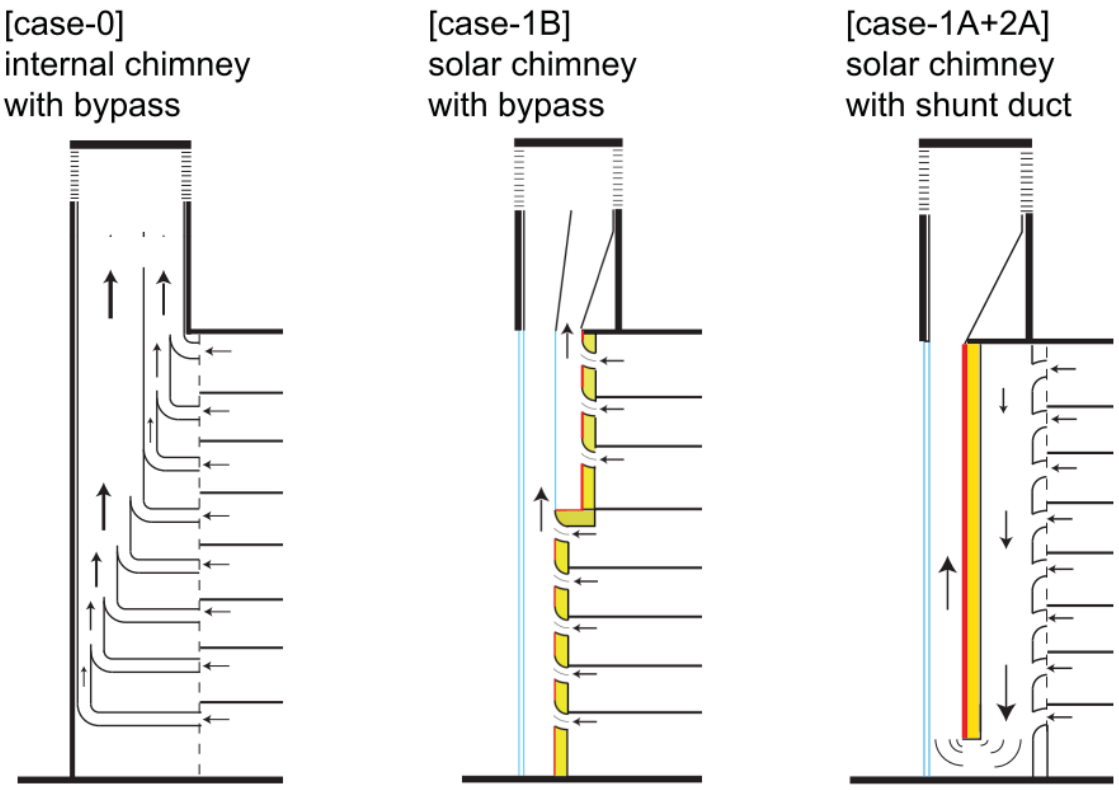

Figure 9.6: schematic representation of the chimney types used in the different building cases

Part 4: Driving ventilation components

In the final building model, three elements are included which are designed in such a way that a positive effect on ventilation flow and fan energy savings is obtained.

- The first is the solar chimney which takes advantage of the sun to boost the buoyancy which naturally occurs in the chimneys.
- The second is the 'venturi' roof which takes advantage of the wind by inducing under pressure over the exhaust.
- The third is the strategic placement of the air intake and design of the inlet plenum and supply shaft. The placement of the intake is crucial for obtaining a positive pressure in the supply flow.

For the design of the 'venturi' roof and the placement of the air intake several wind studies were done with use of CFD-software in order to obtain the ideal design for the shape and placement within the design boundaries of the project.

Chapter 10: Solar chimney

The solar chimneys in this project are in essence double facades in which the second plane is an absorber wall. The design of the chimneys is based on the Earth, Wind & Fire PhD. research at Delft University of Technology by Bronsema (November 2011,a). In this research project, numeric analysis of solar chimney performance is compared to a mock-up of an 11 meter high solar chimney at Peutz in Mook, The Netherlands. The construction of the chimney used in the mock-up is used in this project to model the solar chimneys in the TRNSYS building simulations.

Figure 10.1: Mock-up of solar chimney in the E,W&F research. project at Peutz in Mook

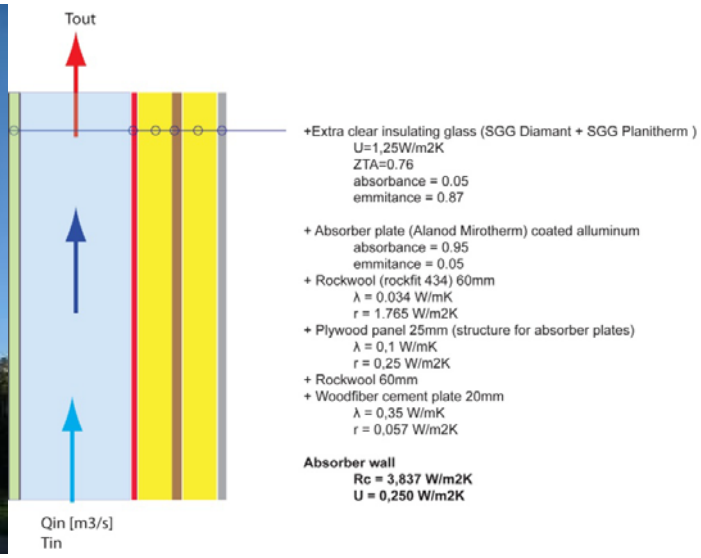

Figure 10.2: schematic section of the solar chimney construction

10.1: Numeric analysis of temperatures in the solar chimney in MS-Excel

As a quick scan tool for the performance of a vertical solar chimneys with given dimensions, a MS-Excel model was made. Its purpose is to get a first idea of the stack pressure created for a given set of input variables. For this model a five temperature node model is made. It is a set of 5 equations with 5 unknown temperatures which are solved in a matrix. An example of this static MS-Excel model can be found in [Appendix A].

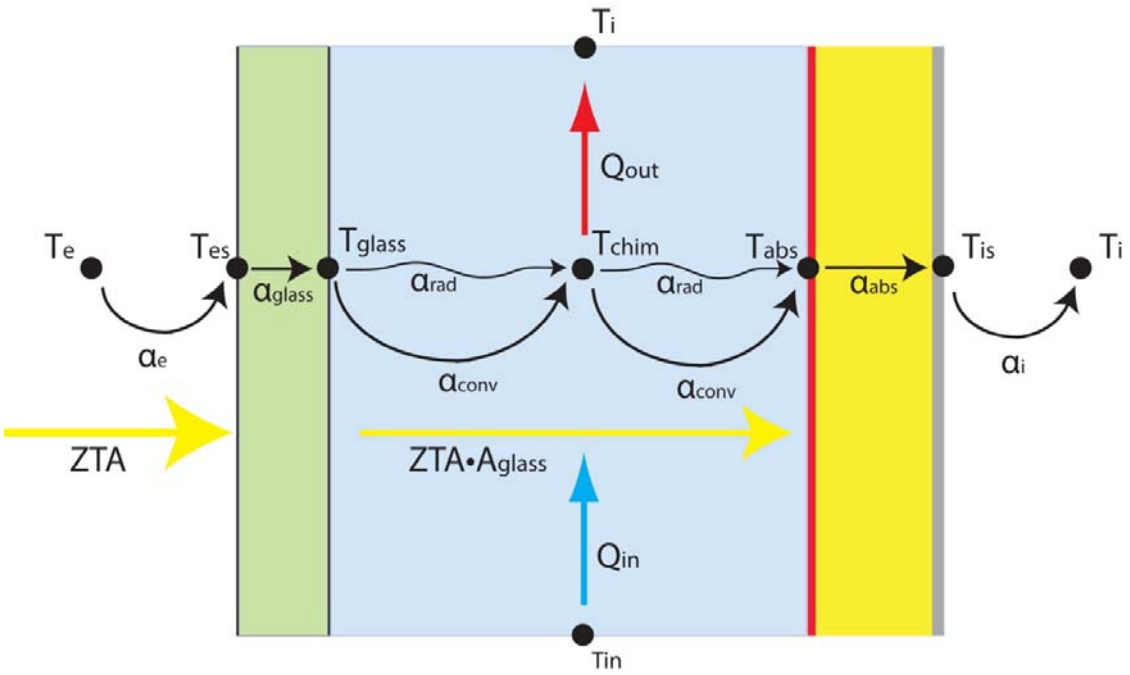

Figure 10.3: 5 node analytical model of the solar chimney

Figure 10.4: solar chimney 5 node equation model		
T_{es}	$A_{glass} \cdot \Phi_{solar} + \alpha_i \cdot (T_e - T_{es}) = \alpha_{glass} \cdot (T_{es} - T_{glass})$	(10.1a)
T_{glass}	$\alpha_{glass} \cdot (T_{es} - T_{glass}) = \alpha_{conv} \cdot (T_{glass} - T_{air}) + \alpha_{rad} \cdot (T_{glass} - T_{abs})$	(10.1b)
T_{air}	$\alpha_{conv} \cdot (T_{glass} - T_{air}) \cdot S_{chimney} + Q_{in} \cdot (\rho c) \cdot T_{in} = \alpha_{conv} \cdot (T_{air} - T_{abs}) \cdot S_{chimney} + Q_{in} \cdot (\rho \cdot c) \cdot T_{out}$	(10.1c)
T_{abs}	$A_{abs} \cdot \Phi_{solar} \cdot \tau_{glass} + \alpha_{conv} \cdot (T_{air} - T_{abs}) + \alpha_{rad} \cdot (T_{glass} - T_{abs}) = \alpha_{abs} \cdot (T_{abs} - T_{is})$	(10.1d)
T_{is}	$\alpha_{abs} \cdot (T_{abs} - T_{is}) = \alpha_i \cdot (T_{is} - T_i)$	(10.1e)
	$T_{chim} = (T_{in} + T_{out})/2$	(10.1f)

the variables and factors in the energy balance are:

Q_{in} ➔ volume flow entering the chimney [m3/s]
T_i ➔ internal temperature of the building [K]
T_e ➔ external temperature [K]
T_{es} ➔ exterior glass surface temperature [K]
T_{glass} ➔ temperature of the inner glass surface at the chimney [K]
T_{in} ➔ temperature of the air entering the chimney [K]
T_{chim} ➔ temperature of the air in the solar chimney [K]
T_{out} ➔ temperature of the air exiting the solar chimney [K]
T_{abs} ➔ temperature of the inner absorber surface at the chimney [K]
T_{is} ➔ internal surface temperature of the absorber wall [K]
Φ_{solar} ➔ global radiation (direct + diffuse radiation) [W/m^2]
A_{glass} ➔ absorption factor of the glass [-]
A_{abs} ➔ absorption factor of the glass [-]
τ_{glass} ➔ transmission factor of the glass (ZTA in Dutch building industry) [-]
U_{glass} ➔ heat transfer coefficient of the glass including α_i en α_e [W/m^{2}K]
α_{glass} ➔ heat transfer coefficient of the glass = 1/ (U_{glass}^{-1}- α_i^{-1}- α_i^{-1}) [W/m^{2}K]
U_{abs} ➔ heat transfer coefficient of the absorber wall including α_i en α_e [W/m^{2}K]
α_{abs} ➔ heat transfer coefficient of the absorber wall = 1/ (U_{abs}^{-1}- α_i^{-1}- α_i^{-1}) [W/m^{2}K]
$S_{chimney}$ ➔ glass surface of the solar chimney [m^2]

α_i ➔ heat transfer coefficient at the interior surface of a separation wall [W/m^{2}K]
α_e ➔ heat transfer coefficient at the exterior surface of a separation wall [W/m^{2}K]
α_{conv} ➔ convective heat transfer coefficient at the absorber and glass surface [W/m^{2}K]
α_{rad} ➔ radiative heat transfer coefficient between the glass and absorber surface [W/m^{2}K]
$\rho \cdot c$ ➔ heat capacity of air (1,2x1000) [J/m^3]
S_{facade} ➔ surface glass face and the surface of the absorber [m^2]

As there are five unknown variables and five equations in the energy balance model, this set of equations can be solved using a [5x5] matrix with 5 solution equations to find the values for the unknown variables; $\{T_{es};T_{glass};T_{chim};T_{abs};T_{is}\}$ with the known variables $\{T_i,T_e,T_{in},\Phi_{solar}, Q_{in}\}$. Qin in this case, is the minimal volume flow that is required for the chimney complex with the adjacent office wings.
The stack pressure induced in the chimney due to the heating air in the shaft can be calculated with the stack pressure formula (3.4a).

10.2: Influence of the side planes in the solar chimney - exchange factors of the surfaces
The 5 node analytical model in figure 10.3 is based on a solar cavity which has no side surfaces. However, in the solar chimney the solar irradiation will strike the back plane and the side planes. The sides hence can't be neglected in the analytical model. In *"Earth, Wind and Fire" part I* (Bronsema, 2011a), the relation between the exchange factors and the radiative heat transfer coefficient, α_{rad}, is described. The exchange factors and view factors between the three absorber planes and the glass plane in a rectangular solar chimney have to be calculated to find this relation and determine α_{rad}. The width of the chimney is corrected for the radiation from the back to the glass via the side planes to obtain the radiative width of the chimney:

$$W^*_{rad} = W \bullet \psi_{1-4} + D \bullet \psi_{2-4} + D \bullet \psi_{3-4} \quad (10.2)$$

W^*_{rad} ➔ convective width of the chimney
ψ_{1-4} ➔ exchange factor from plane 1 to plane 4 (figure 10.3)
ψ_{2-4} ➔ exchange factor from plane 2 to plane 4
ψ_{3-4} ➔ exchange factor from plane 3 to plane 4

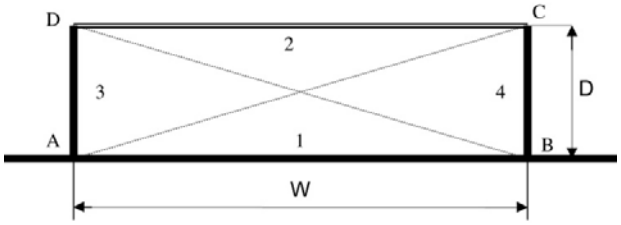

Figure 10.5: planes in the chimney

Through the side absorber planes, heat loss to the interior occurs hence the depth of the chimney is added to the width to obtain the convective width of the chimney:

$$W^*_{conv} = W + (2 \bullet D) \quad (10.3)$$

W^*_{conv} ➔ convective width of the chimney

The exchange factor are derived from the view factors between the planes in the chimney which are calculated by the "crossed string" method. In the MS-Excel model the view factors and the exchange factors are solved in matrices after input of the geometrics of the chimney.

10.3: Heat transfer coefficients

The heat transfer coefficients at the glass plane and the absorber plate in the chimney are influenced by many variables. In his research project Bronsema first described an analytical relation between the convective heat transfer coefficient, α_{conv}, with air velocity and surface temperature in the chimney. Furthermore, extensive studies have been done to obtain a satisfying model of the heat transfer coefficients. In the MS-Excel analytical model the first analytical relation by Bronsema is used.

$\alpha_{conv,abs} = 3{,}98v^{0,8} + 0{,}042v^{-1,55} \bullet (T_{glass}-T_{air})$ [W/m^{2}K] (Bronsema, 2011,a) (10.4)

$\alpha_{conv,abs}$ ➔ convective heat transfer coefficient at the absorber wall
v ➔ air velocity in the chimney

$\alpha_{conv,glass} = 3{,}98v^{0,8} + 0{,}042v^{-1,55} \bullet (T_{glass}-T_{air})$ [W/m^{2}K] (Bronsema, 2011,a) (10.4)

$\alpha_{conv,glass}$ ➔ convective heat transfer coefficient at the glass plane

10.4: Shunt duct

The solar chimneys in the final design are executed with a shunt duct. This is a vertical duct next to the solar chimney which collects the stale air from the office floors and connects to the bottom of the solar chimney. The principal behind this is to provide each floor with the same stack height and hence the same stack pressure in the chimney. The solar chimney plus shunt duct is shown in figure 9.6 in the [case-1A+2A] chimney configuration.
The solar chimney in this project is modeled as a duct next to every solar chimney. The design of the stale air flow pattern from the office floors to the bottom of the solar chimneys can be set up in several other ways which are summarized in chapters 24 and 25.

Chapter 11: 'venturi' roof, conventional exhaust and air supply – CFD-analysis

All building models have an air supply system through a plenum under the roof edge. Next to that every building has an exhaust in some form. In order to determine the wind force on these two ventilation components in every building model, a series of CFD-analyses is done to determine the wind pressure coefficients which are necessary for the TRNSYS-TrnFlow simulations. The CFD-studies where executed by Heleen Doolaard during her internship at Deerns consulting engineers. The boundary conditions of the CFD-analysis and the relevant results of this research are summarized in this chapter. The full results are gathered in the internship report by Doolaard (November 2011)

11.1: 'Venturi' roof C_p-value

In the final building model a 'venturi' roof is placed on the center of the building. All three solar chimneys lead back to this 'venturi' exhaust to take advantage of the wind induced under pressure in the contraction. The ideal contraction ratio of the roof and the performance are investigated by Doolaard. As this specific model for a 'venturi' exhaust is one of many possibilities, a summary of the design possibilities for the integration of 'venturi' exhausts in the building design is given in chapter 26.

Boundary conditions

The 'venturi' roof is in essence a combination of to ellipsoids placed above each other to create a contraction with the narrowest point at the center. At this center in the lower ellipsoid the stale air from the building is extracted. Goal of the CFD-analyses was to determine the $C_{p,e}$. In Phoenics the building is modeled as a block without the air intake holes and without the exhaust hole in the 'venturi' contraction. Therefore the results shown in this report apply to the 'venturi' roof without exhaust stream and without the influence of the exhaust opening in the lower ellipsoid. The results are obtained by evaluating the pressure difference at the narrowest point of the contraction which is the exhaust position. In CFD-analyses in the Earth, Wind and Fire research project (Bronsema, November 2011,b), the influence of the exhaust opening and exhaust flow are analyzed and validated by wind tunnel measurements in the atmospheric boundary layer wind tunnel at Peutz in Mook. This study concluded that the exhaust opening causes a slight drop of the $C_{p,e}$ and the ideal contraction ratio increases slightly. However the principle of the 'venturi' roof holds.

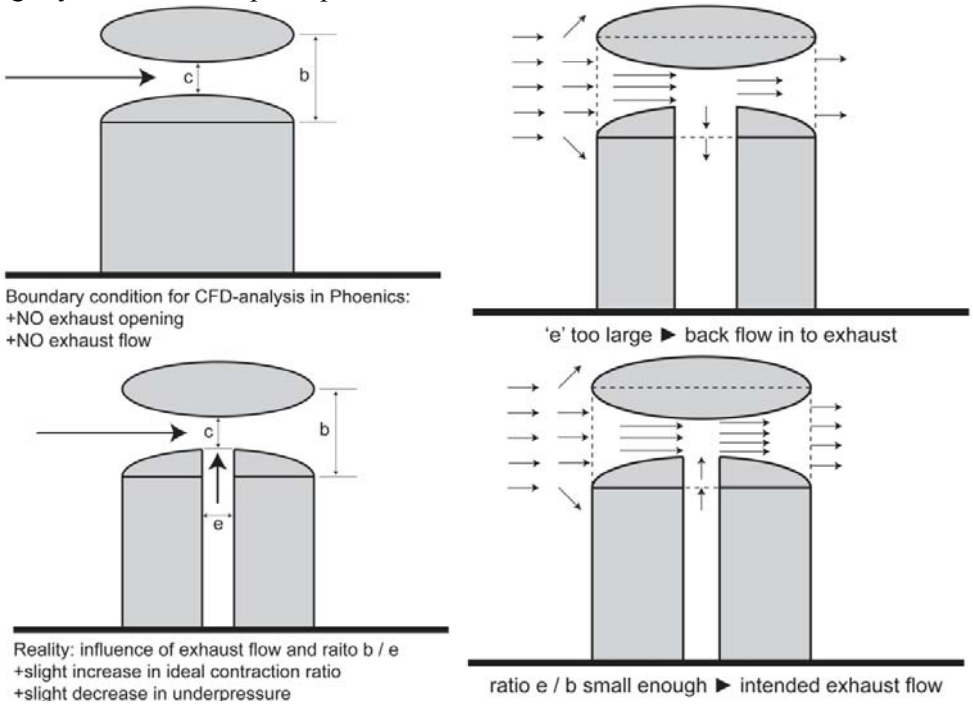

Figure 11.1: a) Boundary conditions for the CFD-analysis in this project,
b) influence of the exhaust flow and opening on the ideal contraction ratio and the resulting pressure difference, c) diagram of expected behavior with a large exhaust diameter, d) diagram of expected behavior with small exhaust diameter relative to the inflow area.

For the CFD-analysis of the air intake and exhausts a logarithmic wind profile was used in Phoenics. TRNSYS-TrnFlow uses a power law equation to describe the wind profile. The corresponding power law wind profile used in TRNSYS-TrnFlow is described by:

$$U(h) = U_0 \cdot (h_0 / 60)^{\alpha_0} \qquad (11.1)$$

$U(h)$ ➔ wind velocity at height h from the ground plane [m/s]
U_0 ➔ wind velocity at reference height at the building site [m/s]
h ➔ height at the building site [m]
α_0 ➔ wind velocity exponent at the building site, 0,226 in this project
60 ➔ height of the boundary layer at the building site

Ideal contraction ratio and correspond wind pressure coefficient

As mentioned in chapter 4, the 'venturi' effect in a construction as in this project is not a confined flow which means that are can flow around and over the 'venturi' roof.

At first a reference venturi model was made to set a reference for the C_p-value. (Figure 10.1a). After setting the reference the, contraction ratio was altered by altering the distance between the lower and upper roof. With this an ideal contraction ration of 0,2 determined by equation (4.3), was found (Figure 10.1b). With this contraction ration of 0,2 the maximum negative C_p-value was sought by stretching the vertical dimension of the lower and upper roof while maintaining R_c =0,2 (Figure 10.1c)

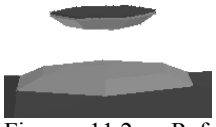

Figure 11.2a: Reference venturi roof. The ellipsoids are 2.4 m high and the minimal separation between them is 5.1 m, which makes a contraction ratio of 0.5.

Figure 11.2b: The separation between the ellipsoids that form the venturi roof is reduced. The ellipsoids are 2.4 m high, just as in the reference case. Their minimal separation is 1.3 m, so the contraction ratio is 0.2.

Figure 11.2c: The roof parts are stretched in the vertical direction. The roof plate is not changed. Both ellipsoids are 4.8 m high and the separation is 2.5 m, so the contraction ratio is 0.2.

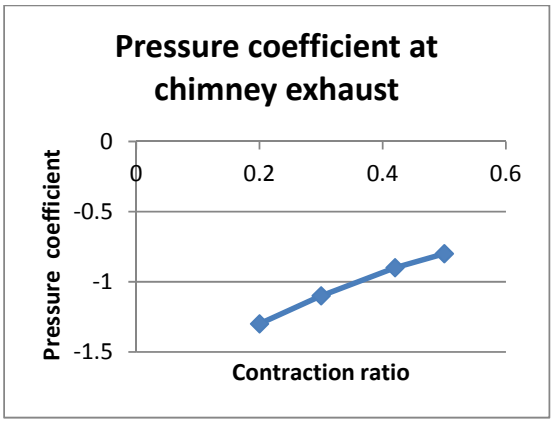

Figure 11.3a: Pressure drop at the chimney exhaust for different contraction ratios. The pressure is given relative to the atmospheric pressure.

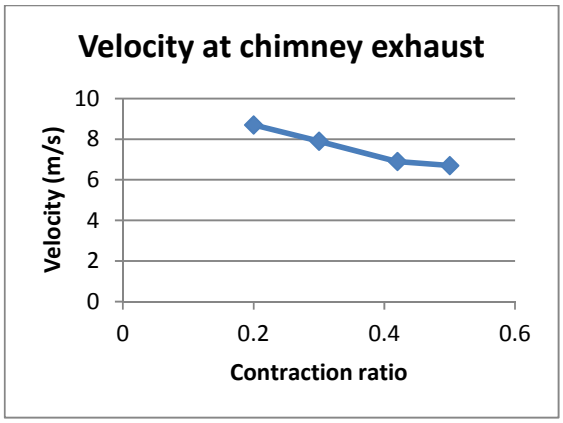

Figure 11.3b: Velocity at chimney exhaust for different contraction ratios.

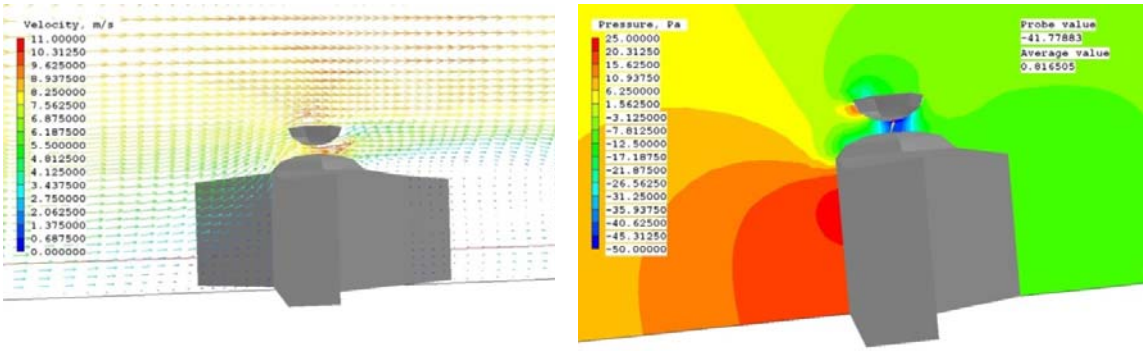

Figure 11.4: Velocity and pressure profile of the venturi chimney with the optimal roof shape for a contraction ratio of 0.2. The velocity at the exhaust is 9.5 m/s and the pressure drop is 41,8Pa, which results in a pressure coefficient of -1.4

Figure 11.5: results for different ellipsoid heights at R_c =0,2			
Distance between roofs (m)	Height ellipsoids(m)	C_p at the exhaust	Velocity (m/s)
1.3	2.4	-1.29	8.7
2.0	3.8	-1.33	9.3
2.25	4.3	-1.36	9.4
2.5	4.8	-1.42	9.5
2.75	5.3	-1.31	9.6
3.0	5.8	-1.35	9.7

The largest negative C_p is obtained by the model with R_c =0,2 and an ellipsoid height of 4,8. As this model has a total 'venturi' roof height of 2x4,8+2,5 = 10,1 meters, the construction of the roof adds an additional 10 meters to the total building height of 32 meters. In [case-2A], the final simulation model, the model with a contraction height of 2,0m in Figure 11.5 is chosen for architectural reasons which still has a C_p-value of -1,33.

11.2: C_p-values of conventional chimneys

For comparison of the performance of the 'venturi' roof with conventional exhaust systems, the C_p-values of the exhaust openings of the chimneys in [case-0] were tested in Phoenics by Doolaard on a model also used to determine the pressure on the air intakes for[case-0] and [case-1].

Boundary conditions

Similar to the 'venturi' roof analysis, the model of [case-0] with conventional exhaust openings is tested without the influence of the exhaust flow and exhaust openings. The results in this model where obtained by evaluating the pressure difference at surfaces on 4 sides of the chimney, which represent the exhaust openings, and averaging them for the 12 analyzed wind directions evenly spread with an intermediate angle of 30° between each simulation. In this manner the C_p-values of the three individual chimneys are known for 12 wind directions which are used in the TRNSYS simulations. TRNSYS interpolates between these 12 data points to model the wind directions over the full 360 degrees of the compass card.

Results for 3 separate chimneys per wind direction

The conventional chimneys in [case-0] and [case-1] have an average C_p-value over all wind directions of -0,31 for the South-East chimney and -0,37 for the North and South-West chimney. In figure 11.6 the results are given for the three chimneys, for the 12 wind directions which were used in the TRNSYS simulations for [case-0], [case-1A] and [case-1B]. The results for the four sides of each chimney are averaged to come to one value per chimney per wind direction.

Pressure on chimney exhaust for [case-0]

Uw,ref@10m	5	[m/s]
Uref	7	[m/s]
ref height	30	[m]
rho	1.2	[kg/m3]

North office wing

wind direction	0_degr		30_degr		60_degr		90_degr		120_degr		150_degr		180_degr		210_degr		240_degr		270_degr		300_degr		330_degr		
orientation	pressu	Cp	pressu	Cp	pressu	Cp	pressu	Cp	pressu	Cp	pressu	Cp	pressu	Cp	pressu	Cp	pressu	Cp	pressu	Cp	pressu	Cp	pressu	Cp	
North	-2.5	**-0.1**	-5.4	**-0.2**	-15.2	**-0.5**	-4.7	**-0.2**	-14	**-0.5**	-20.2	**-0.7**	-10	**-0.3**	-19.9	**-0.7**	-13.9	**-0.5**	-14	**-0.5**	-2.2	**-0.1**	-4.2	**-0.1**	average
East	-10.6	**-0.4**	-8.4	**-0.3**	-14.8	**-0.5**	-0.6	**0.0**	-8	**-0.3**	-13.3	**-0.5**	-9.4	**-0.3**	-20	**-0.7**	-16.6	**-0.6**	-17.1	**-0.6**	-2.2	**-0.1**	-14.1	**-0.5**	over all
South	-6.7	**-0.2**	-15.3	**-0.5**	-17.4	**-0.6**	-4.1	**-0.1**	-7.4	**-0.3**	-9.8	**-0.3**	-9.5	**-0.3**	-14.4	**-0.5**	-10	**-0.3**	-13.3	**-0.5**	-11	**-0.4**	-12.3	**-0.4**	directions
West	-7.1	**-0.2**	-13.3	**-0.5**	-16.6	**-0.6**	-4.9	**-0.2**	-12	**-0.4**	-18	**-0.6**	-9.7	**-0.3**	-17.8	**-0.6**	-6.4	**-0.2**	-9.1	**-0.3**	-15.5	**-0.5**	-5.4	**-0.2**	
average		**-0.23**		**-0.36**		**-0.54**		**-0.12**		**-0.35**		**-0.52**		**-0.33**		**-0.61**		**-0.40**		**-0.45**		**-0.26**		**-0.31**	**-0.37**

South-East office wing

wind direction	0_degr		30_degr		60_degr		90_degr		120_degr		150_degr		180_degr		210_degr		240_degr		270_degr		300_degr		330_degr		
orientation	pressu	Cp	pressu	Cp	pressu	Cp	pressu	Cp	pressu	Cp	pressu	Cp	pressu	Cp	pressu	Cp	pressu	Cp	pressu	Cp	pressu	Cp	pressu	Cp	
30_degr	-7.5	**-0.3**	-2.4	**-0.1**	-15.5	**-0.5**	-12.5	**-0.4**	-7.1	**-0.2**	-7.6	**-0.3**	-15	**-0.5**	-15	**-0.5**	-18.2	**-0.6**	-10.4	**-0.4**	-7	**-0.2**	-15.5	**-0.5**	average
120_degr	-16.3	**-0.6**	-6.4	**-0.2**	-2.2	**-0.1**	-6	**-0.2**	0.5	**0.0**	1.3	**0.0**	0.2	**0.0**	-12.4	**-0.4**	-18	**-0.6**	-12.6	**-0.4**	-12.1	**-0.4**	-14.3	**-0.5**	over all
210_degr	-14.9	**-0.5**	-7.5	**-0.3**	-2.2	**-0.1**	-15.9	**-0.5**	-7.9	**-0.3**	-1.2	**0.0**	6.5	**0.2**	-5.3	**-0.2**	-14.5	**-0.5**	-5.8	**-0.2**	-7.5	**-0.3**	-9.8	**-0.3**	directions
300_degr	-10.5	**-0.4**	-5.7	**-0.2**	-11	**-0.4**	-18.1	**-0.6**	-6.4	**-0.2**	-7.6	**-0.3**	-5.8	**-0.2**	-10.6	**-0.4**	-16.2	**-0.6**	-3.7	**-0.1**	-5.8	**-0.2**	-12.2	**-0.4**	
average		**-0.42**		**-0.19**		**-0.26**		**-0.45**		**-0.18**		**-0.13**		**-0.12**		**-0.37**		**-0.57**		**-0.28**		**-0.28**		**-0.44**	**-0.31**

South-West office wing

wind direction	0_degr		30_degr		60_degr		90_degr		120_degr		150_degr		180_degr		210_degr		240_degr		270_degr		300_degr		330_degr		
orientation	[Pa]	Cp	[Pa]	Cp	[Pa]	Cp	[Pa]	Cp	[Pa]	Cp	[Pa]	Cp	[Pa]	Cp	[Pa]	Cp	[Pa]	Cp	[Pa]	Cp	[Pa]	Cp	[Pa]	Cp	
60_degr	-16.1	**-0.5**	-9.8	**-0.3**	-5.8	**-0.2**	-14.4	**-0.5**	-10	**-0.3**	-13.3	**-0.5**	-11	**-0.4**	-12.3	**-0.4**	-6.7	**-0.2**	-15.3	**-0.5**	-17.4	**-0.6**	-4.1	**-0.1**	average
150_degr	-11.3	**-0.4**	-18	**-0.6**	-7	**-0.2**	-17.8	**-0.6**	-6.4	**-0.2**	-9.1	**-0.3**	-15.5	**-0.5**	-5.4	**-0.2**	-7.1	**-0.2**	-13.3	**-0.5**	-16.6	**-0.6**	-4.9	**-0.2**	over all
240_degr	-13.6	**-0.5**	-20.2	**-0.7**	-12.1	**-0.4**	-19.9	**-0.7**	-13.9	**-0.5**	-14	**-0.5**	-2.2	**-0.1**	-4.2	**-0.1**	-2.5	**-0.1**	-5.4	**-0.2**	-15.2	**-0.5**	-4.7	**-0.2**	directions
330_degr	-5.7	**-0.2**	-13.3	**-0.5**	-7.5	**-0.3**	-20	**-0.7**	-16.6	**-0.6**	-17.1	**-0.6**	-2.2	**-0.1**	-14.1	**-0.5**	-10.6	**-0.4**	-8.4	**-0.3**	-14.8	**-0.5**	-0.6	**0.0**	
average		**-0.40**		**-0.52**		**-0.28**		**-0.61**		**-0.40**		**-0.45**		**-0.26**		**-0.31**		**-0.23**		**-0.36**		**-0.54**		**-0.12**	**-0.37**

Figure 11.6: C_p-values for the conventional chimney exhausts

11.3: Air intake and inlet placement

In an early stage of the project several options for air intake placement and supply ducting design have been investigated. The options which are not used in this project but are nevertheless possible for other building projects are summarized in paragraph 26.3 which describes the architectural possibilities for air intake placement and the integration of air supply in the building design.

In all building cases the supply side of ventilation system is taken care of by an inlet plenum with air intakes on 3 sides. This is done to obtain a positive wind pressure at all times on at least one of the air intakes. When an intake is experiencing a negative pressure it will be closed. This behavior is modeled in the TRNSYS simulation by a series of controls.

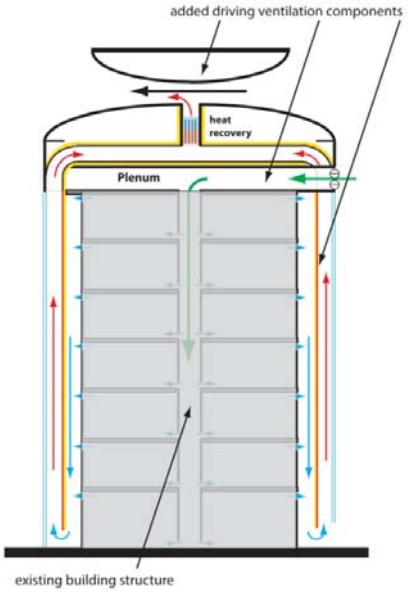

Figure 11.7: supply system and exhaust system placed on an existing building structure

Boundary conditions

The magnitude of the pressure difference at the air intake is tested in Phoenics to obtain the C_p-values at these air intakes for 12 wind directions in a similar manner as the results for the conventional exhausts are obtained. The 3 air intakes have a cross sectional area of 1x10,2m. For this wide spread area a single point value for the pressure difference is not representative. Instead the pressure difference at the 4 corners of the area and 2 at the center of the long edges

are evaluated and averaged to obtain the C_p-values for the 12 wind directions which are used as input in TRNSYS.

Results for Air intake C_p-value

The pressure difference on the air intakes is evaluated on the [case-0] model. For the building simulations of [case-2A] with 'venturi' roof, the same C_p-values are used.

Pressure on inlet openings [case-0] 28.5 to 29.5m; building height is 32m

average pressure coefficient over a plane, 2.5meters under the roof edge

Uw,ref@10m	5	[m/s]
Uref	7	[m/s]
ref height	30	[m]
rho	1.2	[kg/m3]

wind direction	0		30		60		90		120		150		180		210		240		270		300		330	
inlet	[Pa]	Cp	[Pa]	Cp	[Pa]	Cp	[Pa]	Cp	[Pa]	Cp	[Pa]	Cp	[Pa]	Cp	[Pa]	Cp	[Pa]	Cp	[Pa]	Cp	[Pa]	Cp	[Pa]	Cp
90_DEGR	5.43	**0.18**	4.74	**0.16**	8.76	**0.30**	5.85	**0.20**	10.77	**0.37**	6.21	**0.21**	-15.84	**-0.54**	-8.42	**-0.29**	-8.74	**-0.30**	-8.96	**-0.30**	-9.83	**-0.33**	-15.21	**-0.52**
210_DEGR	-8.74	**-0.30**	-8.96	**-0.30**	-9.83	**-0.33**	-15.21	**-0.52**	5.43	**0.18**	4.74	**0.16**	8.76	**0.30**	5.85	**0.20**	10.77	**0.37**	6.21	**0.21**	-15.84	**-0.54**	-8.42	**-0.29**
330_DEGR	10.77	**0.37**	6.21	**0.21**	-15.84	**-0.54**	-8.42	**-0.29**	-8.74	**-0.30**	-8.96	**-0.30**	-9.83	**-0.33**	-15.21	**-0.52**	5.43	**0.18**	4.74	**0.16**	8.76	**0.30**	5.85	**0.20**

Figure 11.8: C_p-values for the air intakes at the three sides of the inlet plenum.

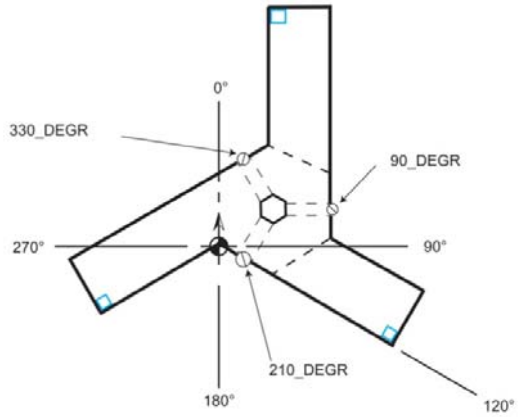

Figure 11.9: Three inlet orientations in the building

Part 5: Method of simulation and data processing

This part of the project report describes the methods followed in setting up the building simulations and the processing of the output data from the simulations done with TRNSYS-TrnFlow.

Chapter 12: Modeling the building cases in TRNSYS-TRNFLOW

In this project the amount of fan energy that can be saved by ventilating an office building through solar chimneys and venturi-shaped exhausts is the central question. As the contribution to ventilation of these measures is dependent on the natural driving forces of the sun and wind and the fact that it is applied on a free running building, a dynamic calculation of the building and its total ventilation system is needed to determine the performance of the building. This chapter describes the method in which the building cases are modeled in TRNSYS-TrnFlow.

12.1: TRNSYS-TrnFlow model of building cases

In order to isolate the performances of the individual components, the solar chimneys and venturi-shaped exhaust, the dynamic calculation is done over a set of cases in which each case a component of the ventilation system is added.

As the main question in this research is the amount of fan energy that can be saved, at first a reference is needed of the amount of energy needed to ventilate the building without the naturally driven ventilation components. The reference case [case 0] is remotely based on the design project of the Ministry of Defense in Paris, France, which consists of a mechanical supply system and a natural exhaust system which consists of internal chimneys which exits under a yet undefined roof shape. In this project the possibility of replacing the internal chimney with solar chimneys and defining the roof space as a venturi-shaped exhaust is investigated.

[test-case]

The test case is the first model to investigate the free running behavior of the buildings ventilation system. It is also used to get a grip of the working principles of the controls which can be applied in the simulation such as heating and cooling, inlet and outlet valve control in time and all other possible control figures applied in TRNSYS-TrnFlow. Figures 12.1 and 12.2 show the thermal zones used in the model and the defined air links between the thermal zones to represent the ventilation system.

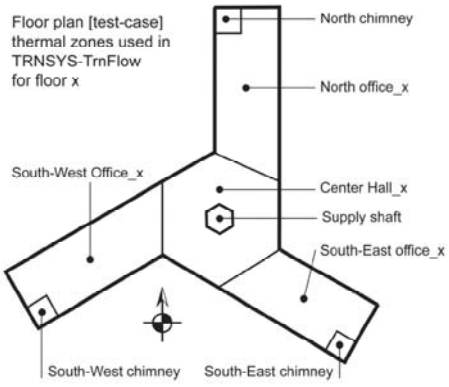

Figure 12.1: plan of [test-case] with thermal zones

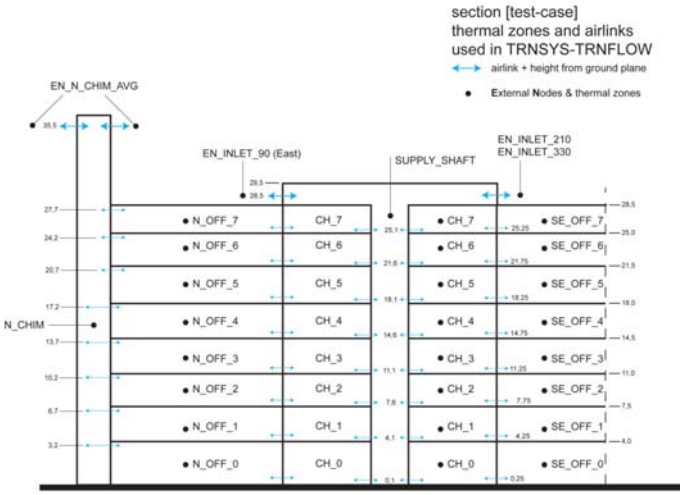

Figure 12.2: section of [test-case] with thermal zones, external nodes and air links

[case-0]

[case-0] is the reference case in this project. It contains three chimneys which are partitioned to prevent back flow at the top floors (figure 9.6).

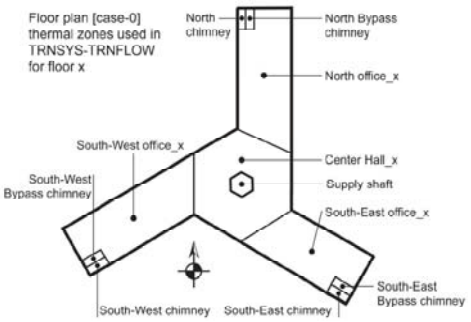

Figure 12.3: plan of [case-0] with nodes thermal zones

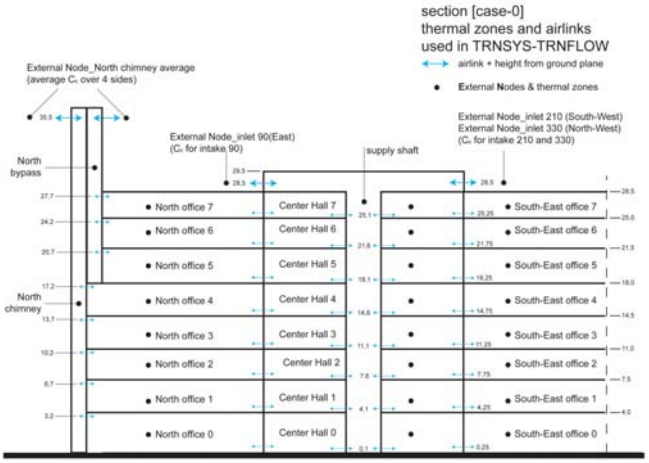

Figure 12.4: section of [case-0] with thermal zones, external and air links

[case-1A]

In [case-1] the solar chimneys are added to the model. These are placed at the corner of each wing in such a way that the most solar radiation is collected throughout the workday. As mentioned two types of solar chimney configurations are tested. [case-1A] has solar chimneys in combination with a shunt duct for each chimney. The shunt duct redirects the stale air from all floors down towards the bottom of the solar chimney (figure 9.6).

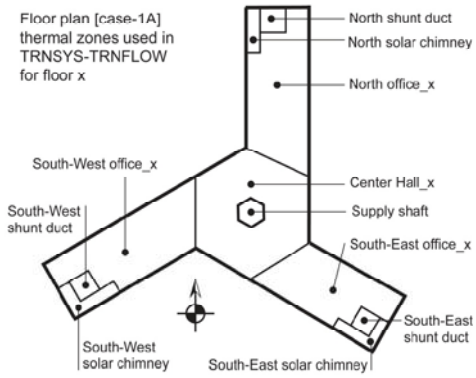

Figure 12.5: plan of [case-1A] with external nodes thermal zones

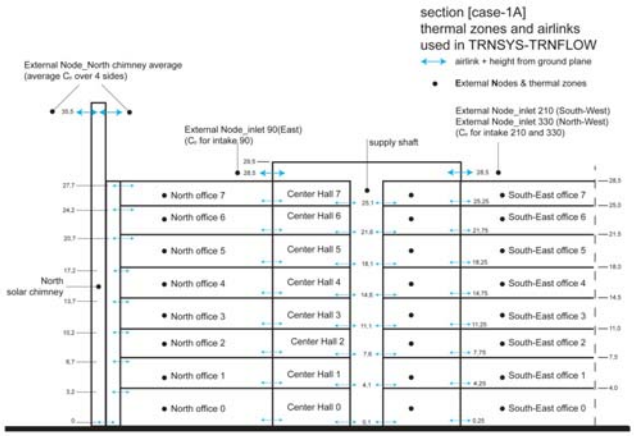

Figure 12.6: section of [case-1A] with thermal zones, and air links

[case-1B]

In variant B of case-1 the solar chimneys are modeled without shunt ducts. The solar chimney configuration is similar to the internal chimneys in [case-0] with bypass chimneys for the fifth, sixth and seventh floor. As a consequence the thermal zones and air links are similar to those of [case-0]. (figure 12.3 and 12.4)

The absorber walls are solar chimneys are constructed in the same manner as those in [case-1A]. The partition wall between the solar chimney and the solar bypass is a single glass pane in order to let the absorber wall of the solar bypass heat up (figure 9.6). A variant with a steel partition with attached absorber plate was investigated shortly but the temperature and hence the stack pressure in the solar bypass in this configuration was significantly lower.

[case-2A]

In the final design the model of [case-1A] is extended with the central 'venturi' roof with as described in chapter 4 with a C_p-value of -1,33.

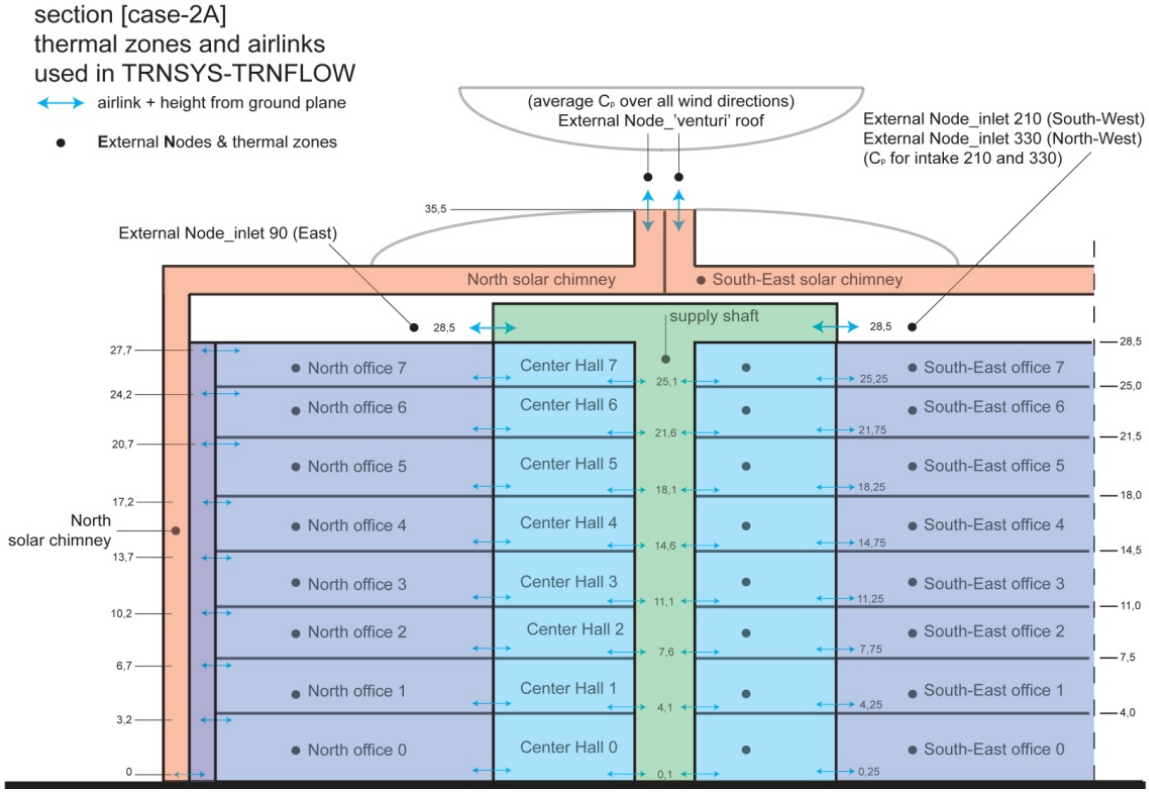

Figure 12.7: section of [case-2A] with thermal zones, external nodes and air links

12.2: Boundary conditions

For a valuable comparison of the cases, a set of boundary conditions is used for all cases. A summary of the most important boundary conditions:

- Building structure
  - Office zones 362,9m^2 GFA (3 per floor)
  - Center Hall zones 539,6m^2 GFA (1 per floor)
  - Total GFA = 13.026m^2 GFA (8 floors)
  - Opaque façade element ➔ U=0,23W/m^2•K
  - Transparent façade elements
    - ZTA = 0,61
    - U_{glass}= 1,1W/m^2•K
    - U_{window}= 1,6W/m^2•K
    - Typical building mass ➔ SWM = 105kg/m^2 GFA
- Occupancy
  - Office zones 86% of GFA as office space ➔0,86x362,9 = 312,1m^2
  - Center Hall zones 25% of GFA as office space ➔0,25x539,6 = 134,9m^2
  - Average occupancy 65% of GFA
- Cooling capacity
  - Office zone 60W/m^2 for 362,9m^2 = 21.775,8W floor cooling
  - Center Hall zone 60W/m^2 for 539,6m^2 = 32.274W floor cooling
- Heating capacity
  - Office zone 60W/m^2 for 362,9m^2 = 21.775,8W floor heating
    Radiative part is 60%
  - Center Hall zone 60W/m^2 for 539,6m^2 = 32.274W floor heating
    80.000W per Center Hall zone preheating
    112.374W zone total
    Radiative part is 20%
- Internal gains Typical per m^2 of office space = 35W/m^2
  - Lighting 8W/m^2 40% convective/ 60% radiative
  - Computers 14W/m^2 office space
  - People 15W/m^2 office space
  - Appliances 1 printer/ copier per office zone ➔ 50W per office zone
- Simulation schedules
  - Workday occupation- / lighting- / ventilation schedule
    - 9:00AM ➔ 19:00PM
    - 5 days a week
    - 52 weeks a year
    - 3132 annual occupation hours
  - Heating- / cooling offset schedule
    - 8:00AM ➔ 19:00PM on workdays
- Ventilation
  - 50m^3/h p.p. (13,9dm^3/s p.p.)
  - 3,25m^3/(m^2•h) per m^2 of office space
  - 0,5m^3/s per office zone to the chimney corresponding with sufficient ventilation of the office zone.

The extensive set of boundary conditions is given in [appendix B]

12.3: calculation and modeling of aerodynamic flow resistance

In TRNSYS, Type56b-TRNFlow building module is used to cases the building models and the air-links between the zones representing the ducting. During the project it was found that only one type of air-link is appropriate in evaluating naturally ventilated buildings. This type is the 'large opening' or window. It is capable of processing a two way air flow within one time step whereas other air-link types only allow one way air flow. As the air flow pattern can reverse in natural ventilation within one time step it is necessary to use this type. With use of other types of air-links the model can't convert the outcome in one time step when multiple air flow directions occur during one time step which causes the program to produce errors and ultimately break of simulation.

A consequence of using 'large openings' is that ducts can't be modeled explicitly and that loss factors have to be translated to the coefficient of discharge [C_{di}] of the large openings used in the model. An advantage of modeling ducts as building zones is the thermal interaction of building zones which makes it possible to simulate thermal effects in the ducts. This is particularly important in the solar chimney. As the solar chimney can be modeled as a building zone with the right glass and absorber wall properties a good representation of the solar chimney can be made in the building model.

Modeling a vertical duct

The chimneys and supply duct in the building are vertical ducts which are modeled as building zones in TRNSYS and connected to the office zones with air-links of the 'large opening' type (figure 12.8).

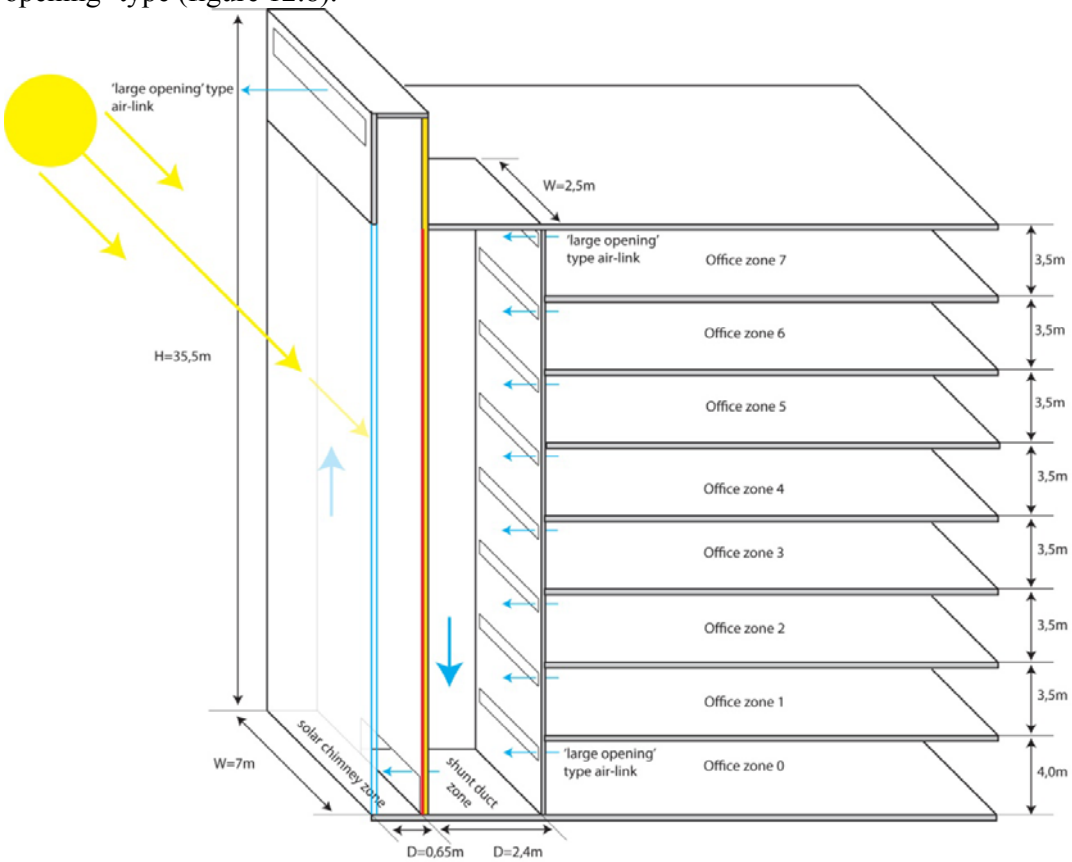

Figure 12.8: solar chimney and shunt duct in [case-1A] modeled as building zones interconnected by 'large opening' type air-links.

In building zones the pressure loss due to friction is suspected to be zero because of low air velocities in the zone. As a consequence the loss factor in the duct represented by the zone has to be determined at a certain air velocity in the duct. Together with the loss factors of the inlet, and outlets ducts between these 'ducts' represented by the building zone, the C_{di} of the total duct is determined which are in turn applied to the 'large opening' type air-links at the building zone. As an example, the determination of the C_{di} values in the solar chimney and shunt duct in building model [case-1A] are shown here.

Example: solar chimney [case-1A] loss factor calculation and determining C_{di} for flow patterns in the TRNSYS-TrnFlow model

The design air velocity in the solar chimney is: Q_v / (W•D) = 4 / (7x0,65) = 0,88m/s. To determine the loss factor at design speed in the chimney the wall roughness is chosen as k_0=4,5x10^{-5} corresponding with aluminum. With this data the loss factor can be calculated with equations (5.3), (5.4), (5.5) and (5.6).

- D_h = 4•(WxD) / 2•(W+D) = 1,190m
- Re = ρ•v•D_h / μ = 1,2041 x 0,88 x 1,190 / 1,8x10^{-5} = 78.431
- Friction factor [λ] is determined by solving the explicit Colebrook-White equation in MS-Excel by iteration (5.5) which results in:
  λ = 0,0191
- ζ = λ • l/D_h = 0,0191 x 35,5 / 1,190 = **0,570**

The loss factors in the shunt duct are calculated likewise and the loss factors of inlets at the office, bends and the exhaust are determined from literature such as the 'Der Recknagel (Recknagel et.al, 2011), the 'Handbook for Hydraulic Resistance' (Idelchik, 2005) and ISSO-publicatie 17 (ISSO, 2010)

The C_{di}-values for the 'large opening' type air-links at the office zones are determined by summation of the loss factors in the flow pattern from the inlet at the office up to the exhaust. For example the flow pattern from office zone 4 in figure 12.8 up to the exhaust includes:

- The inlet at the office
- The merging flow loss factor into the shunt duct
- Merging flow loss factors at floors 3,2,1 and 0
- Wall friction in the shunt duct
- Loss factor of the U-turn to the solar chimney
- Wall friction in the solar chimney (ζ = 0,570).

The combined loss factor of this pattern is $\zeta_{4 \rightarrow ex}$ = 3,96 which results in:
$C_{di,4 \rightarrow shunt}$ = 3,96$^{-0,5}$ = 0,503. This value is used as input in TrnFlow for the C_{di}-value of this 'large opening'.

The determination of all loss factors and C_{di}-values used in the building models in this project are given in [Appendix C].

12.4: Pressure drop in the building cases

After determining the loss factors for all elements in the ventilation system of the building cases, the pressure drop at the design air velocity are calculated which sum up to the total pressure drop in the building cases. All building cases have pressure drops per floor around 10Pa. In figure 12.9 the pressure drop in the flow pattern in every floor is given for all building cases modeled in the TRNSYS simulations. Δp_{total} is built up from :

- Δp_{supply} ➔ pressure drop over the flow pattern from air intake up to the center hall zone
- $\Delta p_{interior\ link}$ ➔ pressure drop over the air-link from the Center Hall zone to the Office zones

- $\Delta p_{exhaust}$ ➔ pressure drop over the flow pattern from the office zones all the way through the chimney to the exterior
- Δp_{static}➔ combined pressure drop of the 3 above flow patterns.
- $\Delta p_{dynamic}$ ➔ dynamic pressure drop due to the largest air velocity in the flow pattern
- Δp_{total} ➔ combined pressure drop of $\Delta p_{static} + \Delta p_{dynamic}$

Total pressure loss for [case-0]

Flow patern through:	Δp,supply	Δp,interior link	Δp,exhaust	Δp,static	Δp,dynamic	**Δp,total**
0th floor	5.88	0.45	3.35	9.68	0.27	**9.95**
1st floor	5.87	0.45	2.93	9.25	0.27	**9.52**
2nd floor	5.86	0.45	2.57	8.87	0.27	**9.14**
3rd floor	5.85	0.45	2.38	8.68	0.27	**8.95**
4th floor	5.85	0.45	1.85	8.15	0.27	**8.41**
5th floor	5.85	0.45	1.60	7.89	0.27	**8.16**
6th floor	5.84	0.45	1.40	7.69	0.27	**7.96**
7th floor	5.84	0.45	1.21	7.50	0.27	**7.76**

Total pressure loss for [case-1A]

Flow patern through:	Δp,supply	Δp,interior link	Δp,exhaust	Δp,static	Δp,dynamic	**Δp,total**
0th floor	5.88	0.45	1.82	8.15	0.45	**8.60**
1st floor	5.87	0.45	1.94	8.25	0.45	**8.71**
2nd floor	5.86	0.45	2.03	8.34	0.45	**8.79**
3rd floor	5.85	0.45	2.10	8.40	0.45	**8.86**
4th floor	5.85	0.45	2.16	8.45	0.45	**8.91**
5th floor	5.85	0.45	2.19	8.49	0.45	**8.94**
6th floor	5.84	0.45	2.22	8.51	0.45	**8.96**
7th floor	5.84	0.45	2.24	8.53	0.45	**8.99**

Total pressure loss for [case-1B]

Flow patern through:	Δp,supply	Δp,interior link	Δp,exhaust	Δp,static	Δp,dynamic	**Δp,total**
0th floor	5.88	0.45	3.13	9.46	0.31	**9.76**
1st floor	5.87	0.45	2.83	9.14	0.31	**9.45**
2nd floor	5.86	0.45	2.56	8.87	0.31	**9.18**
3rd floor	5.85	0.45	2.34	8.64	0.31	**8.95**
4th floor	5.85	0.45	1.79	8.08	0.31	**8.39**
5th floor	5.85	0.45	1.49	7.79	0.31	**8.09**
6th floor	5.84	0.45	1.55	7.85	0.31	**8.15**
7th floor	5.84	0.45	1.53	7.82	0.31	**8.13**

Total pressure loss for [case-2A]

Flow patern through:	Δp,supply	Δp,interior link	Δp,exhaust	Δp,static	Δp,dynamic	**Δp,total**
0th floor	5.88	0.45	2.69	9.02	0.60	**9.62**
1st floor	5.87	0.45	2.81	9.13	0.60	**9.73**
2nd floor	5.86	0.45	2.90	9.21	0.60	**9.81**
3rd floor	5.85	0.45	2.97	9.28	0.60	**9.88**
4th floor	5.85	0.45	3.03	9.32	0.60	**9.92**
5th floor	5.85	0.45	3.07	9.36	0.60	**9.96**
6th floor	5.84	0.45	3.09	9.38	0.60	**9.98**
7th floor	5.84	0.45	3.11	9.40	0.60	**10.00**

Table: 12.9: Pressure drop in the flow patterns for all cases modeled in TRNSYS.

12.5: operation of ventilation the system

The ventilation openings in the building models are not set to control the amount of air flow to maintain even air flows in the building because an 'flow controller' type of air-link does not allow two-way air flow during one time step. However, the inlets at the air supply plenum

and the exhaust openings at the chimneys are controlled to open and close the building ventilation system during and outside occupation.
The exhaust openings are time controlled in the TrnFlow-module by the workday time schedule described in the boundary conditions. They are only opened during occupation in order to not cool down the building unnecessarily which would result in high heating demand.
The inlet openings are controlled with a time schedule and a pressure check. The pressure check is constructed by using the current pressure difference output in the inlet air-links from type56b, the building module, as input in type2b, an iterative controller. This controller checks if the differential pressure is positive. The output from the type2b controller is combined with a workday time schedule produced by two type14h forcing functions in the simulation studio. The two outputs are combined in a calculator to create an on/off signal for the inlet openings which is used as input in the inlet 'large opening' air-links in the building model. In a later study model this inlet control system is extended with a night ventilation switch to evaluate the effect of night ventilation on cooling demand in the cooling season. This system and the results are described in paragraph 23.4.

12.6: simulation boundary conditions

The parameters for simulation are:

- Simulation time step ➔ 10min.
- Maximum iterations per time step in the building module, type56b ➔ 100
- Simulation time ➔ 0 to 8760h (one year)
- Solution method ➔ successive substitution
- Minimum relaxation factor ➔ 1
- Maximum relaxation factor ➔ 1
- Equation solver ➔ 0
- Tolerance integration ➔ 0,001
- Tolerance convergence ➔ 0,001

The parameters for the internal solver of type56b, the building module, are:

- Comis output / Time step ➔ 1
- Altitude of building ➔ 0m
- Height of meteo pylon ➔ 10m
- Altitude of meteo station ➔ 0m
- Wind velocity profile at meteo station ➔ 0,14 (open terrain without obstacles)
- Tolerance for internal iterations ➔ 0,01
- Maximum internal iterations ➔ 150
- Minimum relaxation factor ➔ 0,1

The parameters in the TrnFlow module in type56b are:

- Wind velocity profile at building ➔ 0,226 (sub urban landscape)

Chapter 13: Post simulation data processing

The output of a TRNSYS-TrnFlow simulation is typically a sheet with the desired outputs for every time step in the simulation time, in this project one year from January 1st to December 31st. The type of output is data that has to be processed in MS-Excel to obtain meaning full information. This chapter describes the manner in which the raw output from the simulations is processed to results.

13.1: Volume flow assessment

In the building simulation in TRNSYS-TrnFlow the mass flow through all air-links is marked as output to MS-Excel. The mass flow output from TRNSYS is given in [kg/h] for each time step which is recalculated in MS-Excel to [m^3/s]. The minimum, maximum, average volume flow and the relative standard deviation during occupation are determined.
To evaluate the statistic distribution volume, the number of hours is evaluated in which Q_v>-2,0m^3/s up to Q_v>1,5m^3/s with intervals of 0,1m^3/s. To asses if an office floor is sufficiently ventilated the specific case of Q_v>0,5m^3/s is expressed in percentage of occupation for every floor and for the entire building model. This concludes for which percentage of occupation the building is sufficiently ventilated and offers a quick way to compare the effectiveness of the individual cases to each other.

13.2: Fan energy assessment

The main question in this project is how much fan energy can be saved by the natural ventilation components applied in the building models. To assess this, the fan energy consumption of the building models is calculated in data post-processing in MS-Excel. The fan energy consumption calculation is based on how much air is already flowing through the building and how much is to be forced through additionally by use of auxiliary fans. As described in paragraph 13.1, the actual volume flow for every time step is known as wall as the amount of hours in which volume flow exceeds a certain value. With equation (6.1) the amount of energy needed to drive the needed extra air through the office floors is calculated per time step and summed per floor, per office wing and per total building model. This is compared to the amount of fan energy needed if no driving pressure was at hand in the building which corresponds to a 100% mechanically ventilated building.
The combined efficiency of the auxiliary fans and electric engines necessary in the building is assumed to be 40%. The fan efficiency used in the calculations is therefore η_{fan}=0,4 which corresponds to the efficiency of low pressure radial fans.

13.3: Heating and cooling demand assessment

The energy efficiency of the building regarding heating and cooling is evaluated in order to compare the building models with the building practice and assess if the designed models are energy efficient. While heating and cooling demand is a large expense the models have to be comparable to current building practice regarding heating and cooling in order to make the investments in natural ventilation and fan energy saving worthwhile.
The heating and cooling output per zone in the TRNSYS-TrnFlow models is marked used as output data for MS-Excel for every time step. The output of heating and cooling power in the models is given in kJ/hr for every time step. The total energy demand is retrieved by summing the heating and cooling for the whole year in kWh. This is done for the total building and for the building zones of a number of representative floors. These are the top and bottom floor and floors 3 and 5.
The heating and cooling demand is also expressed in kWh/m^2 GFA annually and natural gas consumption for heating in m^3/m^2 GFA annually. This is done to compare the models with other buildings on the basis of specific demand per square meter.

13.4: Thermal comfort assessment

The thermal comfort of the building models in the project is assessed by using the comfort output function in the type56b building module in TRNSYS. The PPD output is retrieved in MS-Excel for every occupied zone together with the operative temperature in the zones. With use of the GTO-method the weighted temperature exceedance hours over one year are calculated for each occupied zone.

For every time step the weighted temperature exceedance is determined. This is done by with equations:

$GTO_{timestep} = (T_{op} – 25{,}5°C) \times (PPD/10) / 6$ ➔ temperature exceedance

$GTO_{timestep} = (20°C - T_{op}) \times (PPD/10) / 6$ ➔ temperature undershoot

The GTO per time step is divided by 6 because of the simulation time step of 10 minutes. The totality of GTO hours per occupied zone is then calculated by summing all time steps during occupation.

While occupation hours in this building model total 3132 hours, the GTO limit is 3132 x 5% x 1,5 = 236h for each individual occupied zone.

13.5: Assessment of the contribution of the driving ventilation components

The driving ventilation components in the building models such as the supply inlet, the solar chimney and shunt duct, the small 'venturi' exhaust and the 'venturi' roof, all have their own specific contribution to the driving pressure in the ventilation system. In order to assess them individually, the driving forces are calculated from the simulation output data in MS-Excel.

The occurring pressure in the driving components is calculated for every time step from which the minimum, maximum, average and standard deviation during occupation are derived. In addition the percentage of occupation in which Δp of the component is larger than: 0Pa, 5Pa, 10Pa and 20Pa is derived.

- Solar chimney contribution is calculated with:
  - Air temperature in the chimney zones
  - External air temperature
  - Height of the chimney
- Shunt duct contribution with:
  - Air temperature in the shunt duct zones
  - Air temperature in the office zones adjacent to the shunt duct zone
  - Height difference of the air-link at the respective office and the bottom of the shunt duct
  - This contribution is most of the time very small as the shunt duct temperature is an average of all office temperatures.
- Solar chimney + shunt duct contribution per office floor with:
  - Solar chimney contribution
  - Shunt duct contribution of the respective floor
- Solar contribution to the solar chimney stack pressure: (figure 21.3)
  - stack pressure in the solar chimney (solar chimney contribution)
  - minus stack pressure calculated with the difference between air temperature in the shunt duct zone and external air temperature
  - The 'solar' contribution can also be negative when $T_{chim} < T_{shunt}$
- Supply shaft contribution with:
  - External air temperature
  - Air temperature in the supply shaft zone
  - Height difference of the air-link at the respective Center Hall zone and the inlet opening at the supply plenum at the roof.
- Inlet plenum contribution
  - Wind pressure on all three openings combined, if opened.

- Exhaust openings contribution in all cases.
    - Wind pressure on each individual opening during occupation
- Wind contribution
    - Inlet plenum contribution
    - Exhaust opening contribution

Part 6: Results, Discussion and Conclusions on the simulations

The results for each building case involve the occurring volume flow per office floor, the driving pressures of the wind and in the chimneys, thermal comfort, energy demand for heating and cooling and the fan energy consumption for each case. Finally the cases are compared after which the fan energy savings due to the solar chimneys and the 'venturi' roof can be obtained. And conclusions can be drawn.

For each building simulation model the results are given for:

- Average volume flow per floor per wing [m^3/s].
  The required flow for fresh air supply is $0,5m^3/s$ per floor per wing.
- Relative standard deviation of the average volume flow [%]
- Percentage of occupation time with $Q_v > 0,5m^3/s$ [%], part of occupation in which an office floor can be ventilated without auxiliary fans.
- GTO-hours for the Center Hall zones and the maximum per floor of the Office zones.
  The GTO requirement is determined by:
    - Annual occupation time x 5% x 1,5 weighting. For this project the GTO requirement per building zone is:
      GTO < 3132h x 5% x 1,5 = 236h
- Average total driving pressure averaged over all office wings [Pa]
- Relative standard deviation of the average total driving pressure [%]
- The relative contribution to the total driving pressure of:
    - Buoyancy minus solar contribution in the solar chimneys
    - Wind pressure
    - Solar contribution in the solar chimneys
- Heating and cooling demand
- Fan energy consumption

For the different driving ventilation components used in the building models the performance is analyzed on:

- Driving pressures in the ventilation component
    - Average driving pressure [Pa]
    - Minimum, maximum and relative standard deviation
    - Percentage of occupation time with exceedance of 0Pa, 5Pa, 10Pa and 20Pa

In [Appendix D] the full results for all research cases and the final case are gathered

Furthermore the results and conclusions are given concerning three additional simulation runs of [case-2A] placed in different climates in Europe to investigate the climate influence on the performance of solar chimneys.
To evaluate the behavior of an internal chimney plus shunt duct and compare it to a solar chimney plus shunt duct, another simulation, [case-1S], was ran in which the glass in the chimney is replaced by opaque façade material as in the rest of the building model façades.

Chapter 14: Average air flow in the building cases

14.1: [case-0]

Results for the reference case with conventional, partitioned chimneys and conventional exhausts.

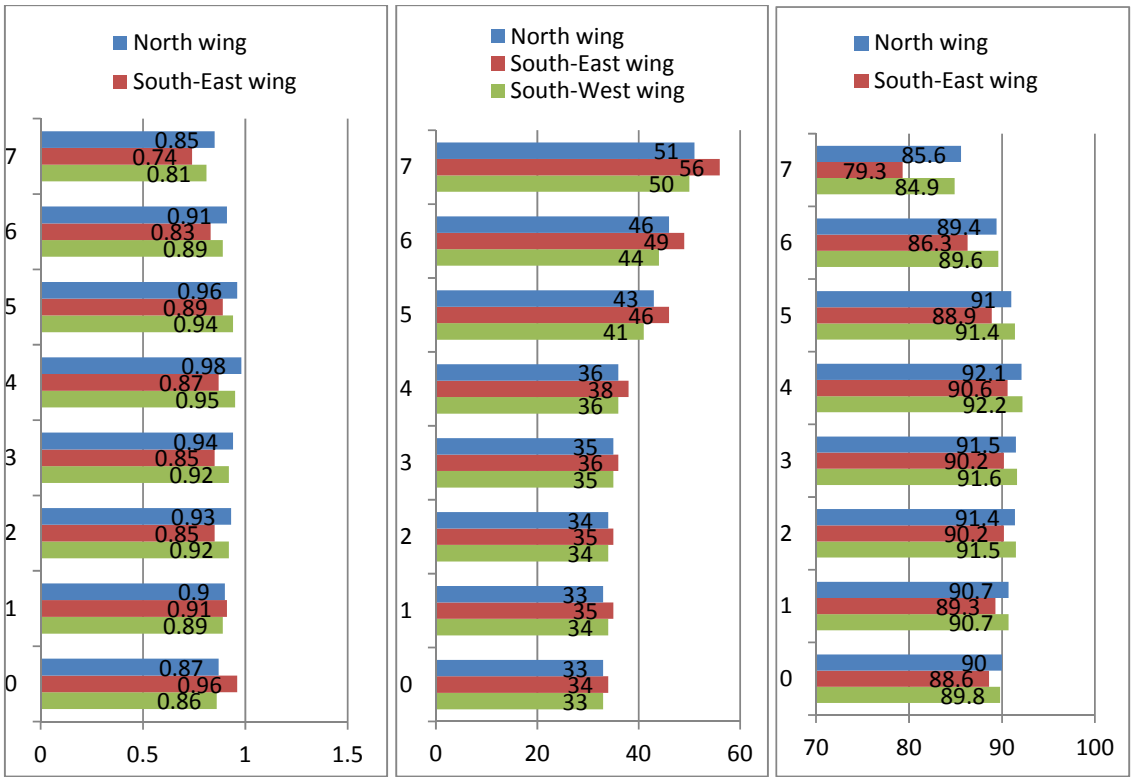

Figure 14.1: a) average volume flow per office floor b) relative standard deviation per office floor, c) percentage of occupation $Q_v > 0{,}5 m^3/s$ per office floor

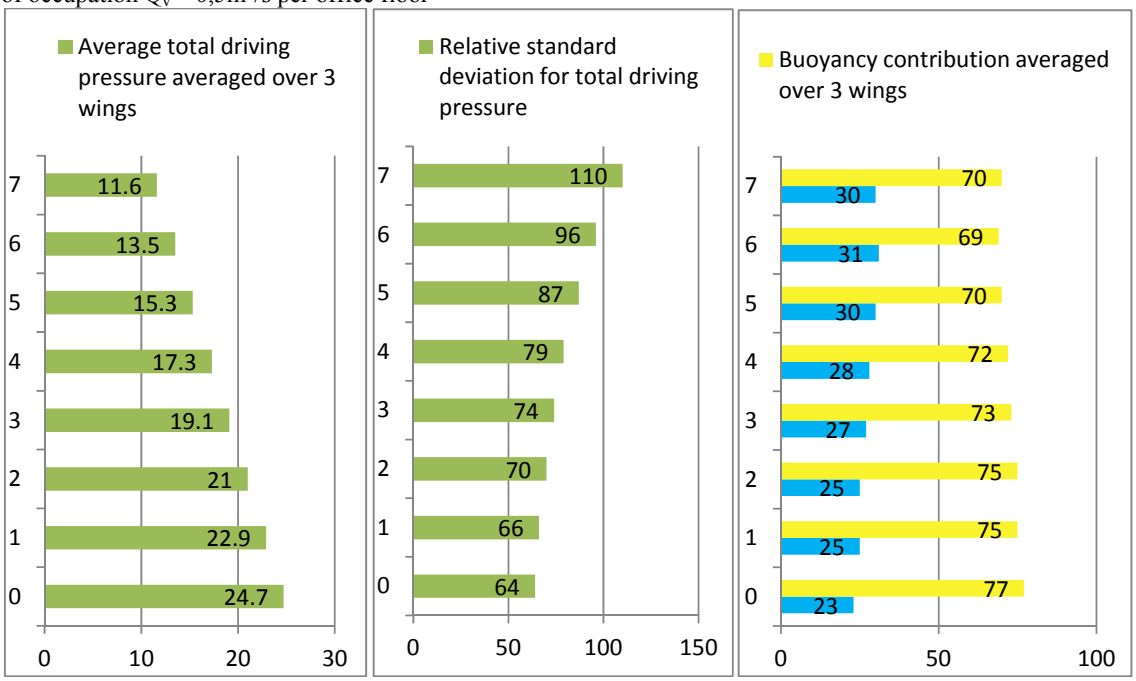

Figure 14.2: a) average total driving pressure per office floor averaged over all 3 wings, b) relative standard deviation of total driving pressure, c) relative contribution of wind and buoyancy to total driving pressure

14.2: [case-1A]

Results for the building model with solar chimneys plus shunt duct and conventional exhausts.

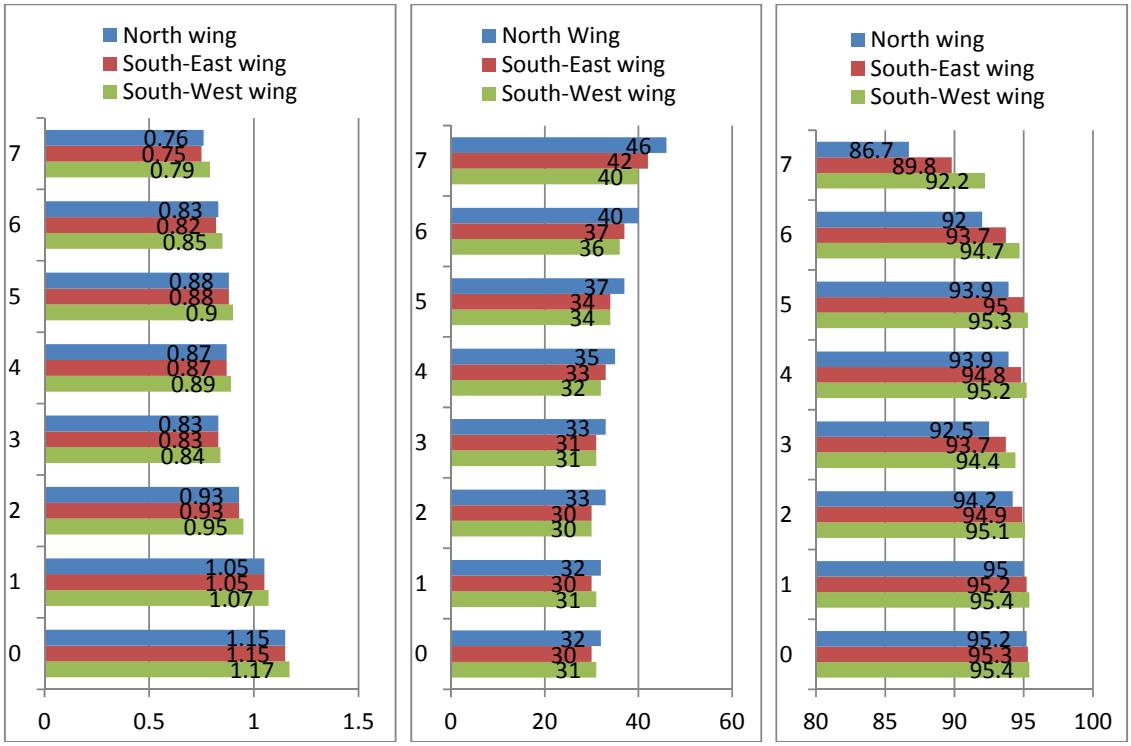

Figure 14.3: a) average volume flow per office floor b) relative standard deviation per office floor, c) percentage of occupation $Q_v > 0{,}5 m^3/s$ per office floor

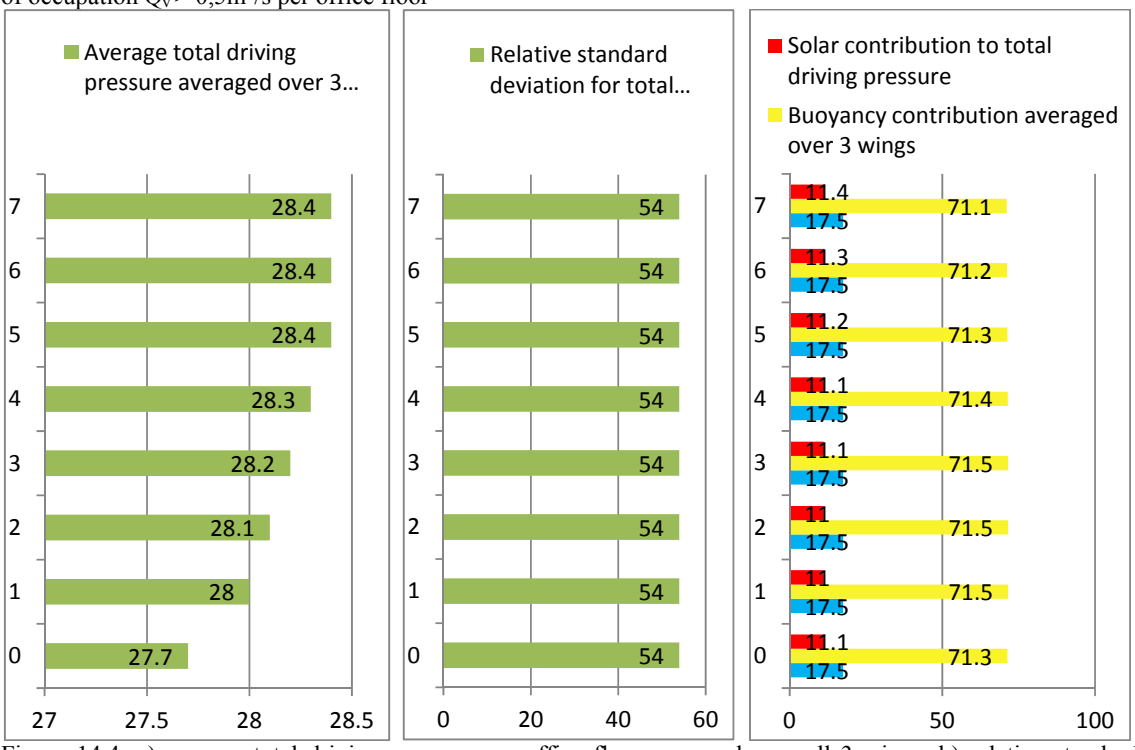

Figure 14.4: a) average total driving pressure per office floor averaged over all 3 wings, b) relative standard deviation of total driving pressure, c) relative contribution of wind and buoyancy to total driving pressure

14.3: [case-1B]

Results for the building model with partitioned solar chimneys with conventional exhausts.

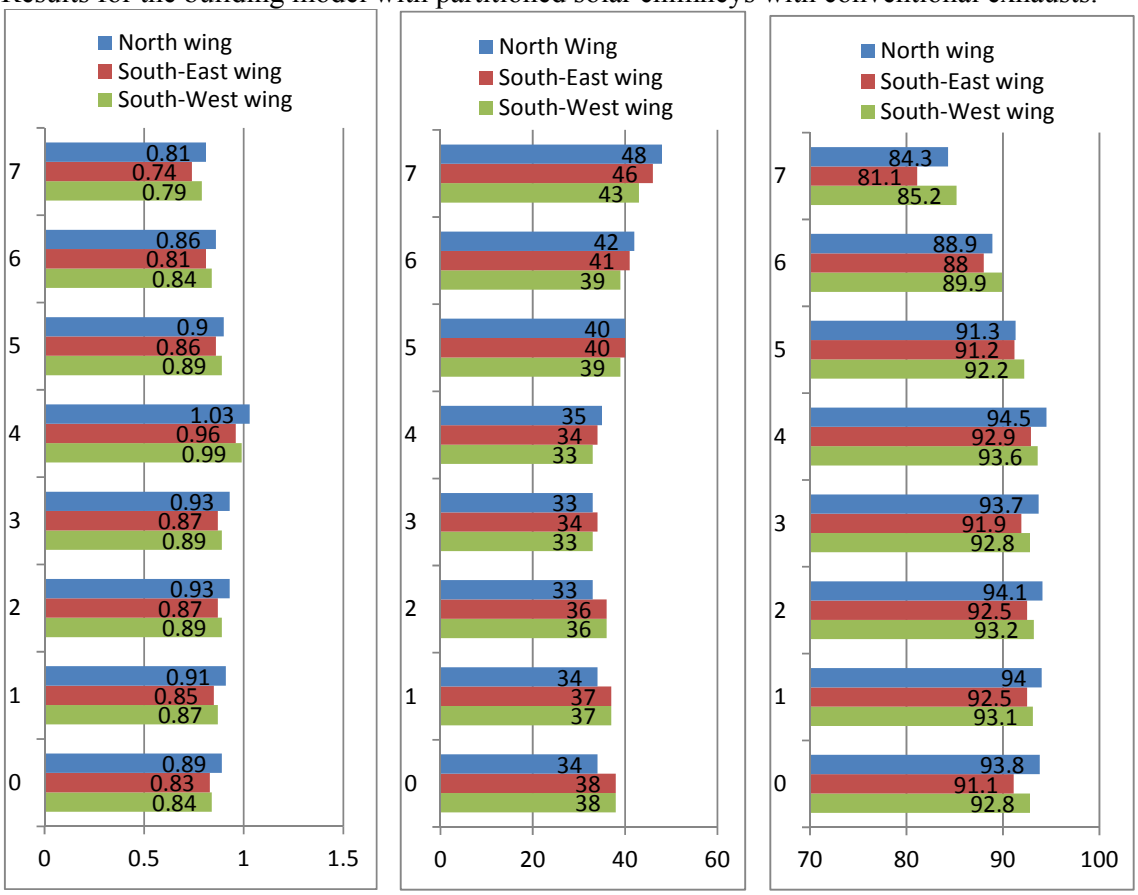

Figure 14.5: a) average volume flow per office floor b) relative standard deviation per office floor, c) percentage of occupation $Q_v > 0{,}5 m^3/s$ per office floor

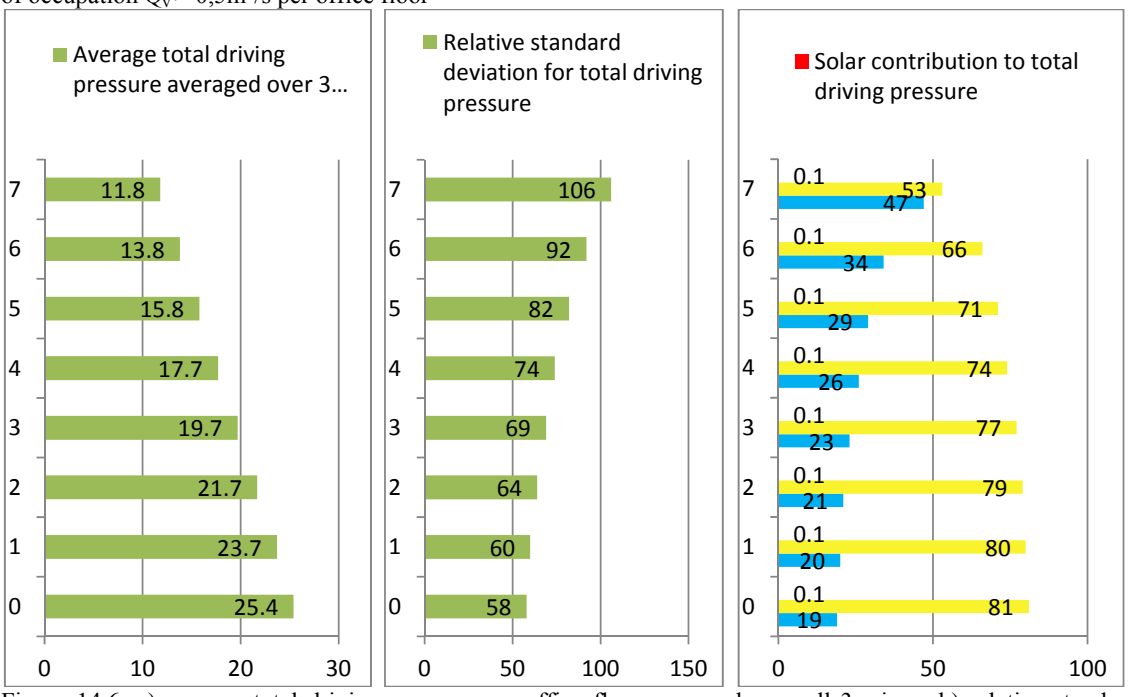

Figure 14.6: a) average total driving pressure per office floor averaged over all 3 wings, b) relative standard deviation of total driving pressure, c) relative contribution of wind and buoyancy to total driving pressure

14.4: [case-2A

The results for the final design with solar chimneys plus shunt duct with one central 'venturi' roof exhaust.

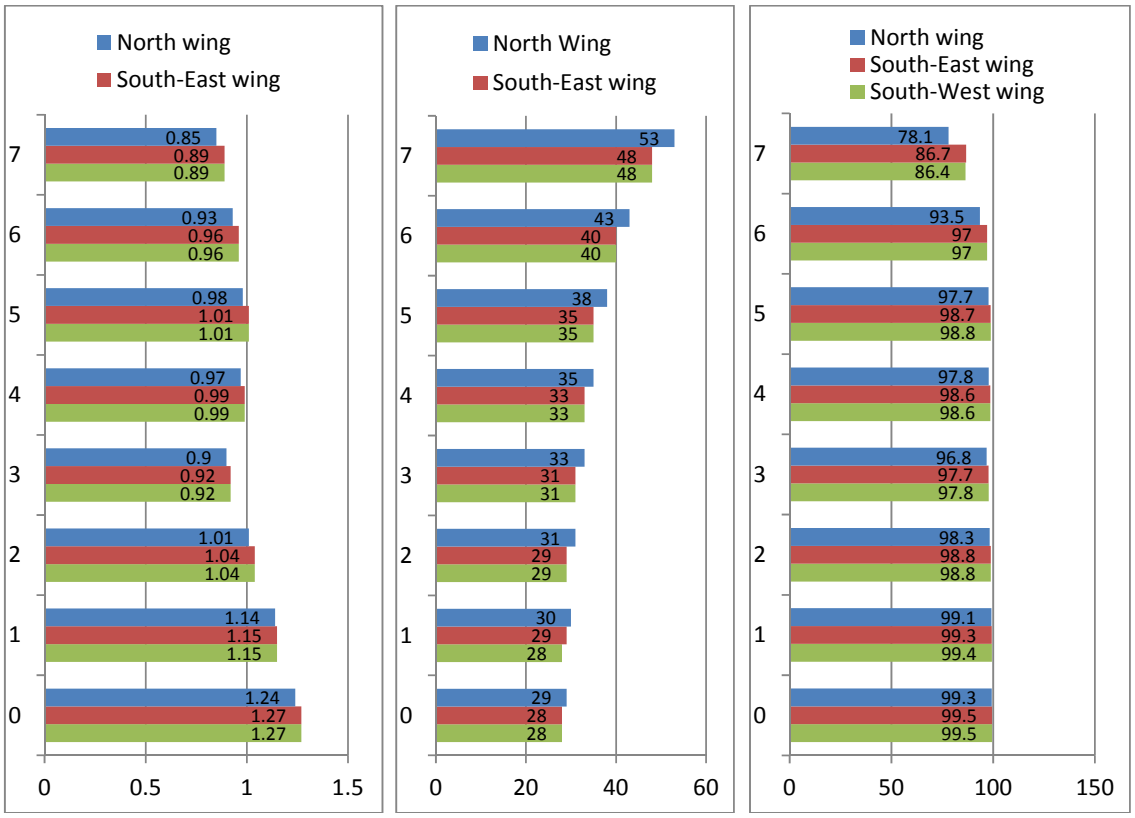

Figure 14.7: a) average volume flow per office floor b) relative standard deviation per office floor, c) percentage of occupation $Q_v > 0{,}5 m^3/s$ per office floor

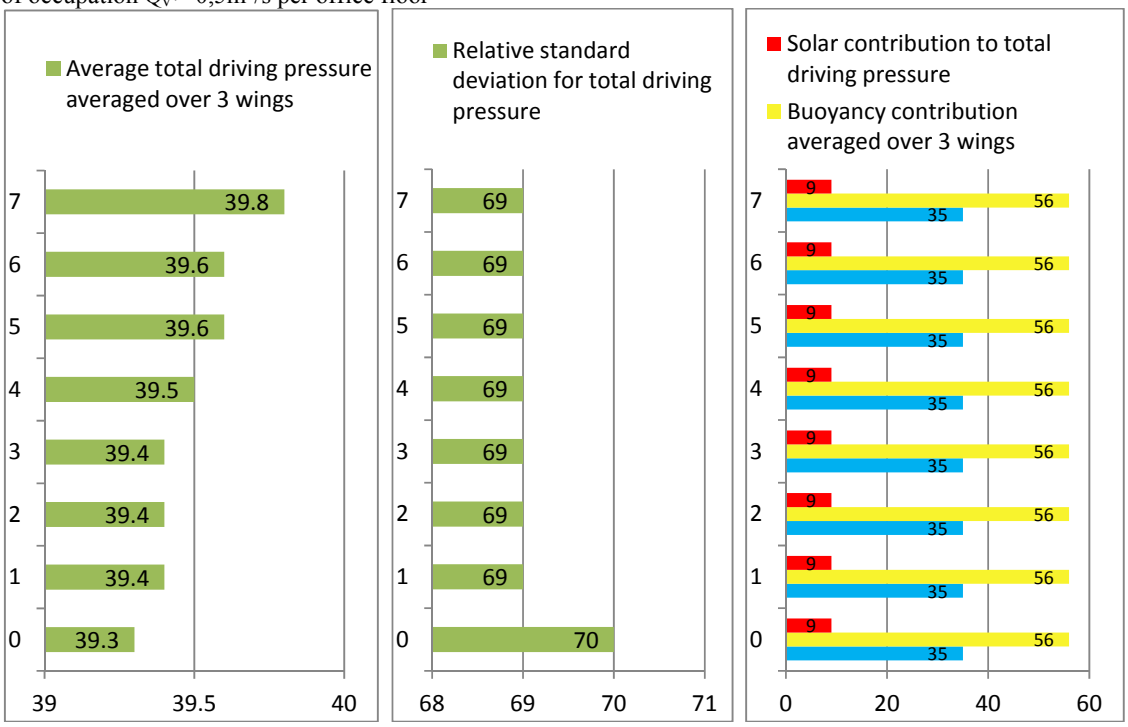

Figure 14.8: a) average total driving pressure per office floor averaged over all 3 wings, b) relative standard deviation of total driving pressure, c) relative contribution of wind and buoyancy to total driving pressure

14.5: [case-1S], non-solar chimney plus shunt duct

Results for the building model with non-solar chimneys plus shunt duct. This is meant to clarify if it is possible to construct an internal chimney with shunt duct in order to generate even stack pressure over all floors in the building and still have better performance than with conventional partitioned chimneys as in [case-0].

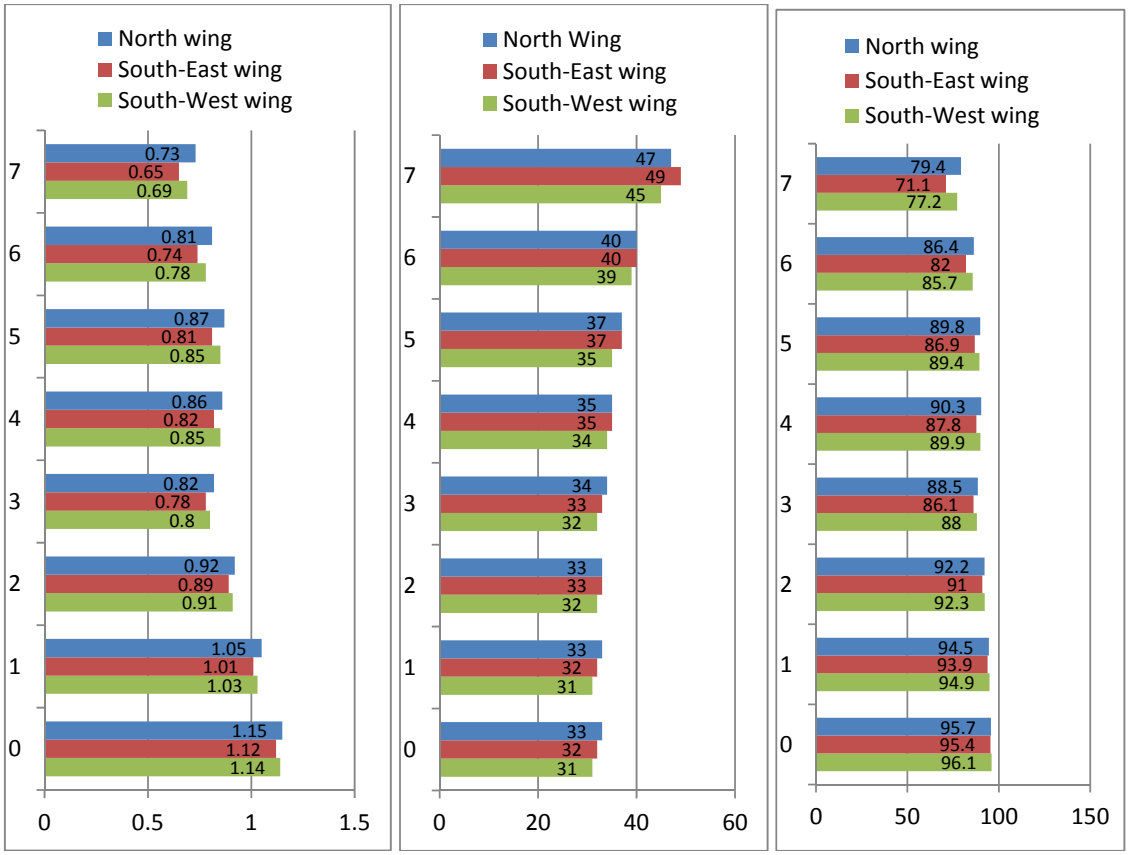

Figure 14.9: a) average volume flow per office floor b) relative standard deviation per office floor, c) percentage of occupation $Q_v > 0{,}5 m^3/s$ per office floor

14.6: Discussion on average volume flow

Of the building cases with conventional exhausts: [case-0], [case-1A] and [case-1B], [case-1A] has the best performance. This implies that the solar chimney plus shunt duct delivers the most stack pressure and is the most effective solar chimney configuration.

In [case-2A] with solar chimneys plus shunt duct and 'venturi' roof exhaust, the South-East and South-West wing have similar average ventilation rates and are both ventilated sufficiently for 97% of occupation. The performance in the North office wing is worse which can only be subscribed to the orientation of the solar chimney as all three wings are exhausted through the 'venturi' roof which creates the same under pressure for every wing.

This implies that solar chimney in the North wing with West orientation creates less stack pressure on average than the solar chimneys in the two other wings which have multiple orientations ranging from South-East to South-West orientation.

Figure 14.10: average volume flow and % of occupation with sufficient ventilation										
	[case-0]		[case-1B]		[case-1A]		[case-2A]		[case-1S]	
	Q_v avg. [m^3/s]	sufficient vent. [%]	Q_v avg. [m^3/s]	sufficient vent. [%]	Q_v avg. [m^3/s]	sufficient vent. [%]	Q_v avg. [m^3/s]	sufficient vent. [%]	Q_v avg. [m^3/s]	sufficient vent. [%]
North wing	0,92	90,2	0,91	91,8	0,91	92,9	1,00	95,1	0,90	89,6
South-East wing	0,86	88,0	0,85	90,4	0,91	94,1	1,03	97,0	0,85	86,8
South-West wing	0,90	90,2	0,88	91,6	0,91	94,7	1,03	97,0	0,88	89,2
Total case	**0,89**	**89,5**	**0,88**	**91,2**	**0,93**	**93,9**	**1,02**	**96,4**	**0,88**	**88,5**

[case-1S] was meant to investigate if a non-solar chimney plus shunt duct will work. The time in which [case-1S] is sufficiently ventilated is with 88,5% lower than in [case-0] with 89,5%. This suggests that a non-solar chimney with shunt duct is not better then a non-solar chimney without shunt duct. This points towards the conclusion that the temperature in the chimney has to be higher than in the shunt duct in order to "pull" the air flow down in the shunt duct. The solar irradiation in the solar chimney provides this extra temperature in [case-1A] and [case-2A]. After the air from the shunt duct reaches the solar chimney due to the extra buoyancy in the solar chimney created by the sun, the positive effect of the shunt duct is reached which provides every floor with an equal stack pressure in the chimney.

Chapter 15: Driving pressure of ventilation components

The driving pressure of each ventilation component in the different building models is evaluated as described in paragraph 13.5. For every component the average, minimum, maximum and relative standard deviation is determined. Also the percentage of occupation in which driving pressure exceeds: 0Pa, 5Pa, 10Pa and 20Pa is given. (figure 15.1)

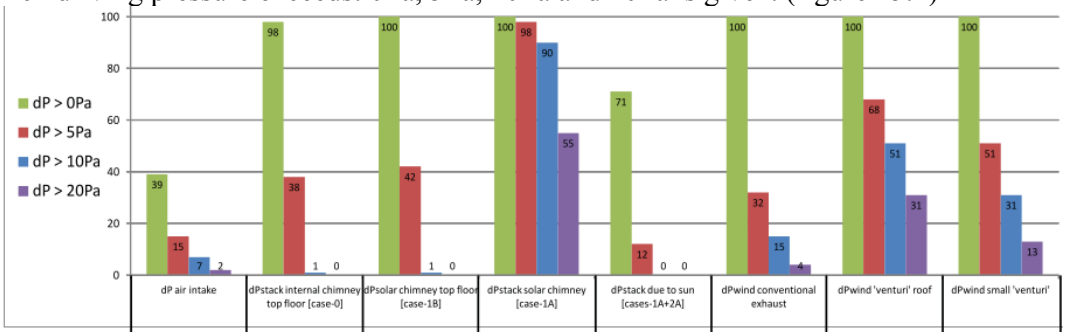

	dP air intake	dPstack internal chimney top floor [case-0]	dPsolar chimney top floor [case-1B]	dPstack solar chimney [case-1A]	dPstack due to sun [cases-1A+2A]	dPwind conventional exhaust	dPwind 'venturi' roof	dPwind small 'venturi'
Δp minimum [Pa]	-103	-3.1	-0.4	-1.1	-2.8	-92.2	-229.0	-108.6
Δp maximum [Pa]	83	11.3	11.4	53.0	11.0	0.0	0.0	0.0
Δp average [Pa]	**0.1**	**4.3**	**4.6**	**21.8**	**1.8**	**-5.0**	**-18.3**	**-9.2**
RSD[%]	7289	55	46	43	137	-134	-126	-125

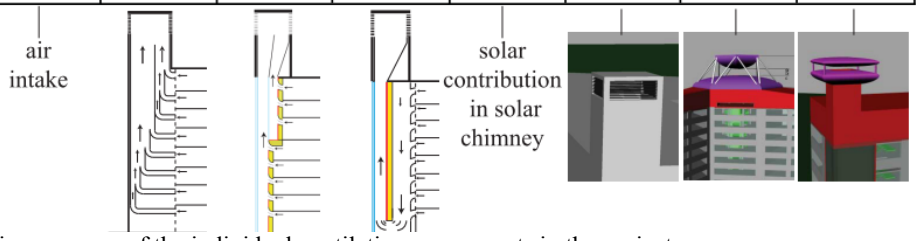

Figure 15.1: driving pressure of the individual ventilation components in the project

15.1: Discussion and conclusion on exhaust types

The pressure contribution of the three exhaust types is linearly comparable with the wind pressure coefficient of the exhaust types. With C_p=-1,33 the average pressure in the 'venturi' roof exhaust is -18,3Pa while the small 'venturi' exhaust with C_p=-0,7 has an average driving pressure of -9,2Pa. A 'venturi' roof creates a great amount of under pressure to drive ventilation in the building but the structure of this exhaust type has a big impact on the total building structure and appearance of the building. The small 'venturi' exhaust still creates significantly larger under pressure than the conventional exhaust in this project, but has far less impact on the total building than the 'venturi' roof does. The implication of one of the 'venturi' type exhausts hence will be a compromise between investment and performance which has to be dealt with by designers.

15.2: Discussion on chimney configuration

The partitioned solar chimney in [case-1B] barely improves stack pressure in the critical top floor compared to the non-solar partitioned chimney in [case-0] as can be seen in the average driving pressure of 4,6Pa compared to conventional chimney with 4,3Pa. This implies a solar contrition of only 0,3Pa on average in the top floor.

The solar chimney plus shunt duct in [case-1A] and [case-2A] provide an even stack pressure in the chimney and shunt duct configuration for every floor. Hence the driving stack pressure for the top floor in [case-1A] and [case-2A] is significantly larger than the stack pressure in the top floor for [case-0] and [case-1B]. The average solar contribution in the solar chimney plus shunt duct is 6 times larger for the top floor with 1,8Pa compared to 0,3Pa in the [case-1B] chimney.

Chapter 16: Conclusion on solar chimney configuration

Regarding the results on average volume flow in the cases and the driving pressure in the individual ventilation components, it can be concluded that a solar chimney plus shunt duct delivers the most stack pressure. The orientation of the chimney is best in the range from South-East to South-West and even better when one chimney has multiple orientations within this range. The solar chimneys in the South-East and South-West wing have this multiple orientation with one side to the South-East and one side to the South west.

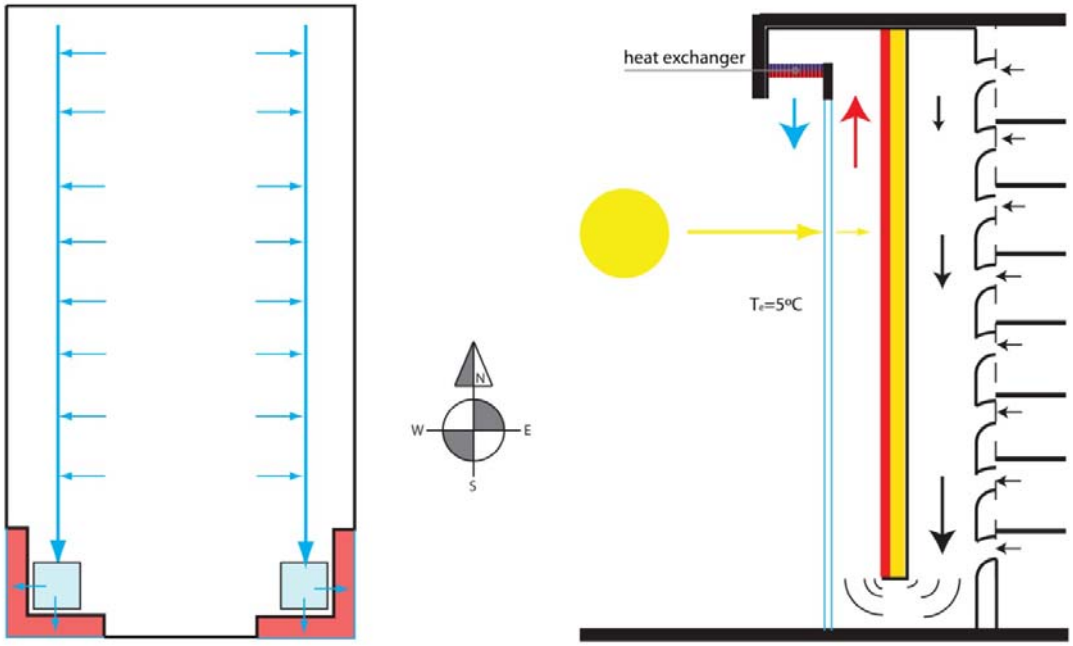

Solar chimney with multiple orientation - withhin range from South-East to South-West

Solar chimney plus shunt duct with heat recovery in the exhaust flow

Figure 16.1: Best solar chimney configuration with multiple orientations

Chapter 17: Thermal comfort

The thermal comfort in the building models is assessed using the GTO-method in order to determine if the climate in the models is acceptable.

Figure 17.1: temperature exceedance GTO-method for [case-0] with GTO_{max} =236h

	0th floor		1st floor		2nd floor		3rd floor		4th floor		5th floor		6th floor		7th floor	
	CH	OFF	CH	OFF	CH	OFF	CH	OFF	CH	OFF	CH	OFF	CH	OFF	CH	OFF
$T_i <$	221	24	451	21	416	22	410	24	632	46	437	22	328	21	387	87
$T_i >$	0	0	0	0	0	0	0	0	0	0	0	0	0	0	0	0

Figure 17.2: temperature exceedance GTO-method for [case-1A] with GTO_{max} =236h

	0th floor		1st floor		2nd floor		3rd floor		4th floor		5th floor		6th floor		7th floor	
	CH	OFF	CH	OFF	CH	OFF	CH	OFF	CH	OFF	CH	OFF	CH	OFF	CH	OFF
$T_i <$	1796	49	4333	28	383	25	89	9	167	45	172	9	102	5	127	60
$T_i >$	0	0	0	0	0	0	0	0	0	0	0	0	0	0	0	0

Figure 17.3: temperature exceedance GTO-method for [case-1B] with GTO_{max} =236h

	0th floor		1st floor		2nd floor		3rd floor		4th floor		5th floor		6th floor		7th floor	
	CH	OFF	CH	OFF	CH	OFF	CH	OFF	CH	OFF	CH	OFF	CH	OFF	CH	OFF
$T_i <$	211	115	348	64	292	31	329	21	836	51	346	28	224	19	322	77
$T_i >$	0	0	0	0	0	0	0	0	0	0	0	0	0	0	0	0

Figure 17.4: temperature exceedance GTO-method for [case-2A] with GTO_{max} =236h

	0th floor		1st floor		2nd floor		3rd floor		4th floor		5th floor		6th floor		7th floor	
	CH	OFF	CH	OFF	CH	OFF	CH	OFF	CH	OFF	CH	OFF	CH	OFF	CH	OFF
$T_i <$	2134	89	1715	53	659	21	328	14	498	30	589	14	564	15	705	63
$T_i >$	0	0	0	0	0	0	0	0	0	0	0	0	0	0	0	0

17.1: Discussion and conclusion on thermal comfort

GTO exceeds the limit of 236 hours annually in almost every Center Hall zone due to temperature undershoot. This is mainly due to the fact that the volume flow in the model is not tempered at the minimum required ventilation rate. Hence the ventilation rates can be very large when driving pressure in the model is high. With high ventilation rates the heating demand increases as the heating system has to heat up 6 times more air than needed when the ventilation rate is 6 times the required rate. The maximum air flow occurring in [case-2A] is 3,3m^3/s which is about 6 times higher than the required 0,5 m^3/s. This stresses the heating capacity and apparently leads to temperature undershoot. In practice volume flow will be tempered and this problem will not occur.

Chapter 18: Heating and cooling

The heating and cooling demand of the building models is determined to assess if they are comparable with building practice. If a building model saves a significant amount of fan energy but the heating and cooling demands is far larger than in building practice because of it, the fan energy saving could be outweighed and not worthwhile. That is why the heating and cooling demand should be at least comparable, or favorably lower than in building practice.

18.1: Heating and cooling demand results

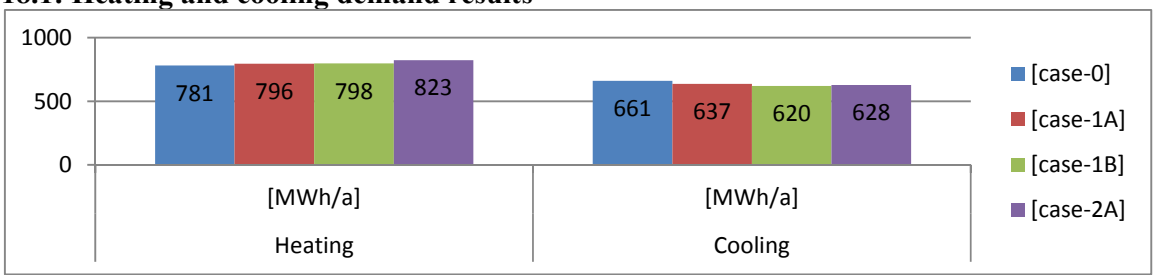

Figure 18.1: Total annual heating and cooling demand for the building cases expressed in output energy, hence not primary energy

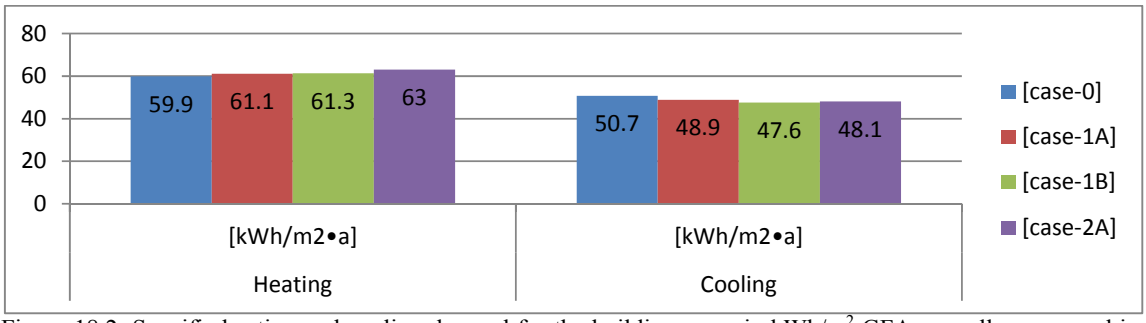

Figure 18.2: Specific heating and cooling demand for the building cases in kWh/m^2 GFA annually expressed in output energy, hence not primary energy

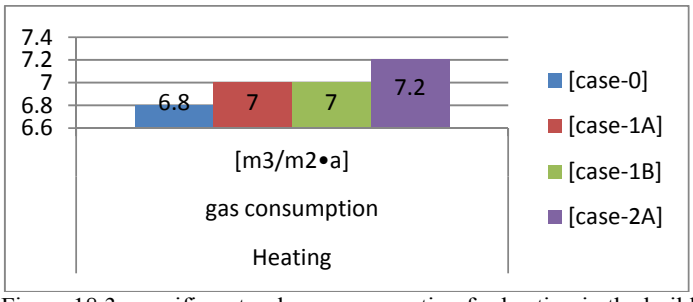

Figure 18.3: specific natural gas consumption for heating in the building cases.

18.2: Discussion on heating and cooling demand

In the comparison of the cases regarding heating and cooling energy, a relation between average volume flow in the building and heating demand is clear. [case-2A] with high average ventilation rate per floor of Q_v=1,02m^3/s, has an increased heating demand compared to [case-0] which has a lower average ventilation rate per floor of Q_v=0,89m^3/s. This confirms the explanation given in paragraph 15.1 for the high GTO scores indicating temperature undershoot which increases with high ventilation rate. This also indicates that with volume flow control at Q_v=0,50m^3/s per floor, the heating demand in the building can be significantly decreased as the average ventilation rate in [case-2A] is 2 times higher than required.

18.3: Conclusion on heating and cooling demand

The heating demand in [case-2A] as modeled with 'free running' volume flow without volume control uses 7,2m^3 natural gas per m^2 GFA. A reference office building from 2005 in The Netherlands uses 15m^3/m^2 (Senter Novum, 2007). This implies that the heating demand in the building models is lower than the average building in The Netherlands. Hence the effect of the fan energy saving due to natural ventilation is not outweighed by increased heating demand and therefore worthwhile in this sense.

Chapter 19: Fan energy consumption

The fan energy consumption for every case is calculated in post simulation data processing as described in paragraph 13.2. In figure 19.1 the percentage of time in which the building cases are sufficiently ventilated by natural driving forces are given to obtain a quick comparison. The actual fan energy savings of the cases is given and compared to the energy consumption for the specific cases if they were 100% mechanically ventilated. The data shows the electrical energy consumption of the fans as output energy, hence not the primary energy consumption.

Figure 19.1: Annual fan energy consumption in building cases

	[case-0]	[case-1B]	[case-1A]	[case-2A]
$Q_v > 0{,}5 m^3/s$ [%]	89,5	91,2	93,9	96,4
Energy consumption for 100% mechanical ventilation [kWh/a]	824,2	743,9	823,5	926,9
Energy consumption for actual case [kWh/a]	24,8	16,7	23	10,6
Energy savings relative to 100% mechanical drive [kWh/a]	799,4	727,2	800,5	916,3
Energy savings relative to 100% mechanical drive [%]	97,0	97,8	97,2	98,9
Energy savings relative to reference [case-0] [kWh]	-	7,5	8,1	14,2

The absolute energy savings in the building cases are low with 916,3kWh annually in [case-2A]. This is largely due to the fact that the reference is 100% mechanical ventilation of the case itself. Due to the very low pressure drop of 10Pa in the system the largest fan energy saving is caused by this low pressure drop system with large ducts. The energy consumption of the building cases should be compared with that of buildings with a higher pressure drop ventilation systems which are more common in building practice which is done in paragraph 19.1.

19.1: [case-2A] compared with high pressure drop ventilation systems

The [case-2A] fan energy consumption is compared to two buildings with ‘venturi’ roof exhaust and solar chimneys which gives them the same driving pressure. However, the pressure drop in the systems is set to 200Pa and 1.000Pa instead of 10Pa.
These comparisons are obtained with MS-Excel by evaluating the volume flows and after that the fan energy consumption of a 200Pa and a 1000Pa pressure drop in the building using the driving pressures in [case-2A]. In this manner a quick evaluation was made of what the performance of solar chimneys and ‘venturi’-exhaust can be on higher pressure drop ventilation systems.

Figure 19.2: Fan energy consumption in building cases			
	[case-2A]Δp=10Pa	[case-2A] Δp =200Pa	[case-2A] Δp =1.000Pa
$Q_v > 0{,}5 m^3/s$ [%]	96,4	0,2	0
Δp_{drive} top floor [Pa]	39,6	39,6	39,6
Fan energy for 100% mechanical [kWh]	926,9	18.792	93.960
Fan energy [kWh]	10,6	10.635	75.196
Fan energy saving relative to 100% mechanical drive [%]	98,9	43	20

19.2: Discussion and conclusion on fan energy consumption

A further comparison is made with building practice. The specific fan energy consumption of [case-2A] expressed in [kWh/m^2] and [kWh$_{pr}$/m^2] is made with that of Δp=1.000Pa reference. As mentioned in chapter 6, the primary energy needed to generate 1kWh op electrical power used by a terminal appliance is 2,5 times higher than the actual energy consumption in the terminal appliance which are the auxiliary fans in the building. The electrical energy cost of [case-2A] is compared with Δp=1.000Pa reference at an energy cost of **0,25€/kWh** and a building size of **10.000m^2 GFA**.

Figure 19.3: Annual primary and output fan energy consumption and electrical energy cost in a 10.000m^2 GFA office building			
	[case-2A] with 100% mechanical ventilation [Δp=1.000Pa]	[case-2A] with 100% mechanical ventilation [Δp=10Pa]	[case-2A] with driving ventilation components [Δp=10Pa]
Specific primary energy consumption [kWh$_{primary}$/m^2•a]	18,0	0,178	0,002
Specific energy consumption [kWh/m^2•a]	7,2	0,071	0,001
Electrical energy cost per building of 10.000m^2 GFA [€ /m^2]	€ 18.000,-	€ 178,-	€ 2,-

When compared to the fan energy consumption and cost in the Δp=1.000Pa reference case with mechanical ventilation, a system with low pressure loss such as [case-2A] even without the favorable effect of the solar chimney and 'venturi' roof can diminish the annual energy bill almost completely. When the solar chimney and 'venturi' roof are taken into account the energy cost drops even further. This result shows that by far the largest fan energy saving can be obtained by applying a low pressure drop ventilation system.

The difference in fan energy saving of the 10Pa system with and without solar chimneys and 'venturi' exhaust emphasizes the presumption that applying a solar chimney solely for the purpose of reducing fan energy consumption does not make much sense. The implementation of solar chimneys can only be substantiated when the thermal energy from the exhaust air and the solar irradiation are recovered in the chimney. The implementation of heat recovery in the solar chimney is argued in paragraph 24.2

Chapter 20: Climate influence on solar chimney – latitude hypothesis

The performance of a solar chimney is dependent on solar irradiation and external temperature. To investigate the influence of the climate on the performance, the final building model [case-2a] is placed in four places in Europe. The results and conclusions on the latitude hypothesis posed in paragraph 1.3 concerning the performance of vertically orientated solar chimneys on different locations on the globe are given in this chapter.

20.1: External temperature and azimuth influence on stack pressure

The final building design, [case-2A], is placed in four places in Europe to investigate the influence on the solar chimney performance of the average external temperature and azimuth ,or solar angle, to the solar irradiation on a vertical plane. The four locations chosen for this study are: Stockholm in Sweden, de Bilt in The Netherlands, Paris in France and Sevilla in Spain. In Figure 20.1 the results of the four cases are given concerning the stack pressures occurring in all three chimneys in the building model. The chimneys in the South-East and South-West office wing have a similar performance. The chimneys in the North office wing have significantly lower performance due to the West orientation of these chimneys.

Latitude influence on vertical solar chimneys

	Latitude [°North]	T_e avg. [°C]	$T_{chimney}$ average in occupaiton [°C]			Δp_{stack} solar chimney for average floor [Pa]			ΔT between chim and shunt duct [°C]			Solar contribution in Δp_{stack} resulting [Pa]			Solar contribution in Δp_{stack} resulting [%]		
			North	South-East	South-West	North	South-East	South-West	North	South-East	South-West	North	South-East	South-West	North	South-East	South-West
Stockholm Sweden	59.2	6.7	23.8	24.7	24.6	25.7	25.6	25.6	0.77	1.46	1.47	1.0	2.0	2.0	3.9	7.8	7.8
De Bilt Holand	52.1	10.5	24.6	25.3	25.3	20.8	21.8	21.8	0.88	1.53	1.52	1.2	2.1	2.1	5.8	9.6	9.6
Paris France	48.5	12.3	24.7	25.3	25.2	18.1	19	18.9	0.91	1.44	1.43	1.2	2.0	2.0	6.6	10.5	10.6
Sevilla Spain	37.2	19.7	26.9	27.7	27.6	10.4	11.5	11.4	1.71	2.85	2.82	2.3	3.9	3.8	22.1	33.9	33.3

In Figure 20.1 the results of the chimney in the South-East office wing are put along each other. This chimney has a South-East / South-West orientation.

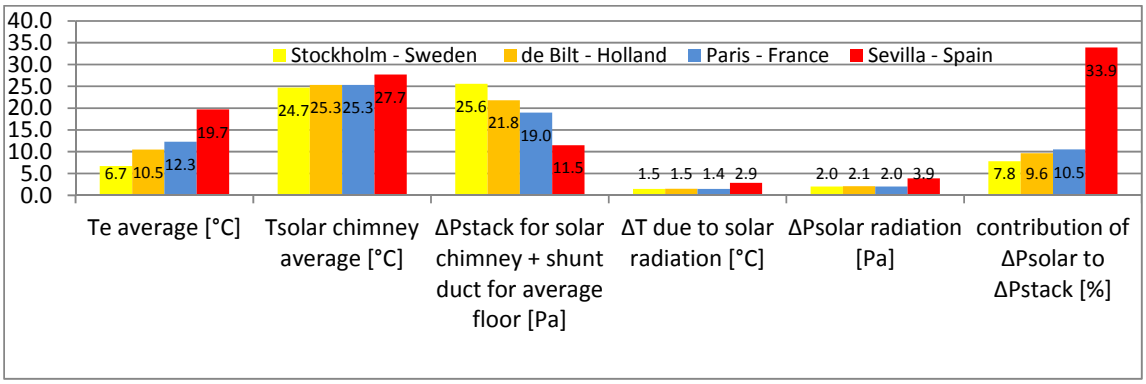

Figure 20.2: Influence of latitude on vertical solar chimneys with South-East / South-West orientation

The conclusion for the hypothesis is that a solar chimney does provide the biggest stack pressure at high latitude due to the lower external temperature. However, lower sun angle at high latitude does result in even solar contribution on the vertical plane for three of four cases. In Sevilla the average solar contribution is 3,9Pa (Figure 20.1) whereas in the other locations it is around 2,0Pa. Hence, except for Spain the lower sun angle compensates the lower general solar power [W/m^2] and results in a similar solar contribution to stack pressure. The higher contribution in Sevilla is probably due to a higher amount of sun hours, hence annual hours with a clear sky.

20.2: Nett heat loss to the exterior through the glass

In winter situations with low external temperature and low solar power the heat loss through the glass plane of the solar chimney can be significant. In case the heat loss through the glass is larger than the heat gain through solar radiation a nett heat loss in the chimney will occur. This results in a lower air temperature in the chimney relative to the interior temperature of the building. When this is the case a negative solar contribution to stack pressure occurs (Figure 20.3).

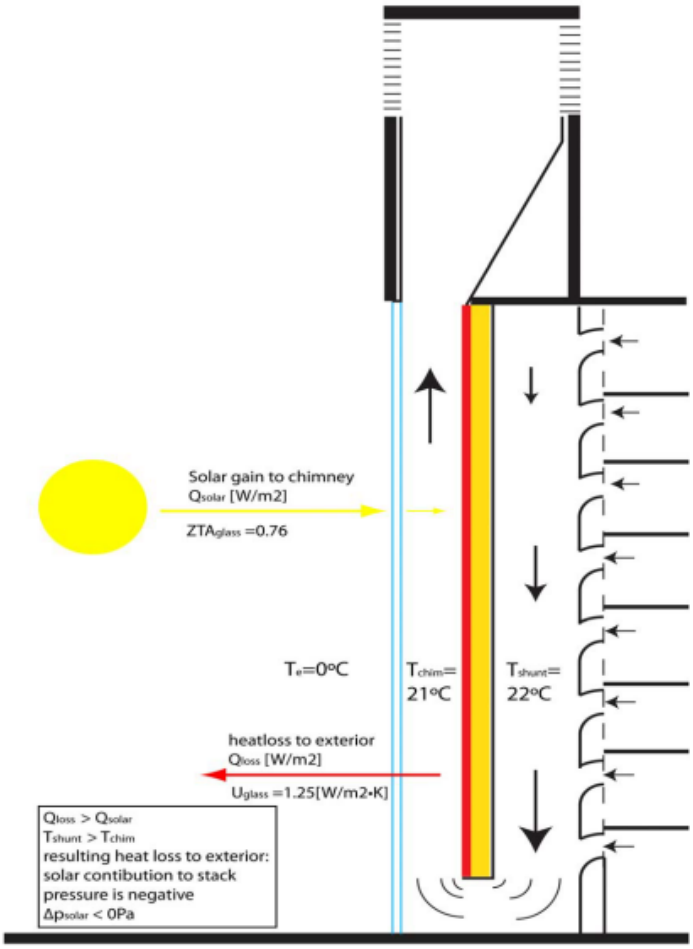

Figure 20.3: Nett heat loss through the glass plane in the solar chimney

The solar contribution to the stack pressure is calculated through deducting the stack pressure which would occur without solar irradiation from the stack pressure actually occurring in the solar chimney.

$$\Delta p_{nett} = \Delta p_{stack,solar} - \Delta p_{stack,non\text{-}solar} \quad (20.1)$$

$$\Delta p_{stack,solar} = \rho_0 \bullet T_0 \bullet (T_e^{-1} - T_{chim}^{-1}) \bullet g \bullet H \quad (20.2)$$

$$\Delta p_{stack,non\text{-}solar} = \rho_0 \bullet T_0 \bullet (T_e^{-1} - T_{shunt}^{-1}) \bullet g \bullet H \quad (20.3)$$

Figure 20.4 shows the solar contribution for the stack pressure in the different locations. The percentage of occupation in which $\Delta p<0$ corresponds with the percentage of occupation in which nett heat loss through the glass occurs.

In Stockholm a solar chimney with favorable orientation in the South-East and South-West office wings, nett heat loss occurs in 28% of occupation. In Sevilla this is only 9%.

Table 19.2: Solar contribution to stack pressure in the solar chimneys												
	Stockholm Sweden			De Bilt Holland			Paris France			Sevilla Spain		
	West orientation	SE / SW orientation	SW / SE orientation	West orientation	SE / SW orientation	SW / SE orientation	West orientation	SE / SW orientation	SW / SE orientation	West orientation	SE / SW orientation	SW / SE orientation
average solar contribution to Pstack [Pa]	1,0	2,0	2,0	1,2	2,1	2,1	2,1	2,0	2,0	2,3	3,9	3,8
resulting heat loss through the glass plane to the exterior; [%] of occupation Δp<0Pa	**42**	**28**	**28**	**37**	**28**	**28**	**31**	**22**	**23**	**14**	**9**	**9**
[%] of occupation Δp>0Pa	58	72	72	63	72	72	69	78	77	86	91	91
[%] of occupation Δp>5Pa	8	15	15	8	17	17	7	12	12	15	32	32
[%] of occupation Δp>10Pa	1	0	0	1	1	0	1	0	0	3	2	2

Figure 20.4: Solar contribution in the solar chimneys + shunt duct for four climates in Europe

20.3: Conclusions on climate influence

The conclusions that can be drawn regarding the climate influence on the performance of a solar chimney are:

- The largest stack pressure occurs at locations with high latitude due to low external temperature
- The relative solar contribution to stack pressure is significantly larger at low altitude due to higher external temperatures, thus a smaller temperature difference with the exterior which results in lower overall stack pressure..
- The nett heat loss through the glass is significant at locations with high latitude due to low external temperatures.

'Conventional' chimneys work best at high latitude. To boost stack pressure in the chimney at low latitude a solar chimney here is a good option.

Part 7: Technical and architectural implementation of the driving ventilation components

To implement one or more of driving ventilation components investigated in this project in a building design, a number of principles have to be followed in order to assure the desired function. The technical principles to assure the functions are described and a number of recommendations is given for the building and ventilation system lay-out which can reduce fan energy consumption by reducing air flow resistance.
Furthermore, this research project focuses on the performance of one specific building design with solar chimneys and a 'venturi' roof exhaust. However in architectural practice a designer will design the ventilation system along with all other aspects involved in the building. This part also describes a number of possibilities in implementing the individual driving ventilation components in architecture. This part is therefore meant to give designers an overview of the criteria and the possibilities in designing a building with solar chimneys, 'venturi' exhausts or both.

Chapter 21: Ducting and air flow design

From the fan energy consumption in the building cases the conclusion was drawn that the greatest part of fan energy reduction was obtained by applying a low pressure drop ventilation system in the ducting and building lay-out. This chapter describes the basic principles with which a low pressure system can be obtained.

21.1: Low air velocity for a low pressure drop ventilation system

The main factor in air flow resistance is the mean air velocity and in the ducting in the building. This implies the use of ducting with larger cross sectional areas than in mechanically ventilated buildings. Whereas in most mechanically ventilated buildings the design air velocity in the main ducts is 3 to 5m/s, the principle in natural ventilation is to have a maximum design air velocity in the ducting of around or under 1m/s. As static pressure loss due to wall friction in the ducts increases by a factor v^2 according equation (5.2), the air velocities have to be kept low.
Low air velocities in the ventilation system can be obtained by ducting with large cross sectional areas but they can also be obtained by using a building lay-out where ventilation through plenums in raised floors or lowered ceilings is applied which provides large cross sectional areas for the same volume flow resulting in lower air velocities. Even more so, displacement ventilation provides even lower air velocities. This principle is used in the building models in this research in the center hall zones and office zones by letting in air at the center hall zone and exhausting it to the chimneys at the end of the office zones.

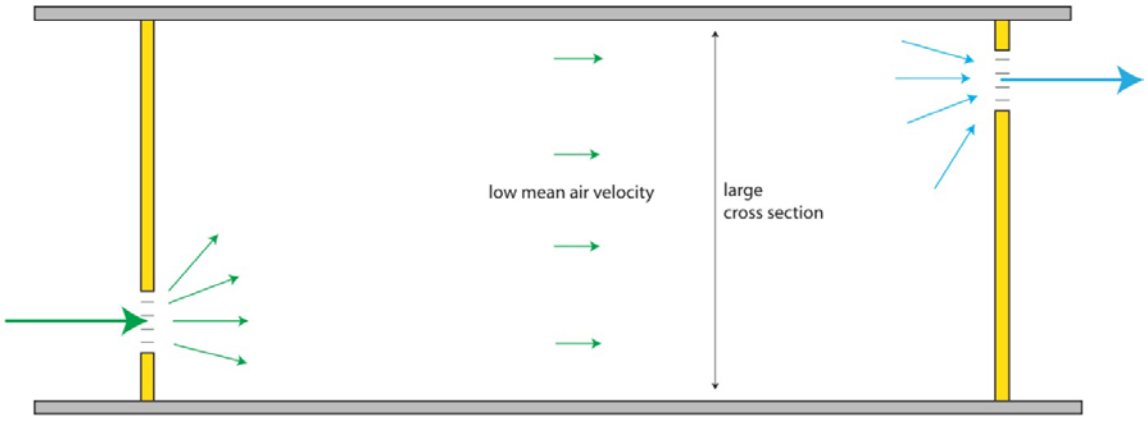

Figure 21.1: Displacement ventilation with low air velocities

21.2: Cost of ducting expressed in Gross Floor Area

The implementation of low velocity ventilation has the advantage of low pressure drop and thereby reduction in fan energy cost. However the ducting takes up space in the building which could otherwise be exploited. Assuming a displacement ventilation system in the horizontal distribution as is done in the building cases, the cost of the vertical ducting with an air velocity of 1m/s is expressed in square meters of GFA in the building needed for vertical ducting and is compared to the use of space of mechanical ventilation systems with air velocities of 3 and 5m/s in the main vertical distribution ducts. Additionally the use of space of all vertical ducting elements including the shunt ducts and solar chimneys in [case-2A] is given in the comparison in figure 21.2. In this comparison the following conditions are used:

- Ventilation rate is 3,25$m^3/(m^2 \bullet h)$ corresponding with 50m^3/h per person
- GFA of the building is 13050m^2 (building cases)
- GFA per floor is 1631m^2 (8 floors)
- Total volume flow through the building is 11,8m^3/s
- Outer dimensions of the vertical ducting elements in [case-2A] are measured in the drawings for the model (figure 8.3)
- Outer dimensions of ducts in other cases are determined with a wall thickness of 0,2m for the duct plus enclosure

Figure 21.2: Use of space of main vertical ducting.

	[case-2A]				Natural ventilation v=1m/s	Mechanical ventilation v= 3m/s	Mechanical ventilation v= 5m/s
	Supply duct per floor v=1m/s	Solar chimneys per floor v=0,88m/s	Shunt ducts per floor v=0,58m/s	Total with 8 floors	Total with 8 floors	Total with 8 floors	Total with 8 floors
Use of space [m^2 GFA]	15,6	19,7	21,1	450,9	235,0	90,8	59,9
Use of space [% GFA]	0,96	1,29	1,21	3,46	1,80	0,70	0,46

The vertical ducting in [case-2A] takes up around 2 times more GFA than the natural ventilation system with v=1m/s due to the air velocities in case-2A which are even lower than 1m/s and due to the double space requirement of the solar chimneys plus shunt duct. Compared to the 5m/s mechanical ventilation case, [case-2A] uses around 7,5 times more GFA for vertical ducting. In the design of a building with solar chimneys it has to be taken into account that the ducting will use significantly more space than in mechanically ventilated buildings. Apart from the larger investment of solar chimneys, the GFA which can't be leased in exploitation has to be weighed against the fan energy savings and the possible reduction in heating demand through heat recovery in the solar chimneys.

21.3: Aerodynamic duct design

While the design air velocity in the ducting is the largest factor which determines pressure loss, wrongly designed bends and fixtures can ruin a low velocity ducting system. This is due to local pressure losses at bends and fixtures described by equation (5.2) in which the loss factor [ζ] is the specific loss factor for a bend, fixture or appliance in a duct. With non-aerodynamic design of these elements, local pressure losses can become significant.

With this the maximum air velocity in the ducting will increase locally which increases the dynamic pressure needed to drive the air through the ducting. The maximum air velocity in the system determines the dynamic pressure loss for the whole system described in equation (5.1).
Loss factors for specific elements in ducting can be found in literature such as the Handbook for Hydraulic Resistance (Idelchik, 2010), Der Recknagel (Recknagel, 2011), and in the Dutch ISSO-publicatie 17 (ISSO, 2010). In this literature, guidelines for aerodynamic duct design can be found.

21.4: Low pressure drop appliances in the ventilation system
Appliances in the ventilation system such as air heaters, filters and humidifiers cause pressure drop in the air flow due to flow resistance. For example, an air heater heats the passing air by exchanging thermal energy from the heater surface to the passing air. The efficiency of the heating system increases with transfer surface, but with increasing transfer surface, the pressure drop also increases. When an appliance decreases the cross sectional flow area in a flow pattern, the dynamic pressure will also increase. It is therefore important in case of natural ventilation systems, which typically have low driving pressures, to not decrease effective cross sectional area in appliances in the ducts significantly.
For example, a duct with a cross sectional area of $1m^2$ in which a heater is placed will probably leave an effective cross sectional area of $0,5m^2$ which increases the local air velocity with 100%. An air heater could therefore be placed in a locally widened duct so that the effective area does not decrease as much. In this project the preheating system was simulated by a honeycomb radiator in the supply ducts at the center hall zones. The air passes though the tubes parallel with the air flow direction while the radiator surface is heated by the heated water passing through it. This is similar to the radiator in a car but instead of heating the air the water in the radiator is meant to be cooled by the passing air.
Another type of heat exchanger which can be used in natural ventilation is the fine wire heat exchanger type. This consists of mats of copper wires which are connected to copper tubes through which heated or cooled water flows. This creates a very large thermal exchange area around the thin copper wires. This system can be used for heat recovery in the solar chimneys as well as for the preheating system.

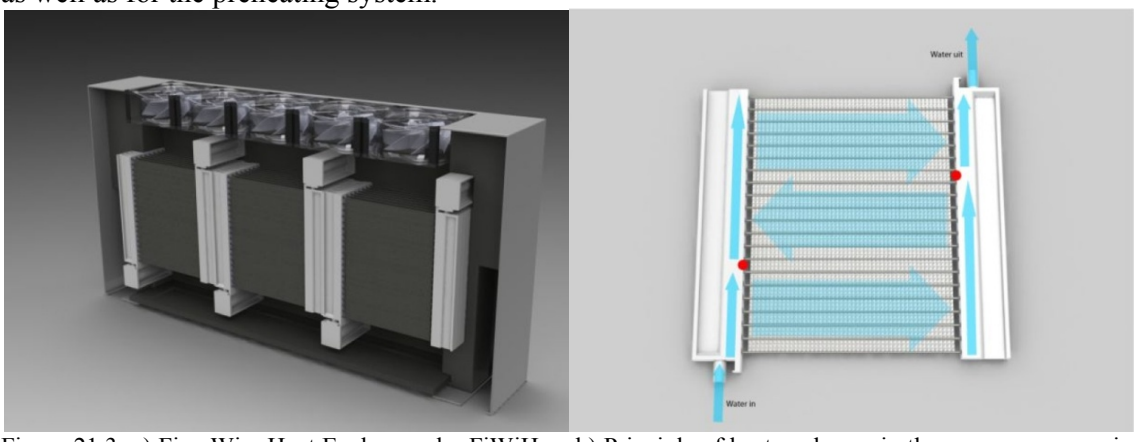

Figure 21.3: a) Fine Wire Heat Exchanger by FiWiHex, b) Principle of heat exchange in the woven copper wire mats


Figure 21.4: Side view of the woven copper wire mats in a linear heat exchanger

Conventional filters also cause large pressure drops. This is due to the fact that the air has to be forced through and along the filter fabric to subtract particles from the passing air. This causes large flow resistance. Electrostatic filters, or electrostatic precipitators, make use of an induced electrostatic charge to subtract particles from the air passing though the filter, which consists of a metal grid through which the air passes. This causes less pressure drop because less contact area is needed, hence wall friction and the wall roughness of the metal is far lower than with other filter types.

Chapter 22: Risk management

Naturally ventilated buildings are more vulnerable to air flow disturbances and draught than mechanically ventilated buildings. The degree of vulnerability depends to large extent on the design of the system. For instance, a single operable window can disturb the air flow pattern in a naturally ventilated building with an open office plan due to the large air flows that can occur in the window and the relatively small driving forces in the ventilation system. The building models in this project do not have operable windows to reduce the complexity of the models and because of the focus of the project which lies at fan energy reduction.

22.1: Operable windows

In Dutch building practice and especially in naturally ventilated buildings there is more and more emphasis on operable windows in office buildings to improve indoor comfort. This is also implemented in sustainability assessment systems such as BREEAM. As mentioned, a single opened window can disturb the entire flow system in a naturally ventilated building. Although the focus in this research is not on risk assessment and probabilistic analysis on the robustness of a natural ventilation system, a number of design guidelines can be given for natural ventilation in combination with operable windows.

In order to make a natural ventilation system work in combination with operable windows a number of aspects should be kept in mind. The natural driving forces of the wind and buoyancy due to the sun in the solar chimney are typically relatively small. This means that an air flow through an operable window can relatively easy cause a disturbance in the ventilation principle resulting in reduced or reversed air flow.

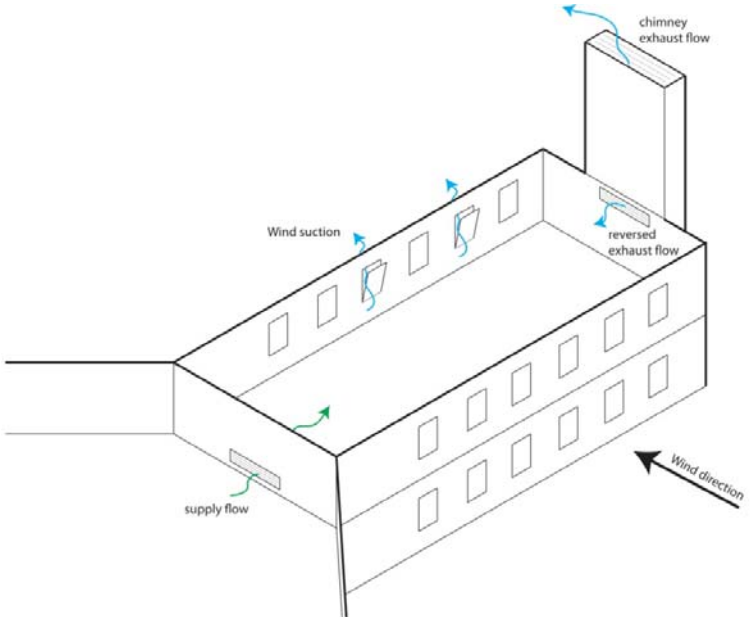

Figure 22.1: reversed air flow in the chimney due to wind suction on an opened window.

A compartment or office floor on which windows are opened could be cut off from the designed flow system by closing the openings to and from the compartment. This compartment would then temporarily be ventilated by cross ventilation or single sided ventilation over the windows. The execution of this principle needs control engineering in which an opened window results in the regarded ventilation compartment being cut off.

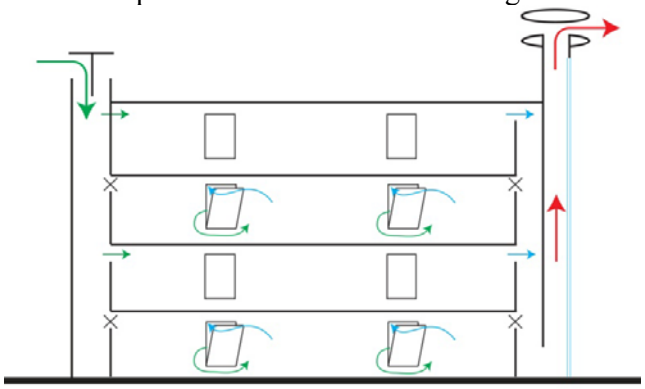
Figure 22.2: section of building with ventilation compartment cut off in case of opened windows.

As a consequence the cut off ventilation compartment has to be ventilated through the opened windows at this compartment. The compartment can therefore only bas as large as the opened windows are able to ventilate. In figure 22.3 one of many possible design solutions for combining natural ventilation through a solar chimney with operable windows is shown.

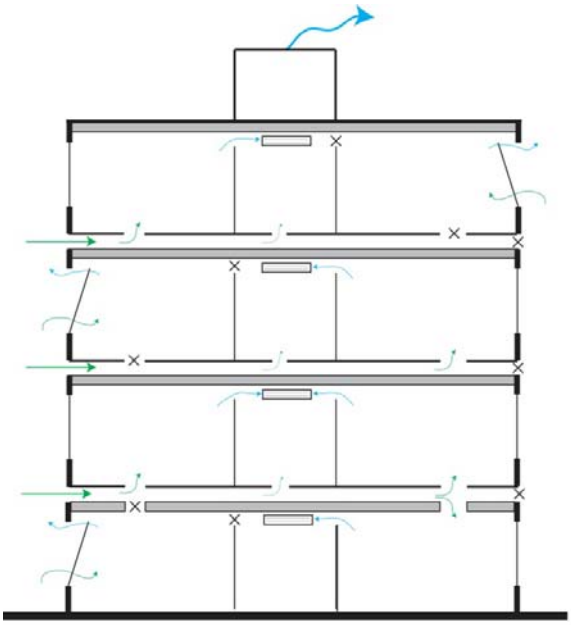

Figure 22.3: compartmentalization of an office with operable windows and natural exhaust ventilation through a chimney and raised floors

22.2: Back flow in the shunt duct

Back flow in the shunt duct occurs when the shunt duct or the zone acting as shunt duct such as an atrium has a higher air temperature as the building zones from which the stale air comes. This is due to the buoyancy between the shunt duct and the building zone. To prevent this back flow, the air which has entered the shunt duct from the building zones can't increase in temperature. It is therefore important that the absorber wall of the solar chimney is well insulated to prevent the heat of the absorber plate from flowing to the shunt duct. A minimum R_c-value of 3,8(m^2•K)/W for the absorber wall construction can be kept as guideline. This corresponds with a U-value of 0,25W/(m^2•K) if it were an external wall.

22.3: Atrium acting as shunt duct

In case of an atrium acting as shunt duct, the insulation of the absorber wall is as well necessary to prevent a high temperature at the internal surface at the back of the absorber wall which would result in uncomfortably high thermal radiation in the atrium near the solar chimney

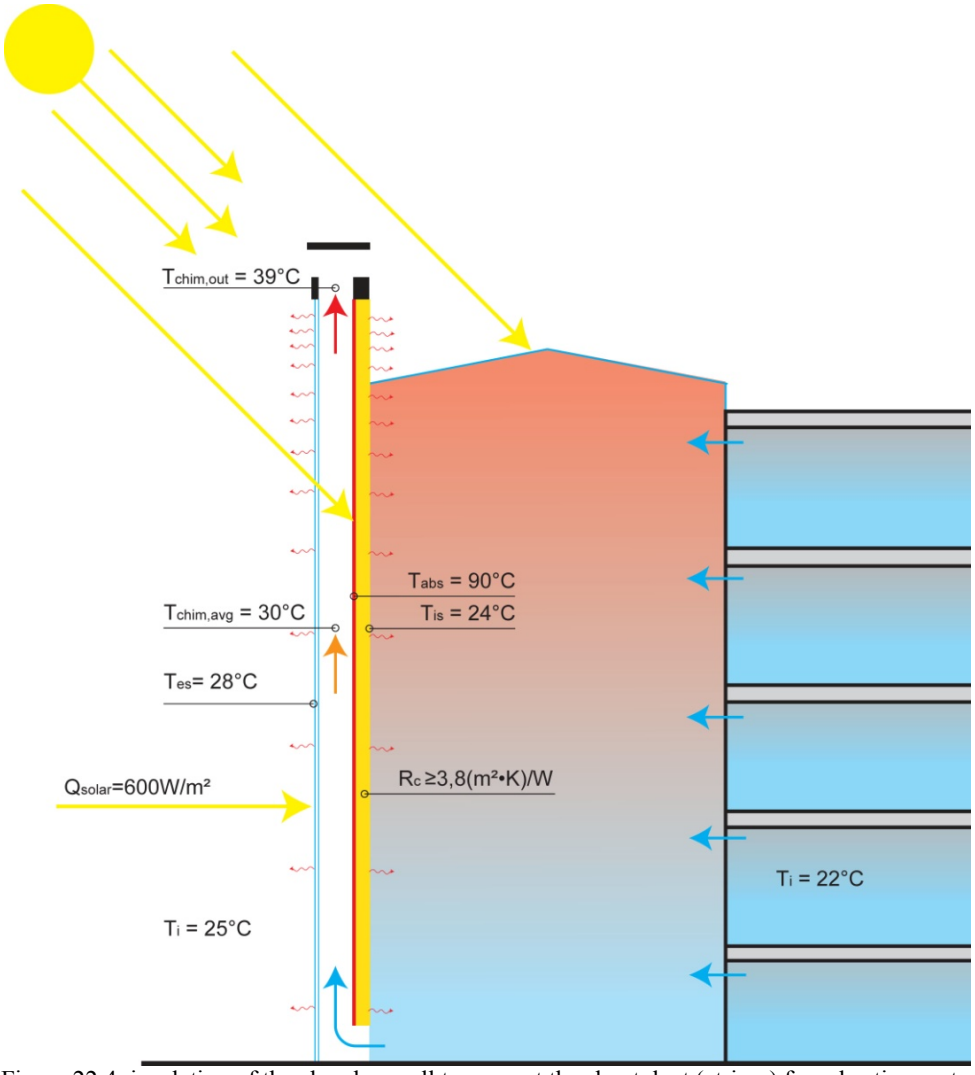

Figure 22.4: insulation of the absorber wall to prevent the shunt duct (atrium) from heating up too much

When a building is designed with a solar chimney including a glazed atrium acting as shunt duct, it is very likely that the air temperature in summer conditions in the atrium will be higher than the air temperature in the building zones. This will result in a buoyant force from the atrium back to the office zones. This could result in reversed flow when this buoyant force is larger than the other driving forces.

An atrium has to be prevented from overheating in summer conditions. With the additional function of the atrium as 'shunt duct' this gets even more significant. The cooling of atria in summer conditions is often done by ventilation to blow out the warm air. However as the ventilation of the building depends on the solar chimney it is advisory to minimize ventilation of the atrium directly to the exterior but maintaining the designed ventilation principle through the solar chimney. Shading of the atrium is therefore of importance. Most direct radiation at the façades can be kept outside by positioning the solar chimney in the right way, orientated South-West to South-East.
Concluding a glazed atrium acting as shunt duct is possible but it needs serious attention in keeping the atrium climate comfortable while maintaining the working principle of the atrium as a shunt duct. A non glazed atrium or an atrium or entrance hall with an opaque roof would be easier to climatize while maintaining the 'shunt duct' function of the atrium.

Chapter 23: Heating and cooling energy reduction

The focus in this research project is on saving energy by reducing the amount of fan energy needed to ventilate the building. Another major contribution to the total energy consumption of a building is the heating and cooling energy. Typically when fan energy consumption is very low, as is the case in the final design, heating and cooling take up a much larger relative part of the energy consumption then fan energy. In this chapter a number of principles are used to reduce heating and cooling demand in the final building model, [case-2A]. Note that volume flow control in natural ventilation described in chapter 20 is also an important measure to reduce heating and cooling demand in the building.

23.1: Volume flow control

With the design of a ventilation system, a desired volume flow is decided. In the first place the desired volume flow has to be met. However a too large volume flow can also cause problems such as draught and too low internal temperatures because the heating capacity of the building is not large enough to heat the large amounts of cold external air passing through the building. In case of natural ventilation especially in winter the driving forces will be large due to low external temperature. This can be seen in the results of the maximum volume flow in the building cases. For example the maximum volume flow in occupation in [case-2A] placed in The Netherlands with solar chimneys and 'venturi' roof is 3,3m^3/s whereas 0,5m^3/s is required. This results in an unnecessarily high heating demand in the building or a situation where the heating can't keep up which is the reason why GTO-hours by temperature undershoot exceed the GTO_{max} limit in the building models in this project. As a consequence the indoor temperatures are too low and air velocities too high which causes draught problems.

To solve this, the ventilation openings could be reduced to reduce the peaks in the air flow but this will also reduce the average air flow and therefore increase fan energy consumption in the building. A better solution is to limit the maximum air flow so that with low driving pressure conditions (high external temperature, no sun and no wind) natural air flow is maximized and fan energy consumption minimized while in high driving pressure conditions (low external temperature, sun and strong wind) the air flow is tempered to the desired air flow.

In addition the volume flow control could be regulated on indoor air quality by CO_2 levels. In case of high occupation of the building the CO_2 production in the building will be high which should result in a higher volume flow. A controls engineering system could then be based on the CO_2 level in the office zones and accordingly decrease or increase the ventilation openings. In principle this means that if an office zone is not occupied, no ventilation is required and fan energy and heating energy for the ventilation air is saved.

23.2: Thermal mass

In a building with a high amount of accessible thermal mass the indoor climate is more likely to be kept constant than in a building with low thermal mass. In Dutch building practice a building is regarded as 'heavy construction' when the specific active mass or SWM (Specifieke Werkzame Massa in Dutch) is above 100kg/m^2 GFA. This can be kept as guideline for naturally ventilated buildings as a minimum.

SWM < 50kg/m^2 ➔ light construction
50 < SWM < 100kg/m^2 ➔ middle weight construction
SWM > 100 kg/m^2 ➔ heavy construction

SWM is the thermal mass of the accessible layers of the construction. Calculation of SWM is described in Dutch standard (NEN-1068).

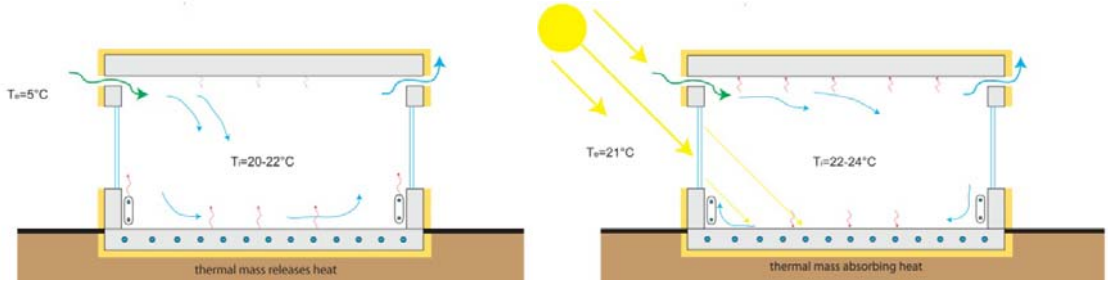

Figure 23.1: Thermal mass and temperature buffering in winter and summer

The thermal mass in a building stores the thermal energy from the solar heat gain and internal gain in summer situations hence keeping the building cool. In winter situations the thermal mass has to heat up the air passing through the building. With small ventilation flows a small amount of heating is needed to keep the thermal mass at the right temperature. This is why in housing natural ventilation is very common.
In utilitarian buildings such as offices the occupancy is higher and therefore the desired volume flows are higher. With larger volume flows more heating energy is needed to keep the indoor temperature comfortable in winter situations.
In summer situations a part of the wanted cooling can be obtained from a slightly higher ventilation flow however when the external air temperature is higher than the internal temperature a higher ventilation flow will result in higher cooling demand because the external air has to be cooled.

As mentioned, in naturally ventilated buildings the ventilation flow has to be kept to the minimum needed for fresh air supply in winter conditions which means that heating can't be done with an all air system. The air flow is only used for fresh air supply. Consequently heating and cooling are applied by terminal equipment such as radiators, fan coils and other devices. Next to mentioned terminal devices which can be controlled by occupants, the thermal mass of the building can be activated. This can be done by applying concrete core activation or in a more passive way by applying phase change materials (PCM) which add virtual thermal mass to the structure.
An activated slab system such as concrete core activation with both thermally accessible floors and ceilings has a heating capacity of around 50 to 60W/m^2. This is not enough to provide the needed heating throughout the whole winter period. A preheating system is often applied in naturally ventilated buildings to heat the supply air up to just below the lower set point of the indoor climate which is typically 20°C in Dutch building practice so a set point of 18-19°C for the supply air is possible. The rest of the heating energy needed to compensate heat loss through the building fabric is provided by the activated thermal mass, the terminal equipment and internal gains.

In order to effectively use the thermal mass of the structure this mass has to be accessible. This means direct exposure of the surface of the mass to the interior space. In case of concrete core activation this is even more significant because a large part of the heating and cooling capacity of the system is based on radiative exchange of thermal energy the surface of the thermally activated slabs. Consequently a complete covering of the ceiling with a lowered ceiling can't be applied. The interior climate of the building needs also acoustically absorbing surfaces to provide a comfortable acoustical climate for the occupants. While this is often taken care of by lowered ceilings, in a naturally ventilated building which takes advantage of a passive or active thermal mass system this has to be dealt with otherwise.

23.3: External shading

In the cooling season a large part of the heat gain which has to be extracted by the cooling system is due to solar gain mainly through the windows of the building. First the glass percentage is to be considered. The curtain wall façade which is often applied to iconic office buildings nowadays is not a very good option in combination with natural ventilation. The large glass area means a large solar gain which results in a large cooling demand. Next to that the façade area has practically no thermal mass which is needed to maintain a comfortable climate.
Secondly an external shading system can be applied to decrease solar gain in the building. This can be applied in form of fixed external shading which can be part of the architecture of the building for instance an overhang or 'brises soleil'. or it can be applied in the form of a movable external shading system or a combination of the two. A movable shading system can be controlled manually by the occupants of the building which will give them a feeling of control of the building climate. It can also be control centrally or in a combination of the two.

A guideline for façade design, with keeping in mind sufficient daylight and reducing solar gain, is a solar heat gain product of the façade of 8% in sunny situations. This implies that the product of glass percentage in the façade, ZTA (SHGC) of the glass and ZTA of a movable external shading system in fully deployed position is 0,08. The building models in this project have an average glass percentage over all facades of 33%. Together with a ZTA of the glass of 0,61 this gives a solar heat gain product of:

Solar heat gain product without shading = 33% x 0,61 = 0,20

In the building models no external shading is applied as the focus of the project was not on heating/ cooling energy reduction. In a short additional study a movable external shading system is applied to the final model, [case-2A]. This shading system has a ZTA of 0,4 in which together with the façade and glazing results in a solar heat gain product of:

Solar heat gain product with shading = 33% x 0,61 x 0,4 = 0,08

In the building model the shading system is controlled by a control engineering system in TRNSYS-TrnFlow which evaluates the total solar irradiation on the corresponding façade.
The system is deployed when the solar radiation exceeds 150W/m^2 perpendicular on the façade plane and is deactivated when it falls below 120W/m^2. In practice a threshold of 150W/m^2 could result in a very early deployment of the system and annoy occupants in the building. A higher threshold could be chosen with the assumption that under that threshold the occupants would already deploy the system manually, giving them a greater sense of control.
However in the simulation no occupant behavior is simulated hence the mentioned thresholds with fully automatic control are applied.

Movable external shading switch modeled in the TRNSYS simulation studio

The external shading systems in [case-2A] are controlled in TRNSYS by type2-controllers which check the solar irradiation on all façade orientations separately. These controllers activate when the solar irradiation output from the weather file in the simulation studio exceeds 150W/m^2 and deactivate when it drops below 120W/m^2. The output of all 10 controllers for the 10 façade orientations is connected back to the type56b building module in which the signal is used to activate or deactivate the movable shading devices on the windows.

Results movable external shading

Figure 23.2: heating and cooling demand with and without external shading system for the final model [case-2A] placed in De Bilt – The Netherlands				
	Specific heating demand [kWh/(m^2•a)]	Total heating demand [MWh/a]	Specific cooling demand [kWh/(m^2•a)]	Total cooling demand [MWh/a]
[case-2A]	63,1	823	48,1	628
[case-2A] with shading	64,4	841	37,8	493

A significant decrease in cooling demand is reached by applying external shading. A further reduction could be reached with a lower ZTA for the shading system or a lower ZTA for the applied glazing. With a reduction of the ZTA of the shading the view to the outside is also blocked. With a reduction of the ZTA of the glass the deployment threshold of the system can be increased providing a view to the outside for a longer time for the occupants, which will benefit comfort of the occupants.

23.4: Night ventilation

To reduce cooling demand in summer conditions, night ventilation can be applied to cool the building and release the stored energy at night from the thermal mass in the building so that the next morning the thermal mass has its full thermal capacity at hand to buffer the solar and internal gain of that day.

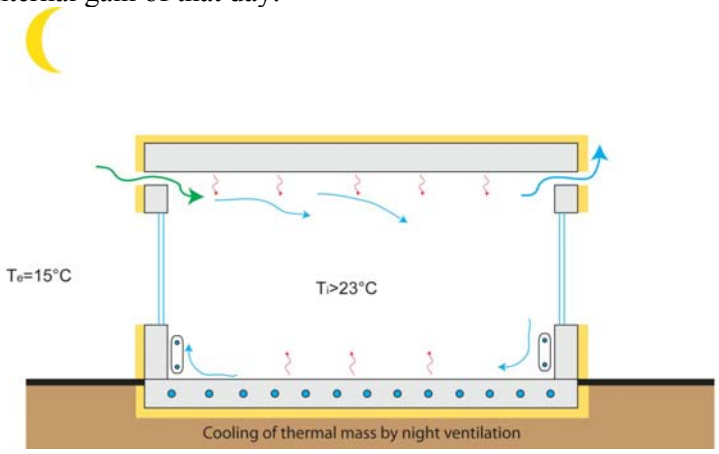

Figure 23.3: night ventilation in cooling season to reduce cooling demand during daytime

A short study is done to evaluate the effect of night ventilation on the final model. Starting point is the building model [case-2A] with external shading described in paragraph 23.3, in order to evaluate the combined effect of night ventilation and movable external shading. The set points for night ventilation used in TRNSYS-TrnFlow are:

- Activation when T_{shunt} exceeds 23°C after occupation
- Deactivation when T_{shunt} falls below 21,5°C after occupation
- Night ventilation is only applied in the cooling season: April 29th to September 28th
- Activation of night ventilation implies opening the inlets at the inlet plenum and the exhaust at the 'venturi' roof.

Night ventilation switch modeled in the TRNSYS simulation studio

The night ventilation system in [case-2A] is modeled in TRNSYS by checking the temperatures in the shunt ducts. The maximum temperature in the three shunt duct is checked by a calculator-type in the simulation studio. The highest temperature of the three is used as input in a type2-controller which checks if the temperature exceeds 23,5°C and when the temperature drops under 21,5°C again. This produces a binary signal which is used in the calculator-type which also controls the pressure check in the inlet openings.

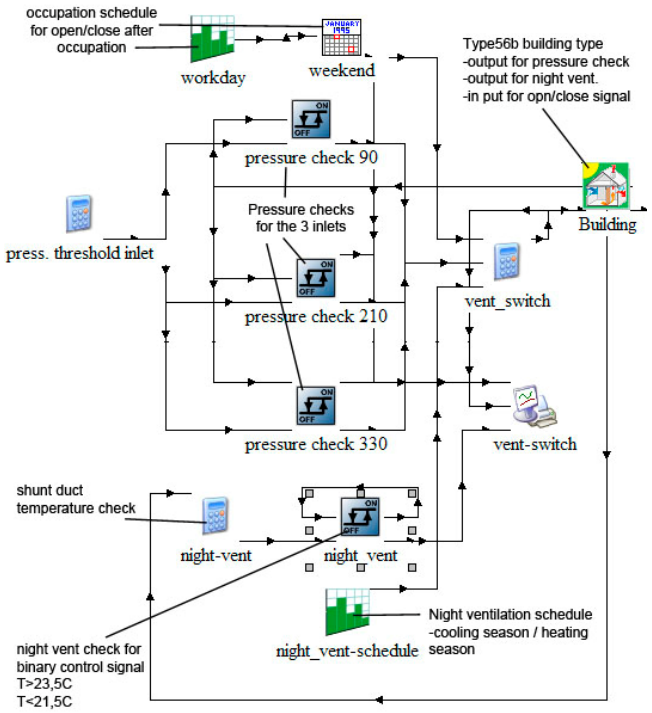

Figure 23.4: screen shot of simulation studio with connections between the controllers which are involved in inlet opening pressure check, occupation open/close switch and night ventilation control

Results night ventilation

Figure 23.5 heating and cooling demand with and without night ventilation and movable external shading system for the final model [case-2A] placed in De Bilt – The Netherlands				
	Specific heating demand [kWh/(m^2•a)]	Total heating demand [MWh/a]	Specific cooling demand [kWh/(m^2•a)]	Total cooling demand [MWh/a]
[case-2A]	63,1	823	48,1	628
[case-2A] with shading	64,4	841	37,8	493
[case-2A] with shading and night ventilation	68,6	895	26,7	349

Compared to the building model with movable external shading but without night ventilation, another significant reduction in cooling demand is reached (Figure 23.5). Simultaneously with decreasing cooling demand, heating demand increases by a small amount. Still the heating and cooling demand combined are lower than without night ventilation but a night ventilation system should decrease cooling demand without increasing heating demand.

Increase of heating demand with night ventilation in simulation model

The increase in heating demand in the model with night ventilation can be explained with the manner in which the building simulation model is built up and specifically how the set points of the supply air preheating and the concrete core activation are controlled. As often mentioned the focus in this project is on fan energy reduction. In order to obtain a quick running simulation model which evaluates ventilation flows and thereby fan energy consumption, the preheating system of the supply air is simplified to an extra heating capacity of the heating in the center hall zones of the model (Figure 23.6).

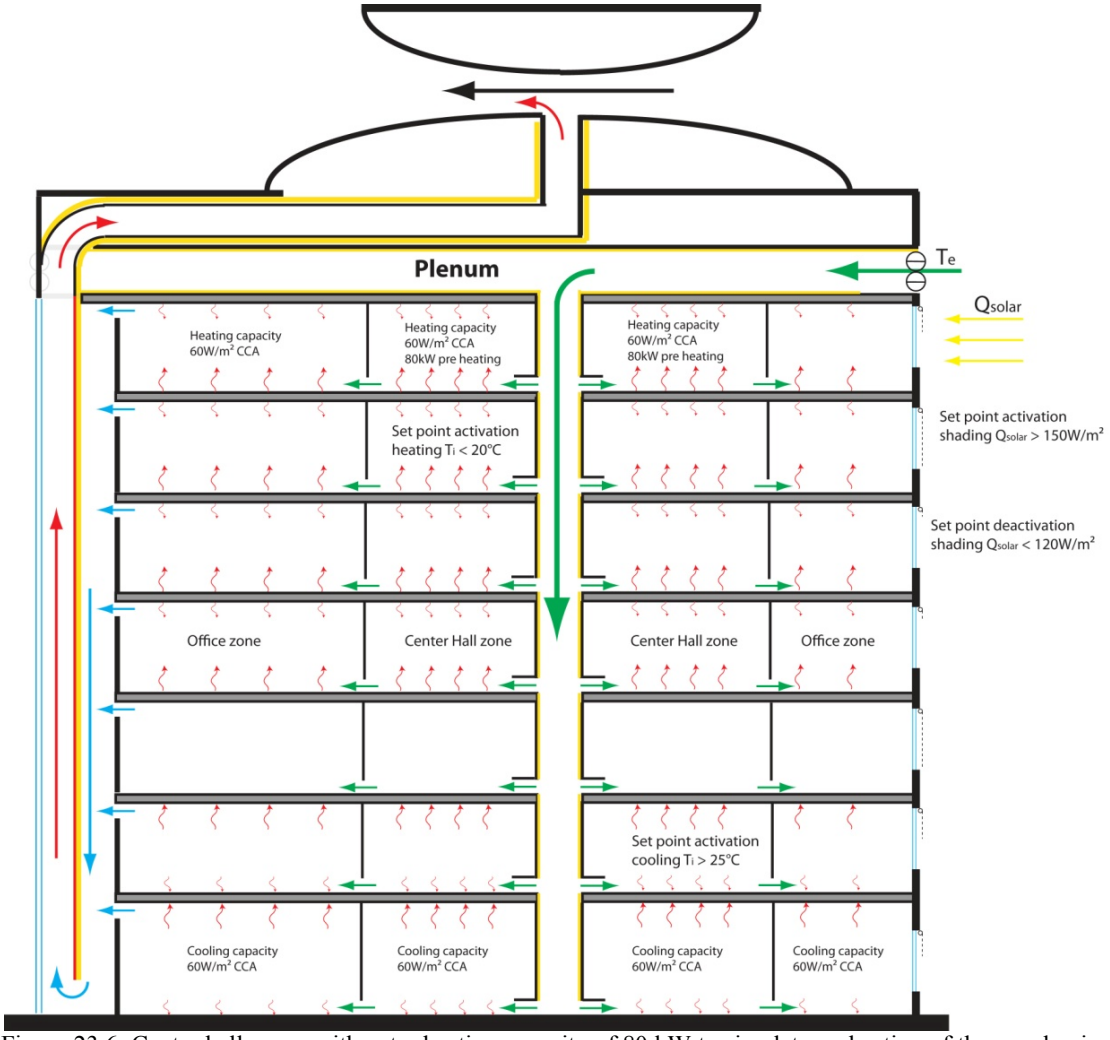

Figure 23.6: Center hall zones with extra heating capacity of 80 kW to simulate preheating of the supply air and set points.

As a consequence of the simplification the set points for preheating and general zone heating are the same and are activated at the same time. In the building simulation model with night ventilation it will occur in the cooling season that in the morning the zone heating in the center hall zones is activated while at the same time in the office zones the zone cooling is activated. This is the case when at night the building is cooled down to around 21°C by night ventilation and in the morning the colder external air (12-15°C) is drawn into the building. The center hall zone heating heats this external air from 12-15°C up to 20°C. At the same time the solar gain and internal gain heat the building. When the indoor temperature reaches 25°C

in the office zones, the zone cooling in the offices is activated resulting in the simultaneous heating and cooling of the building.
This simultaneous heating and cooling in the morning after night ventilation causes the increase of heating energy consumption when night ventilation is used in the building simulation model.

Model improvements - Controls engineering preventing increase of heating demand with night ventilation
Ideally a preheating system will heat the supply air to just below the set point (18°C). The rest of the heating demand in the building zones is then supplied by the zone heating and the internal and solar gain in the building. In this manner the night ventilation can be set to cool the building to just above 20°C. To model this behavior a simulation model should be made with separate preheating of supply air and zone heating and cooling systems. In order to do this the building simulation model used in this project [case-2A] should have been altered extensively.

23.5: Heat recovery
To decrease heating demand, thermal energy in the exhaust air flow is common practice in sustainable building design. The thermal energy which is used in the terminal equipment to heat the building is recovered by heat exchangers. This energy can be directly transported to the supply air flow in case of an air-to-air cross flow heat exchanger. Another way is to use heat exchangers such as a fine wire heat exchanger. These are placed in the exhaust flow in the air ducts. The thermal energy absorbed by the water can be stored in a long term system such as a geothermal storage or in a short term system for use in the heating season. This energy can be used in the preheating system or in the concrete core activation. As the temperature differences in the heat exchangers are low, low temperature systems are favorable to use.

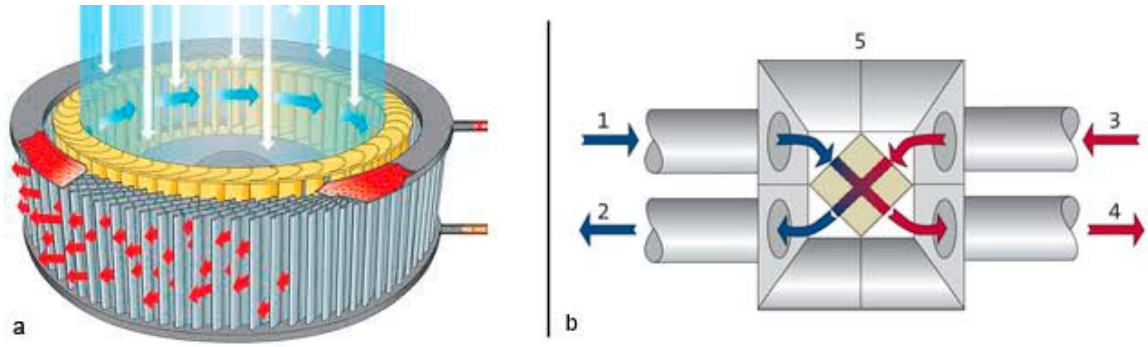

Figure 23.4: a) FiWiHex air-to-water heat exchanger b) air-to-air cross flow heat exchanger for crossing supply and exhaust flow.

Heat recovery in solar chimneys – a solar collector
In buildings with solar chimneys the use of heat recovery in the exhaust flow is even more obvious. Where heat recovery in general decreases heating demand by recycling thermal energy, a heat recovery system in a solar chimney can harvest the additional solar energy gain in the solar chimneys. In fact a solar chimney with heat recovery acts as a solar collector by collecting solar radiation in the chimney and transporting it to the water system in the heat exchanger. In paragraph 24.2 the thermal energy harvest function of solar chimneys is further described.

Chapter 24: Solar chimney design

The main function of a solar chimney is extracting stale air from a building. Another opportunity of solar chimneys is harvesting the solar energy captured in the chimney and using this to heat the building and thereby reduce heating demand. Because of this opportunity the dimensioning of solar chimneys can be based on two principles:

- Minimal ventilation requirement for fresh air supply
- Desired solar energy yield in the solar chimney acting as solar collector.

The construction of the solar chimneys in this project is based on the construction of the solar chimneys in the Earth, Wind and Fire research (Bronsema, November 2011,a). The E,W&F research focuses on the thermal energy harvest in the solar chimneys whereas this project focuses on the ventilation flow generated by the solar chimneys and the fan energy savings it generates in combination with the low pressure loss natural ventilation system designed for this project. In practice the two ways of analyzing solar chimneys can't be seen separately. As the solar chimney is the exhaust of a ventilation system it needs to provide at least the minimum required ventilation flow for the building and in sustainable building design heat recovery in the exhaust flow is common practice. In practice a solar chimney should hence not be designed just to ventilate a building and reduce fan energy consumption but should be combined with heat recovery thus solar energy harvest.

24.1: Dimensioning solar chimneys on desired ventilation rates

Dimensioning the solar chimney on minimal ventilation requirement is very similar to normal duct design. The required air flow per time unit is divided by the wanted air velocity to obtain the needed cross sectional area. In this project a total of $4m^3/s$ of fresh air is required per office wing, hence per solar chimney. The most important variables for the performance of the solar chimney are:

- Height; Higher chimneys produce more stack pressure larger collector area which results in higher temperatures.
- Width; Wider chimneys have larger collector area
- Depth;
- ZTA of glass; a higher solar ZTA will bring better performance while more solar irradiation will enter the chimney
- U-value of glass; low heat loss to the exterior will bring better performance
- U-value of absorber wall; good insulation prevents unfavorable stack effect in the shunt duct
- Absorber plate emittance; low emittance factor gives a higher thermal efficiency of the system
- Air velocity; with maximum air velocities around 1-1,5m/s to reduce pressure loss due to friction.

The depth of the solar chimney should in theory be small to give extra width and thus collector area. However, width greater width the glass area and absorber wall area increase which increases heat loss. In 'Earth, Wind and Fire, airconditioning zonder ventilatoren – Thema fire' Bronsema (November 2011,a) describes the influences of the depth on the performance. A practical argument for a minimal depth is the maintenance of the chimney. If interior planes of the chimneys are cleaned by hand, a minimum depth of 0,65m is required. This is similar to the depth needed to clean and service the cavity of a double skin façade.
The solar chimneys in this project are dimensioned with a depth of 0,65m resulting in a width of 7m to come to a cross sectional area of $4,55m^2$ and an air velocity of 0,88m/s in the chimney.

Volume flow control

The stack pressure in the solar chimney is variable with external temperature and solar irradiation. To obtain a constant volume flow in the chimney a control valve can be applied at the bottom entrance to regulate the desired the air velocity. Control valves can also be applied at the air links from the building zones to the shunt duct. This would be an alternative to combine volume flow control with the possibility to cut off compartments from natural ventilation when windows are opened in the building zone. In this case the control valve at the bottom entrance of the solar chimney could be left out.

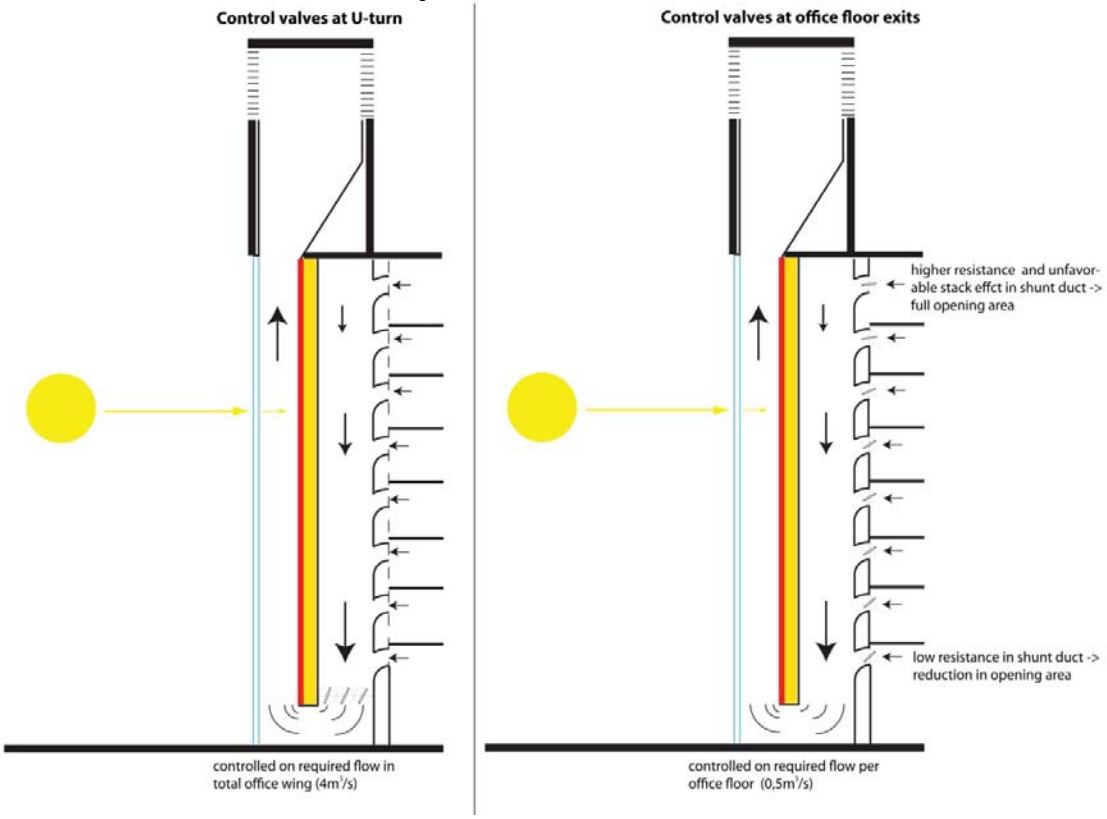

Figure 24.1: a) control valve at solar chimney entrance, b) control valves at shunt duct

24.2: Dimensioning solar chimneys on solar energy harvest.

The possible solar energy harvest in the solar chimney is evaluated by Bronsema (November, 2011,a). The thermal efficiency of a solar chimney with light weight absorber wall is found to be significantly higher than a solar chimney with a heavy weight back wall hence high thermal capacity. This is due to the quick energy release from the absorber wall to the air in case of a light weight absorber wall. With a light weight absorber wall the thermal efficiency is typically around 55-65% calculated in occupation time.

Thermal efficiency of a solar chimney is defined as ratio of the thermal energy transmitted to the passing air divided by the total solar irradiation on the glass surface.

$$\eta_{solar,th} = \frac{Q_v \cdot \rho \cdot c \cdot (T_{out} - T_{in})}{R \cdot W \cdot H \cdot Q_{solar}} \qquad (24.1)$$

$\eta_{solar,th}$ ➔ thermal efficiency of the solar chimney
T_{out} ➔ exit temperature of air [°C]
T_{in} ➔ inlet temperature of air [°C]
R ➔ reduction factor or framing factor in the glass plane by window frames

W ➔ width of the glass surface and solar chimney
H ➔ height of the glass surface and solar chimney
Q_{solar} ➔ total solar irradiation on the vertical glass surface

The thermal efficiency can also be calculated from the wall and glass temperatures with equation (24.2):

$$\eta_{solar,th} = ZTA \cdot \frac{U^*_{gl} \cdot (T_{gl} \cdot T_e)}{Q_{solar}} - \frac{U^*_{abs} \cdot (T_{abs} \cdot T_{shunt})}{Q_{solar}} \qquad (24.2)$$

ZTA ➔ g-value of the glass in the chimney
T_{abs} ➔ average absorber plate temperature
T_e ➔ external air temperature
T_{gl} ➔ average glass temperature at the inside plane
T_i ➔ air temperature in the shunt duct
U^*_{abs} ➔ heat transfer coefficient of the absorber wall
U^*_{gl} ➔ heat transfer coefficient of the glass

From equation (24.2) the three variables which influence thermal efficiency can be derived.

1) The first term is the ZTA of the glass. With a ZTA of 0,7 the thermal efficiency can't exceed 70% as only 70% of the solar irradiation is transmitted through the glass onto the absorber plate.
2) The second term describes the heat loss to the exterior through the glass. A glass type with lower U-value will result in a higher efficiency. However U-value and ZTA of a glass type are linked and with decreasing U-value ZTA will also decrease due to the coatings used on the glass to improve radiative insulation.
3) The third term describes the heat loss through the absorber wall to the adjacent space or duct. In the building cases in this project, the shunt duct

The wall and glass temperatures are interrelated with the heat transfer coefficients in the chimney which are in turn related the geometrical relations, air velocity and solar irradiation. These relations are described in the analytical model in paragraph 10.1. The thermal power of the solar chimney and the thermal energy yield can be calculated with:

$P_{th,ref} = Q_v \bullet \rho \bullet c \bullet \Delta T$ [W] (24.3)

$P_{th,ref}$ ➔ thermal power of the chimney
Q_v ➔ volume flow through the chimney
ρ ➔ density of air in the chimney
c ➔ mass density of air
ΔT ➔ temperature increase in the chimney

By summation of the thermal power over a year the thermal yield can be calculated. For [case-2A] the annual solar irradiation on the façade planes and the theoretical thermal yield in the chimneys is given in figure 24.3.

Figure 24.2: Annual solar irradiation on the vertical plane

Orientation relative to North (0°)	90° East	120°	150°	180° South	210°	240°	270° West
Annual solar irradiation [kWh/m^2]	408	494	553	570	543	472	381

Figure 24.3: Theoretical annual thermal yield in the solar chimneys						
	South-East wing solar chimney		South-West wing solar chimney		North wing solar chimney	Building total
Orientation relative to North (0°)	120°	210°	240°	150°	270°	
Chimney glass area [m^2]	99,8	136,8	99,8	136,8	199,5	672,7
Annual solar irradiation [kWh]	66.667	29.600	47.084	75.621	76.010	294.982
View factor to sky (obstruction factor by the building)	1	0,88	1	0,77	0,77	
Theoretical annual solar energy yield with $\eta_{solar,th}$ = 0,60 [kWh]	55.700		63.187		35.208	154.095

The annual thermal yield given in figure 24.3 per chimney is the amount of solar energy striking the solar chimney which is transferred to the exhaust air temperature, T_{out}, at the top of the chimney. The actual thermal yield also depends on the efficiency of the heat exchanger applied in the chimney. The heat exchanger should have a high efficiency and simultaneously have low air flow resistance. These to variables are interlinked with each other so the choice for a heat exchanger will be a compromise between thermal yield and pressure loss and hence fan energy consumption. The pressure loss over the system should at least be chosen so that the driving force of the chimney is greater than the pressure loss in the solar chimney and the heat exchanger at average annual conditions.
The total heating demand of [case-2A] with applied external shading and night ventilation as given in table 23.2 is 895MWh or 895.000kWh annually. The theoretical thermal yield of solar energy in the solar chimneys is, with 154.095kWh, 17% of annual the heating demand in the [case-2A].
In a solar chimney plus shunt duct design with the possibility to recirculate between chimney and shunt duct (figure 24.4), a solar collector can be realized while the building is not occupied. The solar irradiation striking the chimney in weekends can be harvested and stored in long term storage systems such as geothermal storage (figure 24.4b).

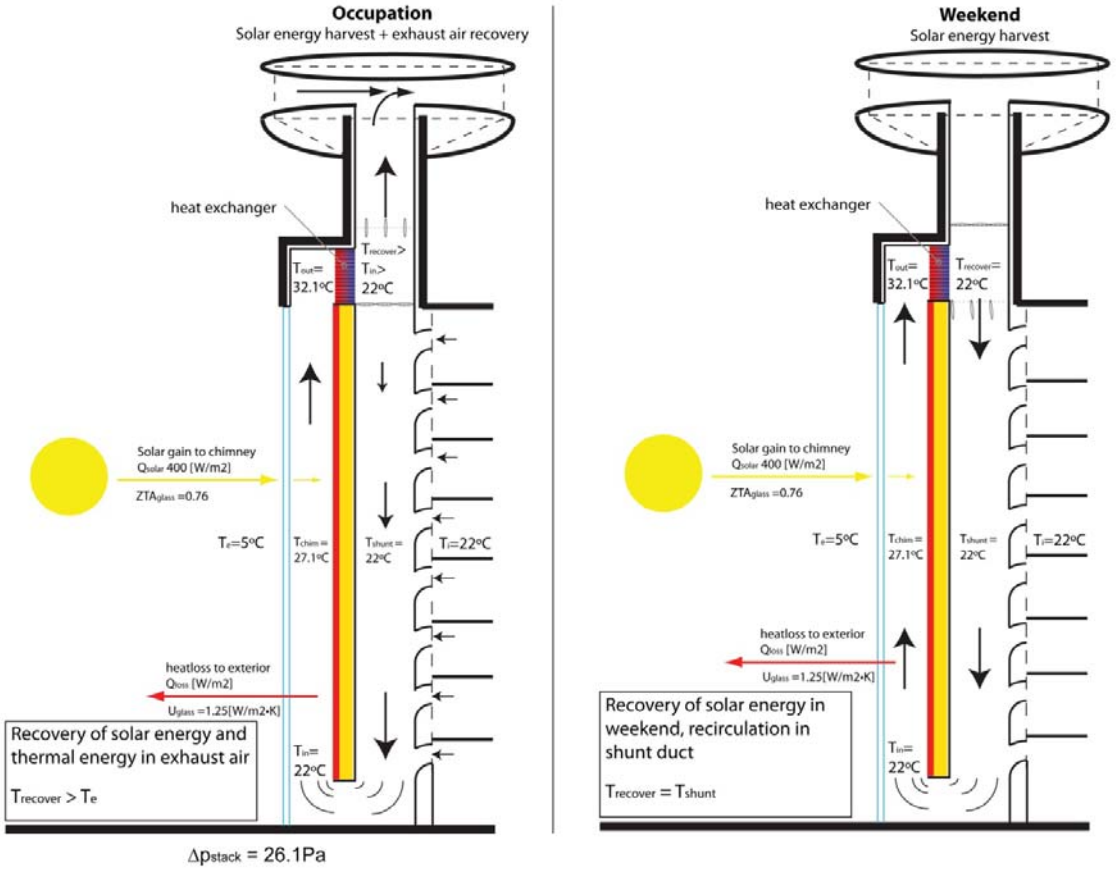

Figure 24.4: a) Heat recovery of exhaust air energy and solar irradiation in occupation, b) heat in the weekend with recirculation in the shunt duct

In conditions with $T_{out} < T_e$ the thermal energy in the exhaust air can be recovered which is also done in ventilation systems without solar chimney. The temperature to which the exhaust air can be cooled in the heat exchanger ($T_{recover}$) has to be larger than external temperature T_e in order to maintain stack pressure in the exhaust. While the heat exchanger cools the air the placement of the heat recovery has to be in a horizontal duct or even better in a downward facing exhaust duct. If the heat exchanger would be placed in the vertical duct of the chimney the cooled air could stall the stack effect in the chimney. A heat exchanger in a downward facing exhaust duct will cause the cooled air to drop and thereby pulling up the air in the solar chimney (figure 24.5)

While the average driving pressure in [case-2A] is around 40Pa (figure 15.8), a heat recovery system with a pressure drop at 1m/s air velocity of around 10 to 20Pa additional to the 10Pa pressure drop in the ducting is well applicable in the building system without dramatically increasing fan energy consumption. Conventional heat exchangers have pressure drops which are significantly higher hence new systems have to be developed to apply in this kind of system. FiWiHex has produced a series of fine wire heat exchangers which have typically far lower pressure drops than conventional systems hence this system could be a starting point.

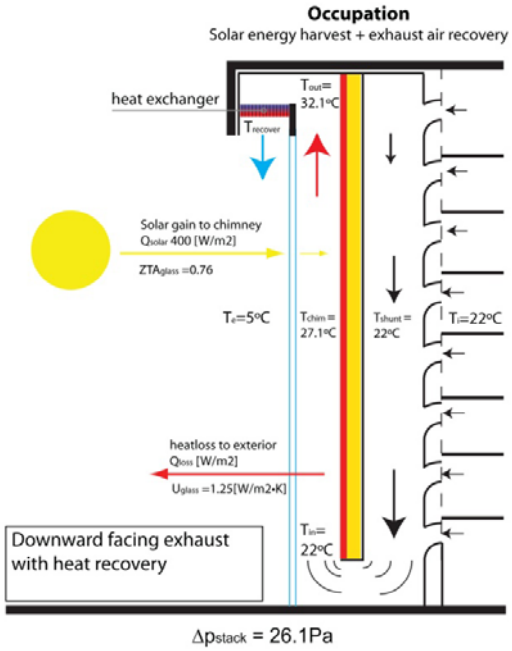

Figure 24.5: Heat recovery in downward facing exhaust which causes cooled air to fall down and draw up air in the solar chimney.

Chapter 25: Possibilities of solar chimneys in architecture

The solar chimney itself is an entity in which not very much can be altered without comprising on performance. From the results in this project is concluded that a solar chimney plus shunt duct works significantly better than one without shunt duct. The combination with a shunt duct can be made in multiple ways which have their advantages and disadvantages. Therefore a summary of possibilities for integration of the solar chimney and specifically the shunt duct in a building is given.

Integration in buildings – shunt duct configuration

The shunt duct configuration as used in the building cases in this project is one with decentral shunt ducts, one at every solar chimney. This means that when one solar chimney does not provide enough stack pressure to ventilate the part of the building connected to it, auxiliary fans have to be activated in the part of the building.

A configuration with central shunt ducts as shown in figure 25.1b and 25.2b connects all multiple solar chimneys to one shunt duct. The stale air from multiple parts of the building is drawn down and can flow to one or another solar chimney regarding in which chimney more stack pressure is created due to more solar irradiation. An advantage is that a building part at the East façade of the building can also exhaust via the solar chimney at the West façade when the sun is in the West. A disadvantage can be the extensive ducting needed at the ground floor or in the basement to connect the central shunt duct and all solar chimneys to each other. Furthermore the solar chimneys should be dimensioned at more than half of the volume flow of the total building in case of two chimneys while more than half of the building could exhaust through one chimney at times in which one chimney produces more stack pressure then the other.

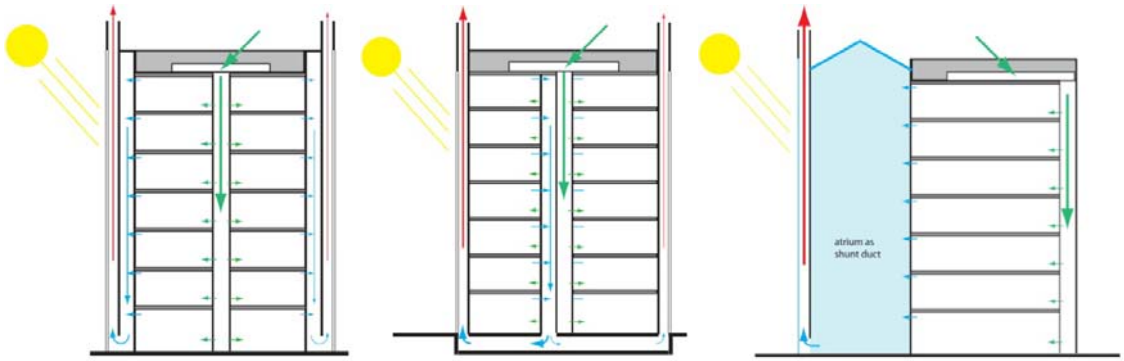

Figure 25.1: schematic section with solar chimney plus shunt duct configuration, a) decentral shunt duct, b) central shunt duct, c) atrium as shunt duct

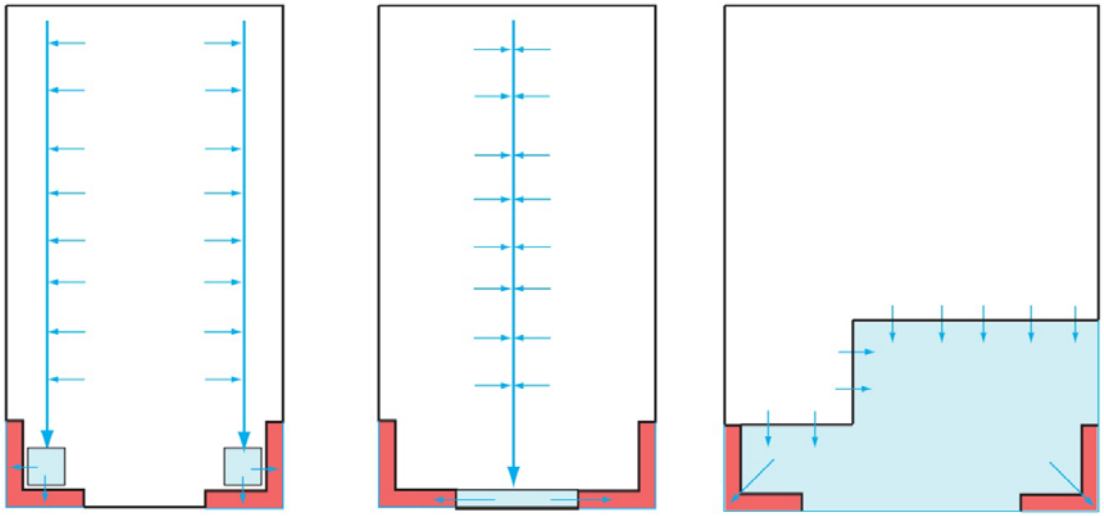
Figure 25.2: schematic plan of solar chimney plus shunt duct configuration, a) decentral shunt duct, b) central shunt duct, c) atrium as shunt duct.

Another way of directing the stale air in the building to the bottom of the solar chimneys in order to provide every floor with a similar stack pressure is to design a building zone as shunt duct which could be an atrium or stairwell. However, it has to be taken into account that stale air is extracted through this zone. In paragraph 23.3 a number of points of attention are given when applying an atrium as shunt duct.

Chapter 26: Possibilities of 'venturi' exhausts and air intake in architecture

The 'venturi' roof design in this project and the small 'venturi' exhaust on the individual solar chimneys are just two of many more possible forms in which a venturi shaped exhaust can be applied. For the air intake and supply shaft in this project this is the same. In this chapter a short summary of possible forms of venturi-shaped exhausts and air-intake design is given. Furthermore the points of attention found in this project in applying one of these elements are described.

26.1: Central 'venturi' roof

The basic principle in a 'venturi'-exhaust is a contracting flow between two elements at which the exhaust of the ventilation system of the building is placed. This can come in many forms. In the Earth, Wind and Fire research by Bronsema a 'venturi' roof of two equally large ellipsoid discs forms the contraction.

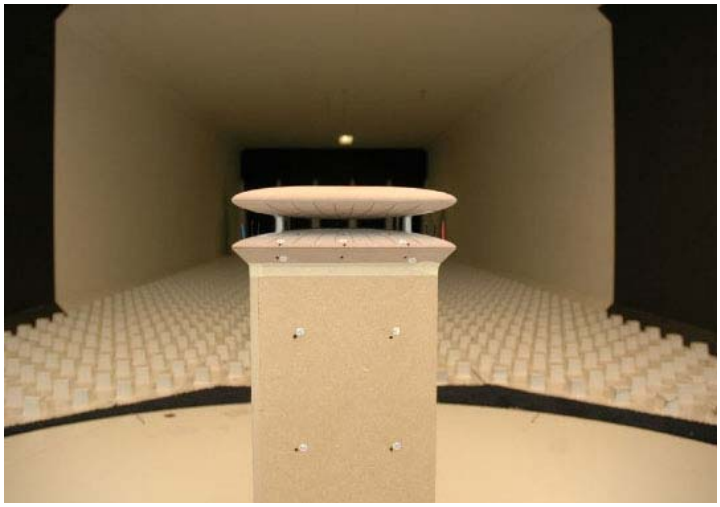

Figure 26.1: ‘venturi’ roof design by Bronsema in E,W&F research in the wind tunnel at Peutz in Mook.

In this project the principle was altered by reducing the upper scale of the ‘venturi’ roof. This principle was also used in roof design of the MoD by Deerns consulting engineers, on which the building case in this project is based (figure 8.1). In this project the void in the roof shape over the chimneys was used to create a contraction between the exhaust and the exhaust cover (figure 26.2). An advantage of this design that was found in CFD-analyses done by Doolaard is the fact that the lower scale in the contraction actual extends into the general roof shape of the building. In this way the air flow is fluently led up to the contraction which results in a larger under pressure than with a ‘venturi’ roof on top of a building such as in figure 26.1.

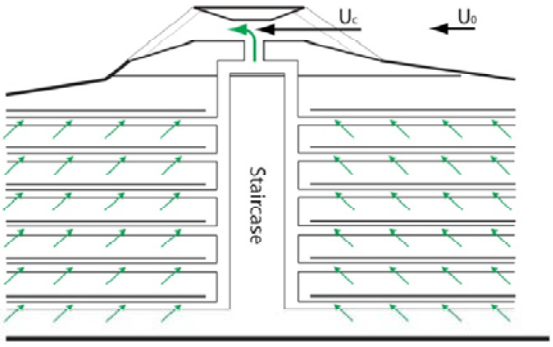

Figure 26.2: venturi-shaped contraction integrated in the roof design of the building.

Louvers in the ‘venturi’ roof

The area between the lower and upper roof is typically very large. In such a contraction all kinds of debris and birds can protrude. This could be prevented by placing louvers between the edges of the lower and upper scale of the roof. These louvers have to be placed in such a way that they do not obstruct air flow. This is typically a horizontal placement of the louvers.

In a CFD-analysis of louvers in a simplified 2D ‘venturi’ model (figure 26.3) it was found that the bottom louvers close to the lower scale could best be placed parallel with the lower scale surface or in other words parallel with the natural air flow towards the contraction. At the louvers a mesh could be placed to prevent birds from nesting in the ‘venturi’ roof.

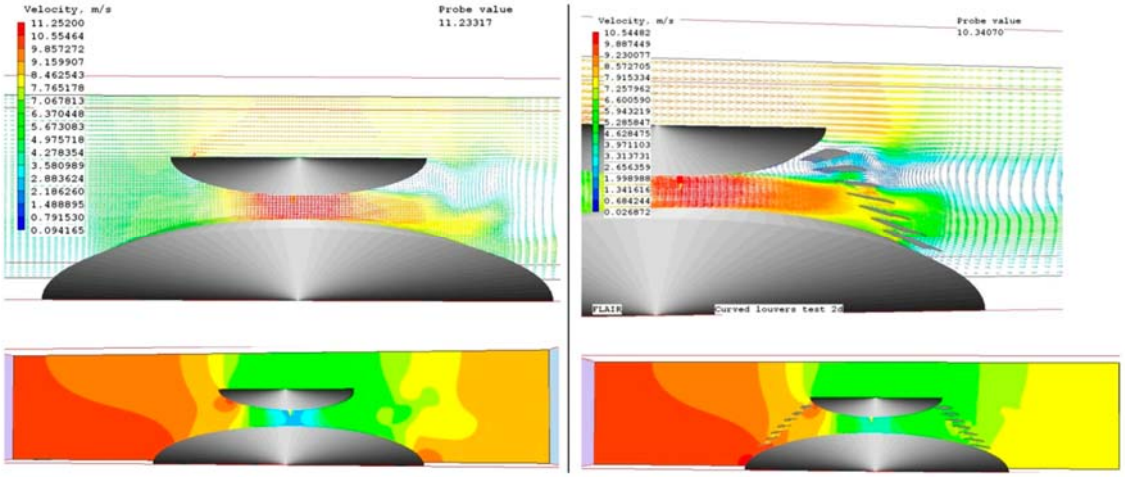

Figure 26.3: a) simple contraction model without louvers, b) model with curved louvers, the lower louvers are placed parallel with the flow direction found in the model without louvers. (retrieved from the internship report by H. Doolaard)

Influence of surrounding buildings

A building with ‘venturi’ roof is ideally higher than the surrounding buildings to obtain an unobstructed air flow towards the contraction. When the building is lower than its surroundings or of similar height, the air flow towards the contraction is obstructed and slowed down. In the Earth, Wind & Fire research regarding venturi-shaped roofs (Bronsema, November 2001,b) the effect of surrounding buildings is analyzed in the wind tunnel.

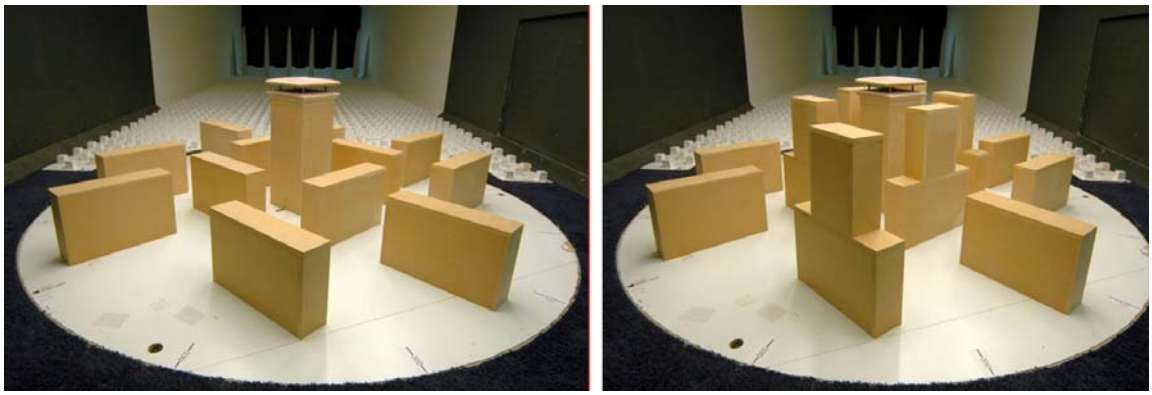

Figure 26.4: building with ‘venturi’ roof in the wind tunnel with surrounding building blocks, a) surroundings lower than ‘venturi’ roof, b) surroundings at similar height as ‘venturi’ roof

26.2: Small ‘venturi’ exhausts

The ‘venturi’ roof in this project has a big impact on the building structure and on the appearance of the building as can be seen in the cover illustration. A ‘venturi’ exhaust directly placed on the chimney also provides extra under pressure compared to a conventional exhaust but has less impact on the building and is easier to construct.

Distance of the 'venturi'-exhaust above the roof

Similar to the influence of surrounding buildings on the 'venturi' roof, the air flow towards the smaller 'venturi'-exhaust is influenced by the building it is placed on. Ideally the 'venturi'-exhaust is placed at significant distance above the roof of the building in order to obtain unobstructed air flow towards the exhaust from all wind directions. The extra height needed above the roof edge is actually extra stack height and therefore favorable for stack pressure in the chimney leading up to the exhaust. Additionally the solar chimney collector surface can be enlarged with the extra height needed above the roof edge.

Exhaust opening dimension

As described in paragraph 11.1, the ratio between the inflow height and the diameter of the exhaust opening is an important point to take into account. For example in this project with a maximum air velocity of 1m/s in the ducting the area of the exhaust is $4m^2$ for all three exhausts. The width of the exhaust opening is therefore 2 meters. With an inflow height of only 1 meter there is a risk that the exhaust opening becomes the 'path of least resistance' for the wind flow through the contraction, resulting in back flow into the exhaust. This could be solved by enlarging the width of the total 'venturi'-exhaust with which the ratio between the exhaust opening and the total construction becomes better. Also the exhaust opening could be reduced which increases the air velocity from the exhaust and increase the resistance for the flow path into the exhaust thereby preventing back flow.

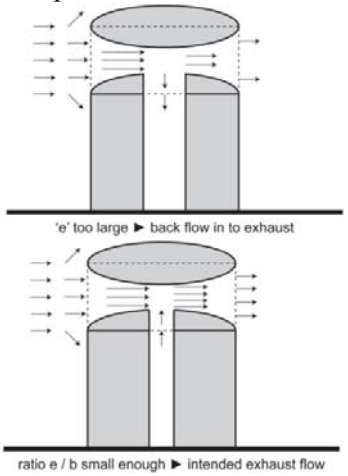

Figure 26.5: decreasing the exhaust opening or enlarging the width of the total construction both result in a better ratio between the width of the construction and the width of the exhaust.

26.3: Air intake and supply route

A correct placement of the air intake and a well designed supply route principle can profit from the wind pressure on the inlet openings and favorable buoyancy in the supply system.

Air intake placement on a flat facade

At a windward façade the largest wind pressure is at approximately 1/6 of the building height under the roof edge. At this so called stagnation height the air flow is split in an upward and downward flow. An air intake placed at this height will profit from the air flow perpendicular to the façade at this height. An air intake place further above this height will experience less over pressure. In practice an air intake can't always be placed at this stagnation height. When placed at the top of the building an air intake should not be placed directly under the roof edge or at the façade edge as the vortexes created at the edges could create suction on the inlet.

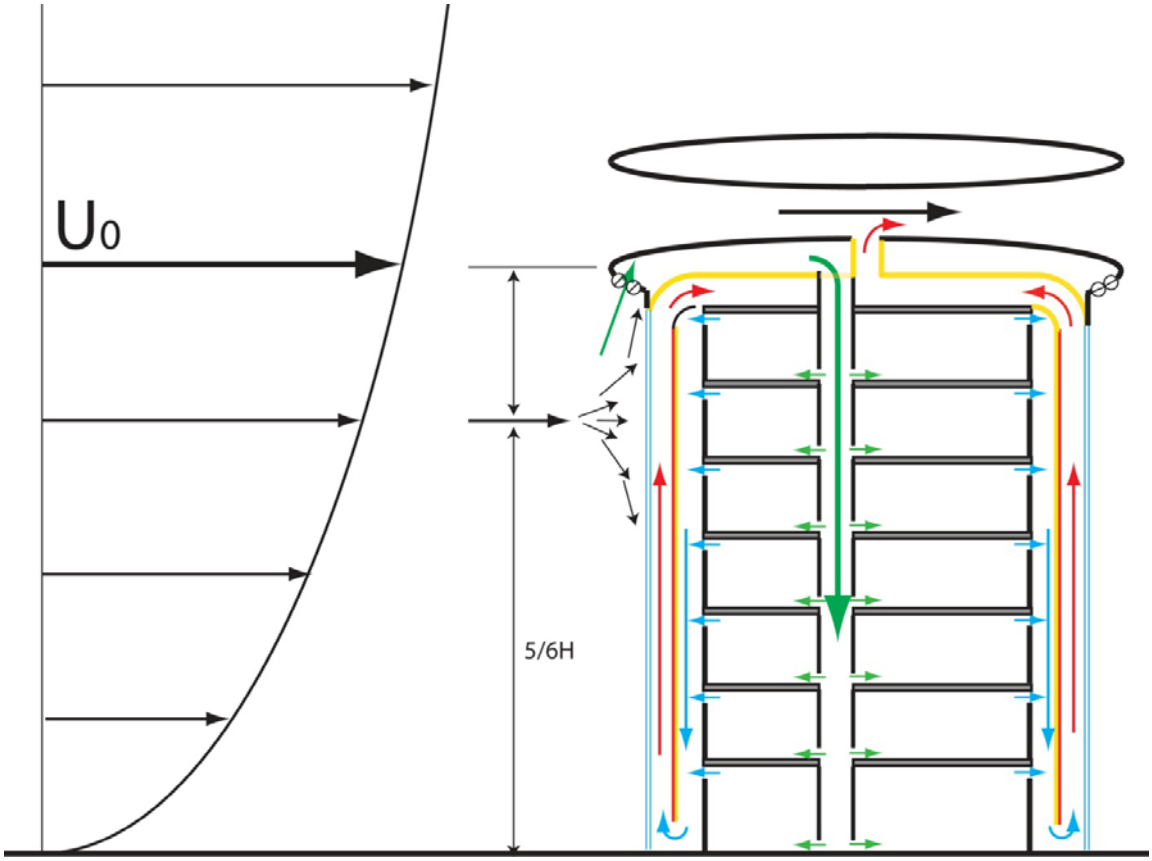

Figure 26.6: stagnation point at the windward façade at 1/6 of the building height under the roof edge and air intake placed under an overhang to 'catch' the wind flowing up along the facade

Plenum configuration and supply system design

The air intake placement influences the characteristics of the vertical supply system in the building. When placed at the top of the building, the air entering the system can't be centrally pre-heated at the top otherwise unfavorable buoyancy would be created in the supply shaft. Therefore the supply shaft in the building cases in this project is insulated and the air is pre-heated at every floor as shown in figure 11.7. When the air intakes are placed at the bottom of the building, favorable buoyancy can be created in the supply shaft by preheating the air at the bottom of the shaft. As the air is heated in this supply shaft, the supply shaft function could be mixed with a building zone such as an internal atrium or stairwell.

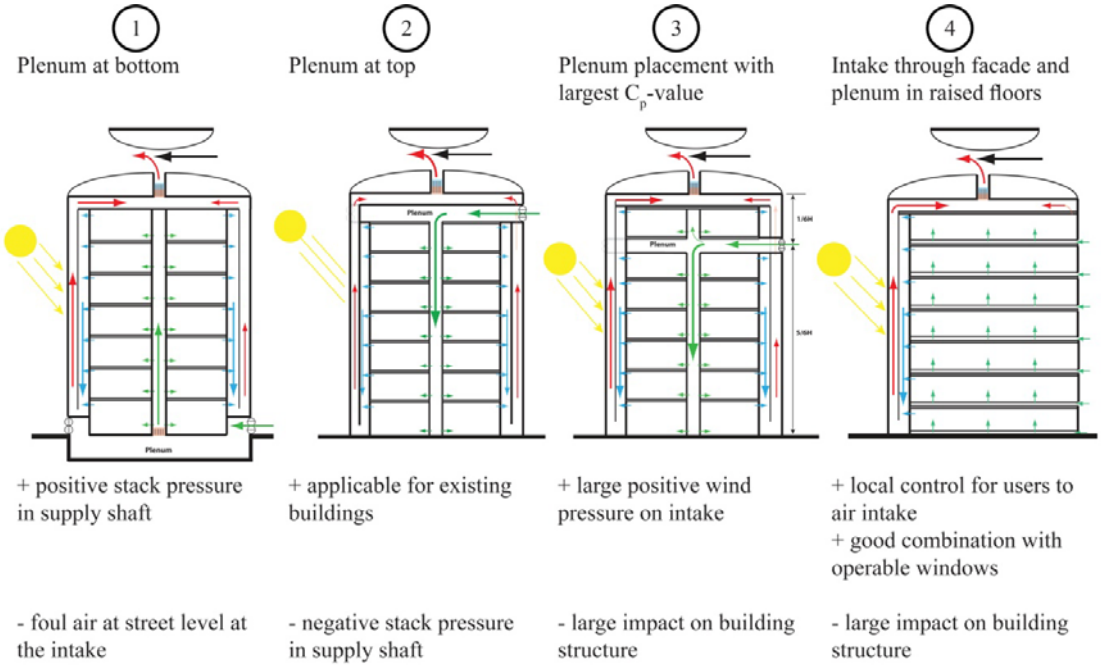

Figure 26.7: Different kinds of intake plenum and supply shaft configuration with their advantages and disadvantages.

Variant number 4) in figure 26.7 is one with air intake at every floor level into raised floors. In this configuration office compartments can be placed on top of the raised floors in which case it is possible to combine the natural ventilation principle with operable windows without losing robustness in the ventilation system by disturbance of the system by opened windows. The characteristics of such a system with natural ventilation and operable windows are described in paragraph 23.1 on risk management in case of operable windows.

Part 8: Conclusion

The general conclusions include the answers to the research questions, conclusions on the implementation of the investigated system and recommendations on possible follow up research.

Chapter 27: Answers to research questions.

The answer to the sub research questions are:

1) *For which configuration of shunt duct(s) and solar chimneys at the end of each office wing does the complex induce the largest resulting stack pressures?*

- A solar chimney in combination with a shunt duct is most effective while it provides even stack pressure over all connected office floors. A solar chimney with multiple orientations ranging from South-East to South-West provides the best performance throughout the day due to the multiple orientations which collect solar irradiation.

2) *What configuration of the venturi shaped exhaust in the given roof shape delivers the largest negative wind pressure coefficient at the exhaust*

A 'venturi' roof with a contraction ratio of 1:5 for the smallest contraction at the exhaust relative to the largest inflow height is ideal. Within the design boundary conditions of this project the 'venturi' roof with a contraction height of 2,5 and inflow height of 12,5m has an wind pressure coefficient of $C_{p,e}$ = -1,42.

The conclusion on the main research question is:

How much fan energy can be saved in an office building ventilated by solar chimneys and venturi-shaped exhausts during occupation time?

- Compared to the naturally ventilated reference building [case-0] with a pressure drop of 10Pa without solar chimneys and venturi-shaped exhaust the energy saving is ➔ 24,8 – 10,6 = 14,2kWh annually
- Compared to mechanical ventilation of the building case with a pressure drop of 10Pa the energy saving is ➔ 926,9 – 10,6 = 916,3kWh annually
- **Compared to mechanical ventilation of the building case with a pressure drop of 1.000Pa the energy saving is in the final design is ➔ 93.960 – 10,6 = 93.949kWh annually.**

The fan energy saving relative to the reference case, [case-0] are negligible. This implies that the greatest saving is due to the low pressure drop ventilation system of 10Pa.
Compared to a reference building with a pressure drop of 1.000Pa in the ventilation system the annual energy savings are significant.

Climate influence on solar chimneys – the latitude hypothesis

The results for the posed latitude hypothesis show that a vertically orientated solar chimney works best at high latitude. However this is largely due to the low external temperatures in high latitude climates. The largest relative solar contribution to the driving pressure of the solar chimney for the investigated climates is found in Spain with lower latitude. It can be expected that with lower latitude the relative solar contribution to stack pressure increases while external temperature rises.

Chapter 28: General conclusions

28.1: Low pressure drop ventilation systems

It is found that by far the largest contribution to fan energy saving is reached by applying a low pressure drop ventilation system. While natural driving forces are significantly lower than driving pressures used in conventional mechanically ventilated buildings with extensive amounts of building services, it is even more important to create a system with a low pressure drop with natural ventilation

28.2: Thermal buoyancy and solar chimneys

From the results in this project is concluded that the largest part of stack pressure in the solar chimneys is due to conventional thermal buoyancy, hence temperature difference between the interior and exterior. The solar contribution in a solar chimney plus shunt duct is in The Netherlands typically around 10% of the total stack pressure for a South-West to South-East orientated chimney. The solar energy is needed as impulse to transport the stale air from the office floors down to the bottom of the solar chimney. When this impulse is provided by the sun, every office floor will experience equal stack pressure. In a solar chimney without shunt duct the positive effect of the sun on stack pressure is negligible.

For the implementation of solar chimneys a lot of things which determine the applicability are still uncertain in building practice. As seen in the energy saving results in the research question, the extra fan energy saving compared to a low pressure drop system is very low. When a solar chimney is applied it is recommended that the solar energy captured in the chimney is recovered together with the thermal energy in the exhaust air while heat recovery in the exhaust flow is very common in the building practice. In potential, a significant amount of solar energy could be harvested in the solar chimneys.

28.2: 'venturi' exhausts

The main conclusion from this research on the applicability of the 'venturi'-exhaust is that a 'venturi'-exhaust is advisable when it can be placed in a built environment where it is higher than its direct built environment to have unobstructed air flow. In general a 'venturi'-exhaust will provide a significant fan energy saving. While a 'venturi' roof is more effective than a local, smaller 'venturi'-exhaust, it has a large impact on the building design and structure. In building practice the smaller 'venturi'-exhaust will be easier applicable.

Chapter 29: Recommendations for follow up research.

29.1: Heat recovery in solar chimneys

The implementation of solar chimneys plus shunt duct is found only to be worthwhile when combined with heat recovery of the thermal energy from the exhaust air plus the solar energy captured in the solar chimney. Further research could be done on the influence of the heat recovery system on the buoyancy in the chimney. For the heat exchanger in the chimney, a very low pressure drop system has to be chosen or developed in order not to let it exceed the typical driving pressure in the chimney which would diminish fan energy saving significantly. Furthermore the behavior of the air flow in the chimney around the heat recovery has to be investigated. While the heat recovery extracts thermal energy from the air, temperature will drop which will alter thermal buoyancy in the air flow after it has passed the heat recovery.

29.2: Robustness of natural ventilation in combination with operable windows

The robustness of a natural ventilation system driven only by natural driving forces could be assessed. Especially in combination with operable windows a natural ventilation system could be easily disturbed when designed in the wrong way. While the driving forces in a natural ventilation system are small, the principle flow pattern can easily be disturbed. The assessment of natural ventilation in combination with operable windows is important because of the significance of operable windows on thermal comfort in the building and because of the developments in sustainability assessment such as BREEAM towards ‘natural ventilation’ in which the definition of natural ventilation is closely related to occupant control and operable windows.

29.3: Volume flow control in low pressure ventilation systems

Further research could also be done on volume flow control in the ventilation system in order to decrease high heating energy demands due to excessively large ventilation rates which occur in an uncontrolled ventilation system such as the building cases in this project. This would be a research topic focused on controls engineering and the development of valves which are robust and react to small pressure differences in order to cope with the typically small pressure differences in natural ventilation.

References

CIBSE guide, *Natural ventilation in domestic buildings*, CIBSE (2005) 36-59

L. Aanen, B. Blocken, B.Bronsema, T. van Hoof, *A venturi-shaped roof for wind-induced natural ventilation of buildings: wind tunnel and CFD evaluation of different design configurations*, publication Building and Environment (February 2011)

H.E.A. van den Akker, R.F. Mudde, *Physishe transport verschijnselen*, VSSD (2003)

C. Biggs, B.Khan, S.B. Riffat, Y. Su, *Performance testing and comparison of turbine ventilators*, Science direct – Elsevier (march 2011)

B. Blocken, T. van Hooff, L. Aanen, B. Bronsema, *Computational analysis of the performance of a venturi-shaped roof for natural ventilation: venturi-effect versus wind-blocking effect*, Computers & Fluids (26 April 2011)

B. Bronsema, *"Earth, Wind and Fire" airconditioning zonder ventilatoren (I) Thema Fire: Onderzoek zonneschoorsteen / Zonnefacade©,* TU Delft, (November 2011,a)

B. Bronsema, *"Earth, Wind and Fire" airconditioning zonder ventilatoren (II) Thema Wind: Onderzoek natuurlijke ventilatie, wind en het Ventecdak©,* TU Delft, (November 2011,b)

G.J. de Bruin-Hordijk, M. van den Voorden, *Geventileerde gevels*, Faculteit Bouwkunde –TU Delft (2000)

D. Clements-Croome, *Naturally ventilated buildings – Building for the senses, economy and society*, E&FN Spon (1997)

M. Cook, B. Krausse, K. Lomas, *Environmental performance of a naturally ventilated city central library*, Science Direct – Elsevier (2007)

H.J. Doolaard, *Natural ventilation using venturi chimneys*, TU Delft – Faculty of Applied Physics / Deerns – internship report (November 2011)

P.J.W. van den Engel, *Thermisch comfort en ventilatie-efficiency door inducerende ventilatie via de gevel*, Publikatieburo Bouwkunde, TU Delft (1995)

I.E. Idelchik, *Handbook of Hydraulic Resistance* – 3rd edition, Jaico Publishing house, (2005)

ISSO-publicatie 74, *Thermische behaaglijkheid, eisen voor de binnentemperatuur in gebouwen*, ISSO, (2004)

ISSO-publicatie 17, Kwaliteitseisen *voor luchtkanaalsystemen in woning- en utiliteitsbouw*, (2010)

N. Khan, S.B. Riffat, Y. Su, *A review on wind driven ventilation techniques*, Science Direct – Elsevier (2008)

Kurvers, S. *Thermisch comfort in gebouwen*, Kennisbank bouwfysica TU Delft (version 19-10-2011)

Liddament, M.W. *Air infiltration calculation techniques – An applications guide*, Air infiltration and ventilation centre (1986)
H. Recknagel, E. Sprenger, E.-R Schramek, Der Reckagel 2011/2012 – Tashenbuch für Heizung und Klimatechnik, (2011)

Senter Novum, *Cijfers en tabellen 2007*, VROM (2007)

C.A. Short, K.J. Lomas, A. Woods, *Design strategy for low-energy ventilation and cooling within an urban heat island*, (online publication, 3 February 2007)

Appendices

[Appendix A]: Example of analytical model of solar chimney in MS-Excel

solar chimney (rectangular configuration)

Uniform temperature in zones

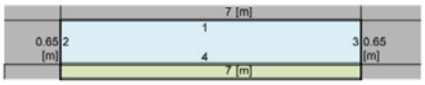

Basic data

gravitation	9.81	[m/s]	
σ	5.67E-08	[-]	
ρ_ref	1.2041	[kg/m3]	
T_ref	20	[°c]	293 [K]

geometry data

width	7	[m]
depth	0.65	[m]
height	28.5	[m]
area	4.55	[m]

view factors

ϕ1->4	0.911444828	[-]	1
ϕ1->2 = ϕ1->3	0.044277586	[-]	
ϕ2->3	0.046328919	[-]	1
ϕ2->4 = ϕ2->1	0.476835541	[-]	
ϕ3->2	0.046328919	[-]	1
ϕ3->4 = ϕ3->1	0.476835541	[-]	

exchange factors

ψ1->4	0.863902079	[-]
ψ2->4	0.843305118	[-]
ψ3->4	0.843305118	[-]

Corrected dimensions

W*rad	7.143611204	[m]
W*conv	8.3	[m]

heat transfer coefficients

α_rad	0.3327	[W/m2K]	α_rad_bronsema	=4*eps_w*sigma*((Twall+Tglass)/2)^3
h_c,m,glass	10.339	[W/m2K]	h_c,m,gl_bronsema	=3,98*v^0,8+0,042*v^-1,55*(Tglass-T∞,avg)
h_c,m,wall	10.491	[W/m2K]	h_c,m,w_bronsema	=3,98*v^0,8+0,042*v^-1,55*(Twall-T∞,avg)
h_c,m,glass	37.219	[(kJ/h)/m2K]	used in TRNSYS-TRNFLOW	
h_c,m,wall	37.768	[(kJ/h)/m2K]	used in TRNSYS-TRNFLOW	
α_i	7.8	[W/m2K]		
α*_e	15	[W/m2K]		
α_i	28.08	[(kJ/h)/m2K]	used in TRNSYS-TRNFLOW	
α*_e	54	[(kJ/h)/m2K]	used in TRNSYS-TRNFLOW	

Climate data

Ti	22	[°c]	295 [K]
Te	10	[°c]	283 [K]
Φsolar,vertical	400	[W/m2]	

flow properties

Qv	15.0000	[m3/s]
v	3.2967	[m/s]
rho_i	1.19593661	[kg/m3]
c	1000	[J/kgK]
rho.c	1195.93661	[J/m3]

glass properties

Type	planitherm solar		
Uglass	1.281	[W/m2K]	
ZTA	0.761	[-]	
alpha_glass	1.6328	[W/m2K]	Rc_glass 0.61243 [m2K/W]
α_glass	0.05	[-]	
ε_glass	0.87	[-]	

absorber wall properties

Type	Mirotherm		
Uwall	0.25	[W/m2K]	
alpha_wall	0.260650196	[W/m2K]	Rc_wall 3.83656 [m2K/W]
α_wall	0.95	[-]	
ε_wall	0.05	[-]	
Rc, wall	3.8366	[m2K/W]	used in TRNSYS
U,wall	0.2497	[W/m2K]	used in TRNSYS

Mirotherm

lambda	202.8	[W/mK]
lambda,(kJ/h)/mK	730	[(kJ/h)/mK]
thickness	1	[mm]
r,layer	4.93151E-06	[m2K/W]
rho	2700	[kg/m3]
c	880	[J/kg K]
c,(kJ/kgK)	0.88	[kJ/kg K]

Rockwool Rockfit 434

lamda	0.034	[W/mK]
lambda,(kJ/h)/mK	0.1224	[(kJ/h)/mK]
thickness	60	[mm]
r,layer	1.764705882	[m2K/W]
rho	70	[kg/m3]
c	1030	[J/kg K]
c,(kJ/kgK)	1.03	[kJ/kg K]

Plywood

lamda	0.1	[W/mK]
lambda,(kJ/h)/mK	0.36	[(kJ/h)/mK]
thickness	25	[mm]
r,layer	0.25	[m2K/W]
rho	350	[kg/m3]
c	1880	[J/kg K]
c,(kJ/kgK)	1.88	[kJ/kg K]

wood cement board

lamda	0.35	[W/mK]
lambda,(kJ/h)/mK	1.26	[(kJ/h)/mK]
thickness	20	[mm]
r,layer	0.057142857	[m2K/W]
rho	1250	[kg/m3]
c	2000	[J/kg K]
c,(kJ/kgK)	2.00	[kJ/kg K]

exchange factor matrix

[A]		
1	-0.04206	-0.04206
-0.45299	1	-0.04401
-0.45299	-0.04401	1
[B]		
0.793		
0.415		
0.415		
[A]^-1		
1.041519	0.045827	0.045827
0.493523	1.023656	0.065813
0.493523	0.065813	1.023656
	[x]	
ψ1->4	0.863902	
ψ2->4	0.843305	
ψ3->4	0.843305	

Solar chimney temperature matrix

Tes	Tglass	Tout	Tabs	Tis
[Y]				
-3318.25	325.75	0.00	0.00	0.00
325.75	-2456.06	2062.57	67.73	0.00
0.00	2062.57	-22483.29	2481.67	0.00
0.00	67.73	2481.67	-2611.06	61.66
0.00	0.00	0.00	61.66	-1906.75
[Z]				
-850867.5	Te + Qsol			
0.0	0.00000			
-5292019.5	Ti * Qv			
-57691.4	Qsol			
-544301.6	Ti			
[Y]^-1				
-0.00031	-0.00004	0.00000	-0.00001	0.00000
-0.00004	-0.00046	-0.00005	-0.00006	0.00000
0.00000	-0.00005	-0.00005	-0.00005	0.00000
-0.00001	-0.00006	-0.00005	-0.00044	-0.00001
0.00000	0.00000	0.00000	-0.00001	-0.00052
	[x]			

Tes	285.6	[K]	12.6	[°c]
Tglass	296.9	[K]	23.9	[°c]
T∞,out	297.9	[K]	24.9	[°c]
Tabs	319.9	[K]	46.9	[°c]
Tis	295.8	[K]	22.8	[°c]
T∞,avg	296.5	[K]	23.5	[°c]

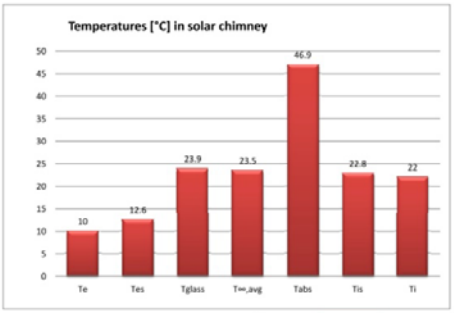

possitive flow pattern

T∞,out	24.9	[°c]
Pstack	15.83	[Pa]

Qsol*A_glass*(H*W) + alpha_e*(Te-Tes)*(H*W)	=	alpha_glass*(Tes-Tglass)*(H*W)
alpha_glass*(Tes-Tglass)*(H*W)	=	h_cm_gl*(Tglass-Tair)*(H*W) + alpha_rad*(Tglass-Tabs)*(H*Wrad)
h_cm_gl*(Tglass-Tair)*(H*W) + rho.c*Qv*Ti	=	h_cm_abs*(Tair-Tabsl)*(H*Wconv) + rho.c*Qv*Tair
Qsol*ZTA*A_abs*(H*W) + h_cm_abs*(Tair-Tabs)*(H*Wconv) + alpha_rad*(Tglass-Tabs)*(H*Wrad)	=	alpha_abs*(Tabs-Tis)*(H*Wconv)
alpha_abs*(Twall-Tis)*(H*Wconv)	=	alpha_i*(Tis-Ti)*(H*Wconv)

[Appendix B]: Boundary conditions building cases

Boundary conditions

People

workspace	10	m2
gain (seated) ISO-7730	150	W
sensibel heat	75	W
Latent heat	75	W
gain per m2	15	W/m2

LBK_case[0]

N_OFF / SE_OFF / SW_OFF

total BVO	362.93	m2
volume	1270.255	m2
%BVO ooc. as workspace	86%	
BVO occupied	312.1198	m2
people	31	#
Qv	1560.599	m3/h
Qv	0.4335	m3/s
personel gain	4681.797	W

Average occupation	0.649	has to be 0,65

CH (Center Hall)

total BVO	539.56	m2
volume	1888.46	m2
%BVO occ. as workspace	25%	
BVO occupied	134.89	m2
people	13	#
Qv	674.45	m3/h
Qv	0.187347	m3/s
personel gain	4210.184	W

Occupation of building Zones

BVO per floor	1651.25	m2
average occupation	65%	NEN-
Ventilated floor area	1073.31	m2
Nett area OFF	1088.79	m2
occupation	86%	
occupied area OFF	936.36	m2
Nett area CH	539.56	m2
occupation	25%	
occupied area CH	134.89	m2
Total occupied area	1071.25	m2/floor

Appliences

computers	0.1	piece/m2
power	140	W/piece
heat production	14	W/m2

printer/ copier	1	piece/ office wing
heat production	50	W/ office wing

Artificial light

power	8	W/m2 (electric output)	
heat production	8	W/m2	
convective part	40	%	Fluorescent lamp

Concrete core activation

Heating	60	W/m2	216	kJ/(hr*m2)
cooling	60	W/m2	216	kJ/(hr*m2)
specific N_OFF/ SE_OFF/ SW_OFF				
Heating power	21775.8	W	78393	kJ/hr
Cooling power	21775.8	W	78393	kJ/hr
specific CH				
Heating power	32373.6	W	116545	kJ/hr
Cooling power	32373.6	W	116545	kJ/hr

Input in TRNYS type56b-TrnFlow building module

Schedule Types

DAYNIGHT	start	end	on/off
morning	0:00	7:00	0
day	7:00	19:00	1
evening	19:00	0:00	0
WORKDAY			
morning	0:00	8:00	0
day	8:00	19:00	1
evening	19:00	0:00	0
WEEKEND			
DAY	1	5	1
DAY	6	7	0
WORKLIGHT			
morning	0:00	8:00	0
day	8:00	19:00	1
evening	19:00	0:00	0

LIGHT	
Monday	WORKLIGHT
Tuesday	WORKLIGHT
Wednesday	WORKLIGHT
Thursday	WORKLIGHT
Friday	WORKLIGHT
Saturday	WEEKEND
Sunday	WEEKEND
SETOFF	
Monday	DAYNIGHT
Tuesday	DAYNIGHT
Wednesday	DAYNIGHT
Thursday	DAYNIGHT
Friday	DAYNIGHT
Saturday	WEEKEND
Sunday	WEEKEND
USE	
Monday	WORKDAY
Tuesday	WORKDAY
Wednesday	WORKDAY
Thursday	WORKDAY
Friday	WORKDAY
Saturday	WEEKEND
Sunday	WEEKEND

Gain Types

GAIN_LIGHT				
total	10	W/m2	36	kJ/(hr*m2)
radiative	6	W/m2	21.6	kJ/(hr*m2)
convective	4	W/m2	14.4	kJ/(hr*m2)
Schedule	"SETOFF"			
GAIN_PEOPLE				
per person	150	W	540	kJ/hr
per m2	15	W	54	kJ/hr
N_OFF etc.	12.9	W/m2	46.44	kJ/(hr*m2)
CH_0 etc.	3.75	W/m2	13.5	kJ/(hr*m2)
Schedule	"SETOFF"			
GAIN_COMP				
computers	14	W/m2	50.4	kJ/(hr*m2)
N_OFF etc.	12.04	W/m2	43.344	kJ/(hr*m2)
CH_0 etc.	3.5	W/m2	12.6	kJ/(hr*m2)
Schedule	"SETOFF"			
GAIN_COPY				
printer/copier	50	W	180	kJ/hr
one for each office wing (N_OFF / SE_OFF / SW_OFF)				
Schedule	"SETOFF"			

heating & cooling types

CCA_CH	(center hall zones)				set point
Heating power	32373.6	W	116545	kJ/hr	Ti <20
Cooling power	32373.6	W	116545	kJ/hr	Ti >24
radiative part	60	%			
Schedule	"SETOFF"				
CCA_OFF	(office wing zones)				
Heating power	21775.8	W	78392.9	kJ/hr	Ti < 20
Cooling power	21775.8	W	78392.9	kJ/hr	Ti >24
radiative part	60	%			
Schedule	"SETOFF"				

pre heating in CCA_CH					%	radiative part
floor heating	32374	W	116545	kJ/hr	28.8	0.6
pre heating air	80000	W	288000	kJ/hr	71.2	0.0
total	112374	W	404545	kJ/hr	100	0.2

[Appendix C]: Loss factors and C_{di} for ventilation elements in TRNSYS-TrnFlow

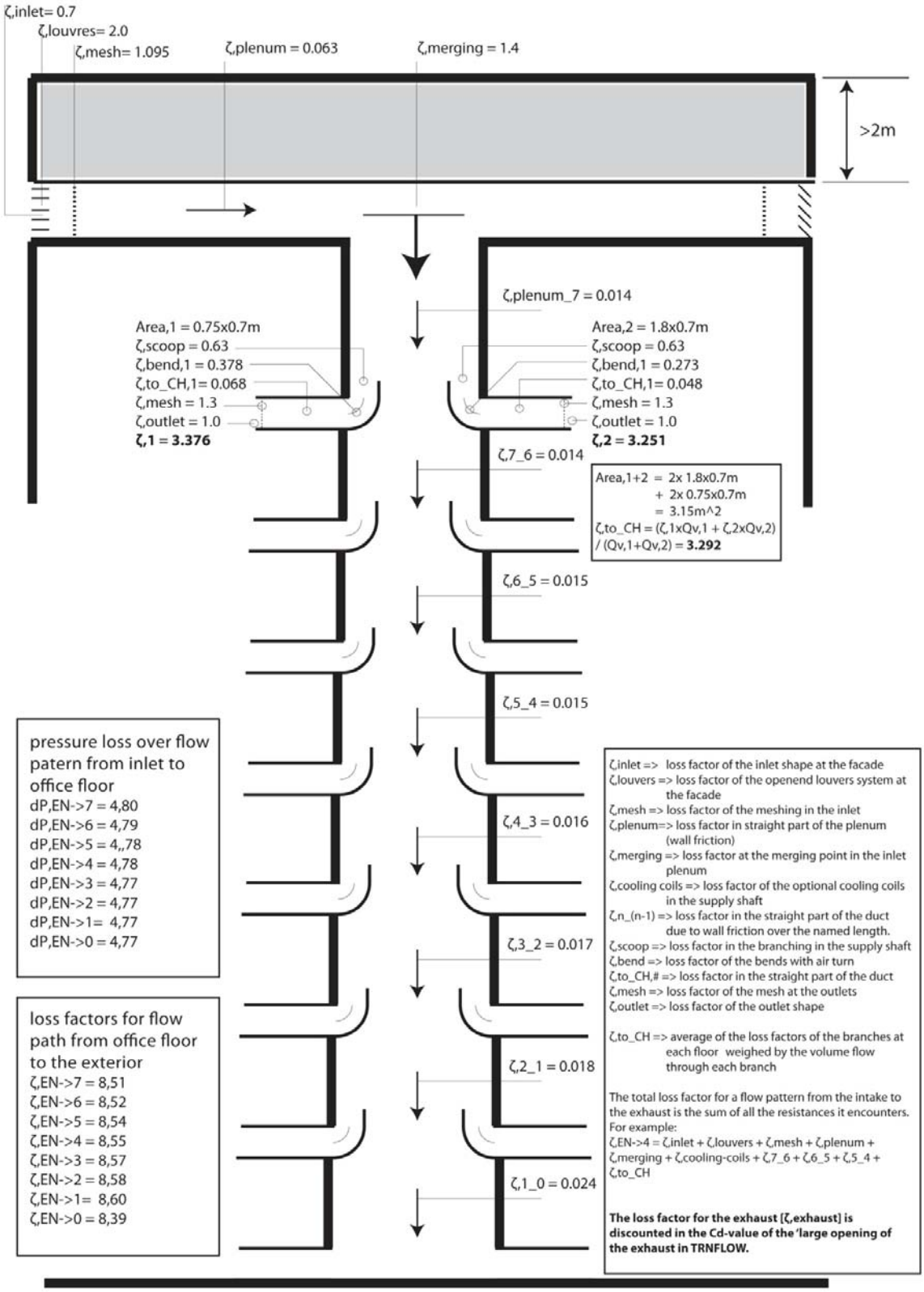

Supply shaft loss factors and static pressure loss

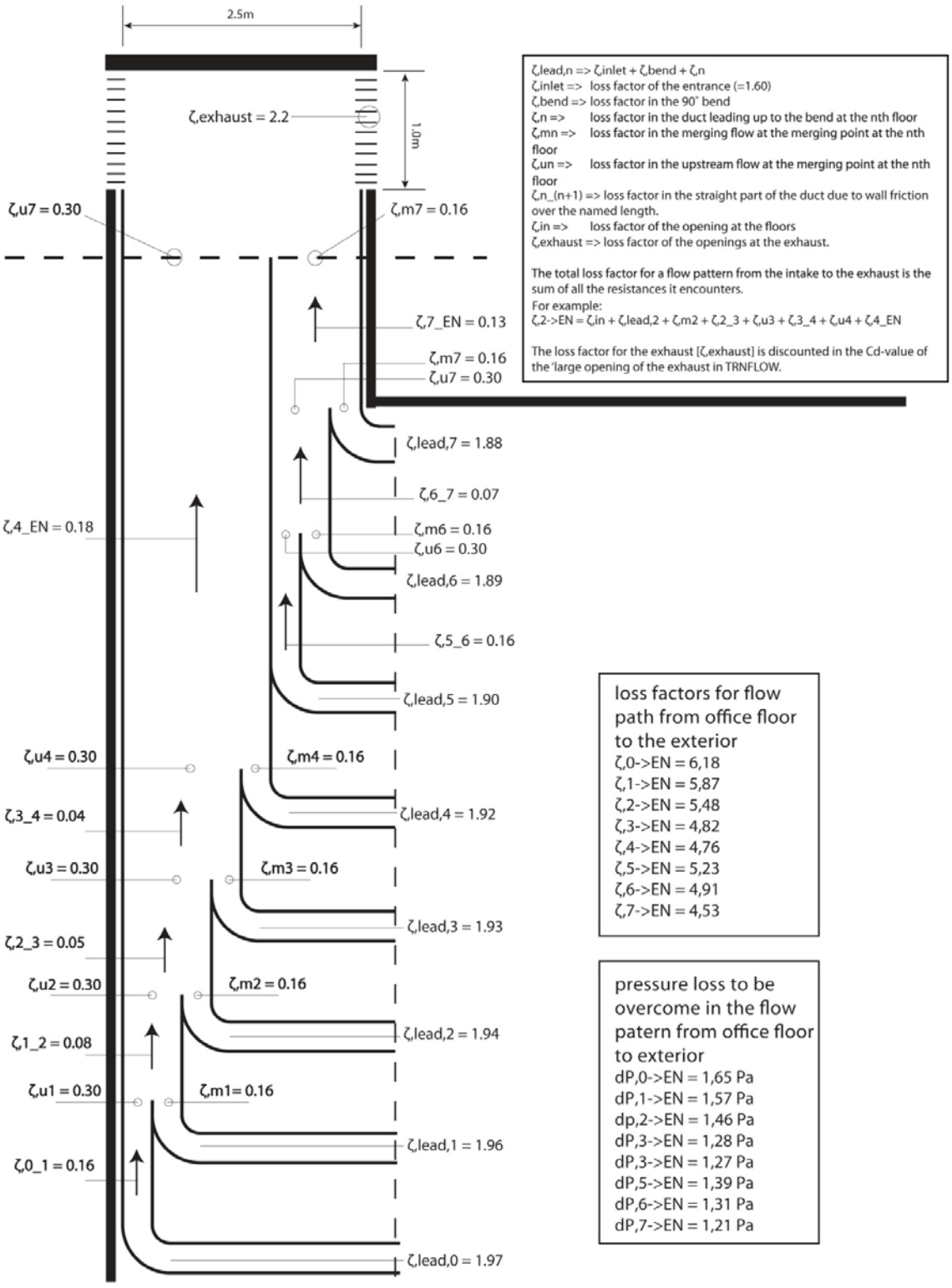

[case-0] conventional chimney loss factors and static pressure loss

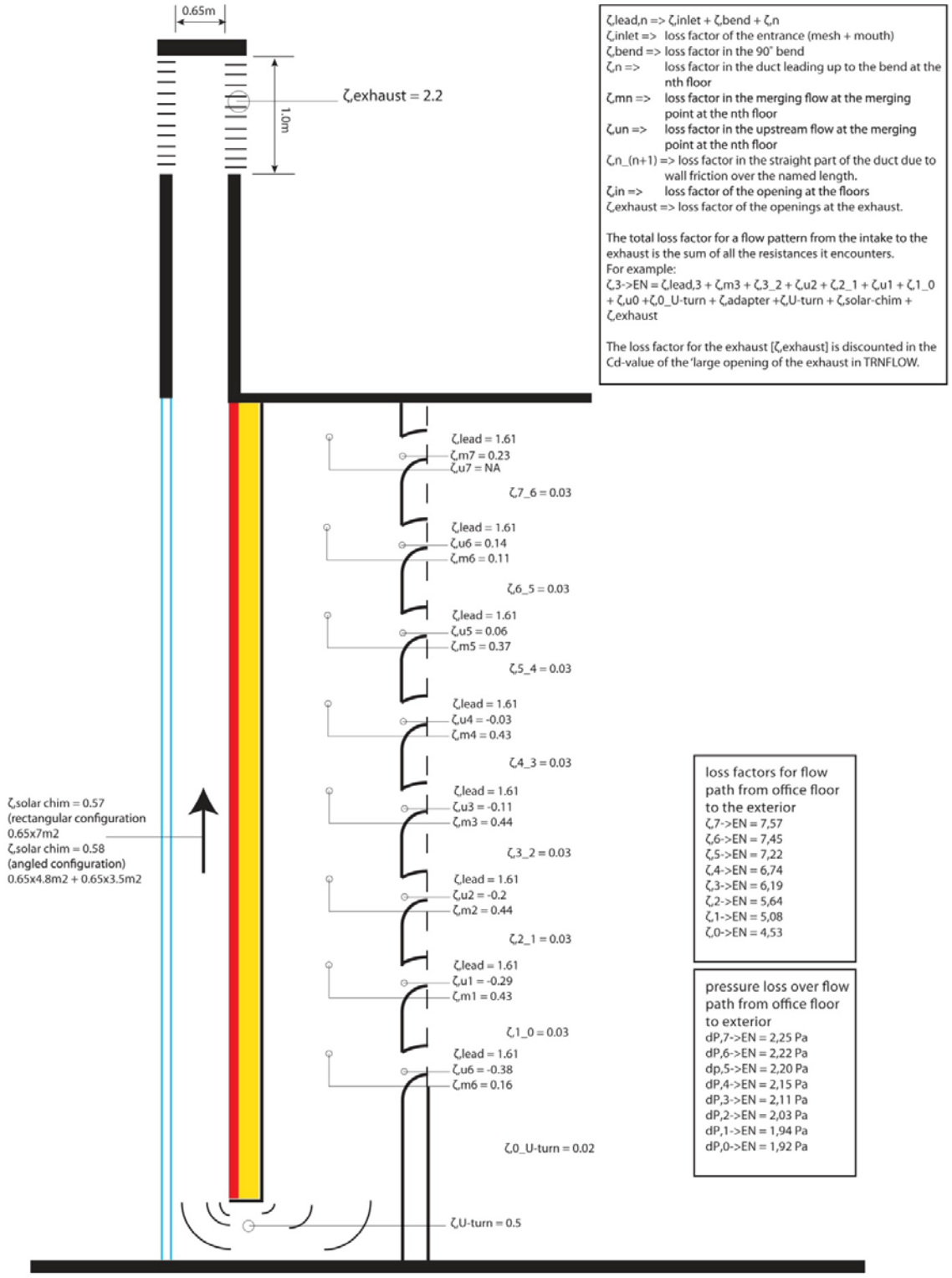

[case-1A] chimney plus shunt duct loss factors and static pressure loss

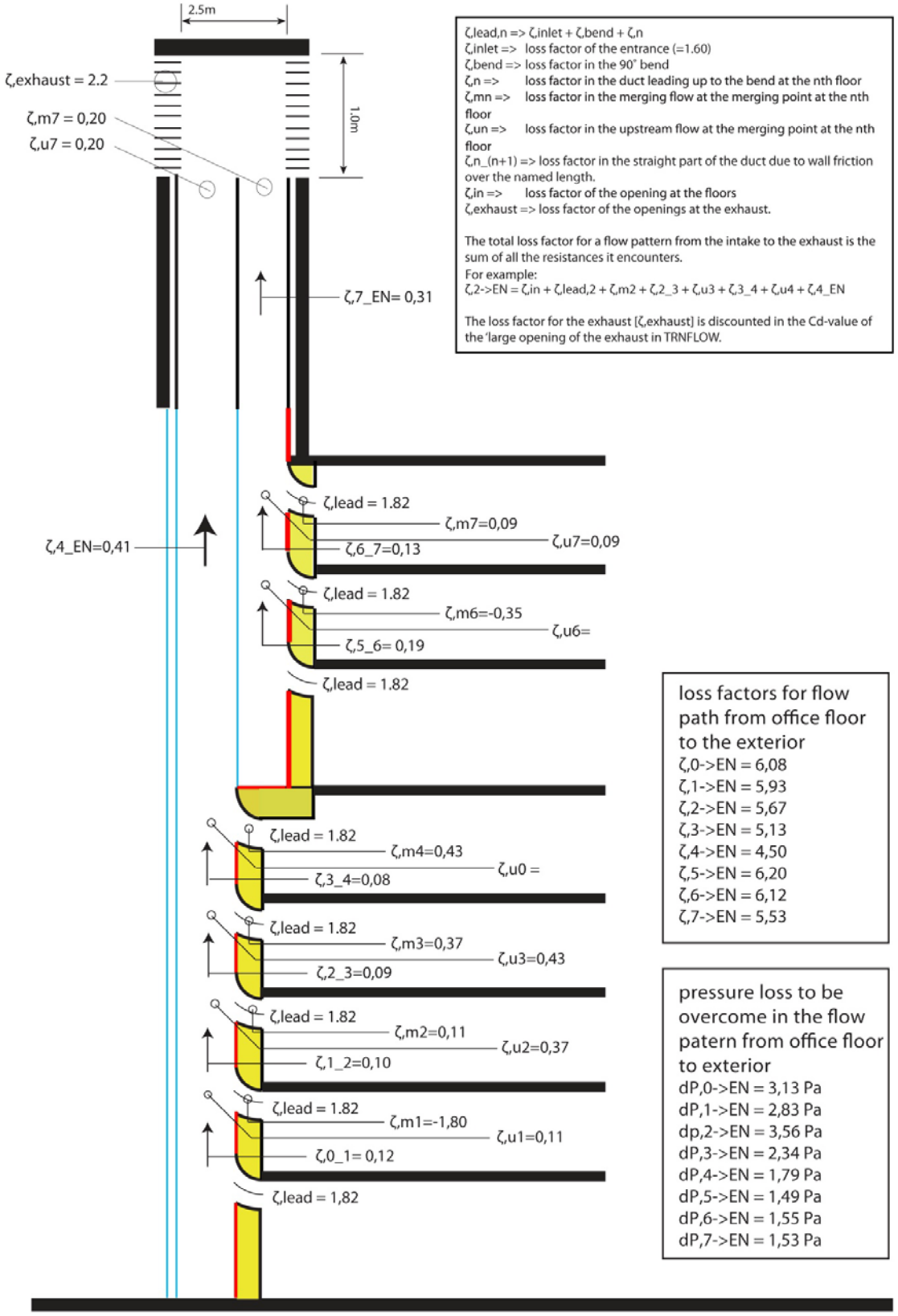

[case-1B] partitioned solar chimney loss factors and static pressure loss

[Appendix D]: Complete results for the building cases

[case-0]- results in office occupation

Volume flow	North office wing							South-East office wing							South-West office wing						
office floor	0th	1st	2nd	3rd	4th	5th	6th	7th	0th	1st	2nd	3rd	4th	5th	6th	7th	0th	1st	2nd	3rd	4th	5th	6th	7th
	[m3/s]	[m3/s]	[m3/s]	[m3/s]	[m3/s]	[m3/s]	[m3/s]	[m3/s]	[m3/s]	[m3/s]	[m3/s]	[m3/s]	[m3/s]	[m3/s]	[m3/s]	[m3/s]	[m3/s]	[m3/s]	[m3/s]	[m3/s]	[m3/s]	[m3/s]	[m3/s]	[m3/s]
maximum in occ.	2.13	2.28	2.46	2.61	2.90	2.96	3.11	3.25	2.26	2.44	2.64	2.81	3.12	3.21	3.38	3.54	2.06	2.21	2.39	2.54	2.82	2.89	3.05	3.21
minimum in occ.	-1.01	-1.04	-1.07	-1.06	-1.09	-1.16	-1.26	-1.36	-1.03	-1.06	-1.08	-1.07	-1.09	-1.24	-1.34	-1.45	-1.04	-1.07	-1.09	-1.08	-1.10	-1.13	-1.02	-1.10
average in occ.	0.87	0.90	0.93	0.94	0.98	0.96	0.91	0.85	0.85	0.87	0.89	0.89	0.92	0.89	0.83	0.74	0.86	0.89	0.92	0.92	0.95	0.94	0.89	0.81
st. dev. In occ.	0.29	0.30	0.31	0.32	0.35	0.41	0.42	0.43	0.29	0.30	0.31	0.32	0.35	0.41	0.41	0.41	0.29	0.30	0.31	0.32	0.34	0.39	0.39	0.40
	[%]	[%]	[%]	[%]	[%]	[%]	[%]	[%]	[%]	[%]	[%]	[%]	[%]	[%]	[%]	[%]	[%]	[%]	[%]	[%]	[%]	[%]	[%]	[%]
RSD [%]	33	33	34	35	36	43	46	51	34	35	35	36	38	46	49	56	33	33	34	35	36	41	44	49
Qv>0,5m3/s [%]	90.0	90.7	91.4	91.5	92.1	91.0	89.4	85.6	88.6	89.3	90.2	90.2	90.6	88.9	86.3	79.8	89.8	90.7	91.5	91.6	92.2	91.4	89.6	84.9
Total driving pressure																								
	[Pa]	[Pa]	[Pa]	[Pa]	[Pa]	[Pa]	[Pa]	[Pa]	[Pa]	[Pa]	[Pa]	[Pa]	[Pa]	[Pa]	[Pa]	[Pa]	[Pa]	[Pa]	[Pa]	[Pa]	[Pa]	[Pa]	[Pa]	[Pa]
maximum in occ.	179.0	175.2	171.4	167.6	163.8	160.1	156.3	152.5	186.1	182.8	179.4	176.0	172.6	168.4	165.2	162.0	184.3	180.3	176.4	172.4	168.5	165.1	161.0	156.9
minimum in occ.	-20.1	-17.1	-14.5	-11.9	-9.3	-7.6	-6.2	-5.7	-4.8	-3.9	-3.2	-2.6	-1.9	-7.6	-4.9	-3.4	-4.3	-3.5	-2.8	-2.2	-1.5	-7.5	-4.8	-3.2
average in occ.	25.0	23.2	21.3	19.5	17.6	15.7	13.9	12.0	24.0	22.1	20.2	18.4	16.5	14.5	12.7	10.8	24.6	22.7	20.9	19.0	17.1	15.1	13.3	11.4
st. dev. In occ.	16.2	15.6	15.1	14.6	14.2	13.8	13.5	13.3	15.4	14.7	14.2	13.6	13.2	12.8	12.5	12.3	15.7	15.1	14.6	14.1	13.6	13.2	12.9	12.7
	[%]	[%]	[%]	[%]	[%]	[%]	[%]	[%]	[%]	[%]	[%]	[%]	[%]	[%]	[%]	[%]	[%]	[%]	[%]	[%]	[%]	[%]	[%]	[%]
RSD [%]	65	67	71	75	80	88	97	110	64	67	70	74	80	88	98	113	64	67	70	74	80	87	97	111
% of occ. Δp>0Pa	99.8	99.8	99.8	99.8	99.8	99.1	99.1	98.9	99.7	99.7	99.7	99.7	99.7	98.7	98.8	98.4	99.7	99.8	99.8	99.8	99.8	98.9	99.0	98.8
% of occ. Δp>5Pa	95.3	94.6	93.8	91.9	89.5	85.2	79.1	67.4	94.8	94.1	93.1	91.1	88.1	83.5	75.9	62.5	95.0	94.4	93.6	91.8	89.1	84.9	77.8	64.6
% of occ. Δp>10Pa	84.5	82.0	79.2	74.9	68.5	59.2	47.3	36.2	83.1	80.5	77.3	72.5	65.7	55.4	43.3	32.5	84.1	81.6	78.5	74.0	67.4	57.3	44.9	34.3
% of occ. Δp>20Pa	56.7	50.6	43.3	35.8	29.2	23.8	20.3	17.9	54.3	47.9	40.5	32.9	26.1	20.6	17.3	14.6	55.3	48.9	41.5	34.2	27.6	22.1	19.1	16.8
Fan energy consumption																								
	[kWh]	[kWh]	[kWh]	[kWh]	[kWh]	[kWh]	[kWh]	[kWh]	[kWh]	[kWh]	[kWh]	[kWh]	[kWh]	[kWh]	[kWh]	[kWh]	[kWh]	[kWh]	[kWh]	[kWh]	[kWh]	[kWh]	[kWh]	[kWh]
Fan energy per floor 100% mechanical	39.1	37.4	35.9	35.2	33.1	32.1	31.3	30.6	39.1	37.4	35.9	35.2	33.1	32.1	31.3	30.6	39.1	37.4	35.9	35.2	33.1	32.1	31.3	30.6
Fan energy per floor natural	1.15	1.18	1.25	0.78	0.63	0.69	1.07	0.93	1.33	1.34	1.38	0.87	0.72	0.81	1.30	1.40	1.20	1.19	1.27	0.77	0.64	0.71	1.13	1.07
fan energy per wing	7.68								9.16								7.99							
Fan energy consumption for building case	24.83																							

[case-1A]- results in office occupation

	Volume flow North office wing								South-East office wing								South-West office wing							
office floor	0th	1st	2nd	3rd	4th	5th	6th	7th	0th	1st	2nd	3rd	4th	5th	6th	7th	0th	1st	2nd	3rd	4th	5th	6th	7th
	[m3/s]	[m3/s]	[m3/s]	[m3/s]	[m3/s]	[m3/s]	[m3/s]	[m3/s]	[m3/s]	[m3/s]	[m3/s]	[m3/s]	[m3/s]	[m3/s]	[m3/s]	[m3/s]	[m3/s]	[m3/s]	[m3/s]	[m3/s]	[m3/s]	[m3/s]	[m3/s]	[m3/s]	[m3/s]
maximum in occ.	2.78	2.62	2.40	2.20	2.47	2.67	2.72	2.76	2.99	2.83	2.60	2.40	2.70	2.93	2.99	3.06	2.74	2.57	2.34	2.15	2.42	2.62	2.66	2.71
minimum in occ.	-0.78	-0.79	-0.74	-0.70	-0.86	-1.00	-1.07	-1.15	-0.71	-0.73	-0.69	-0.67	-0.85	-1.01	-1.10	-1.21	-0.36	-0.44	-0.45	-0.46	-0.62	-0.77	-0.86	-0.96
average in occ.	1.15	1.05	0.93	0.83	0.87	0.88	0.83	0.76	1.15	1.05	0.93	0.83	0.87	0.88	0.82	0.75	1.17	1.07	0.95	0.84	0.89	0.90	0.85	0.79
st. dev. In occ.	0.37	0.34	0.30	0.27	0.31	0.33	0.33	0.34	0.35	0.32	0.28	0.25	0.28	0.30	0.30	0.32	0.36	0.33	0.29	0.26	0.29	0.30	0.31	0.31
	[%]	[%]	[%]	[%]	[%]	[%]	[%]	[%]	[%]	[%]	[%]	[%]	[%]	[%]	[%]	[%]	[%]	[%]	[%]	[%]	[%]	[%]	[%]	[%]
RSD [%]	32	32	33	33	35	37	40	46	30	30	30	31	33	34	37	42	31	31	30	31	32	34	36	40
Qv>0,5m3/s [%]	95.2	95.0	94.2	92.5	93.9	93.9	92.0	86.7	95.3	95.2	94.9	93.7	94.8	95.0	93.7	89.8	95.4	95.4	95.1	94.4	95.2	95.3	94.7	92.2
	Total driving pressure																							
	[Pa]	[Pa]	[Pa]	[Pa]	[Pa]	[Pa]	[Pa]	[Pa]	[Pa]	[Pa]	[Pa]	[Pa]	[Pa]	[Pa]	[Pa]	[Pa]	[Pa]	[Pa]	[Pa]	[Pa]	[Pa]	[Pa]	[Pa]	[Pa]
maximum in occ.	171.3	171.6	171.8	172.0	172.2	172.4	172.6	172.8	176.4	176.6	176.7	177.6	176.8	176.8	176.7	176.5	174.5	174.6	174.8	175.9	175.2	174.9	174.8	174.6
minimum in occ.	-0.1	1.0	0.9	0.9	0.8	0.7	0.6	0.5	3.4	3.7	3.5	3.1	2.8	2.5	2.2	1.7	2.4	2.7	2.7	2.6	2.3	1.9	1.6	1.2
average in occ.	26.6	26.8	26.9	27.1	27.2	27.4	27.6	27.7	28.7	29.3	29.5	29.4	29.2	29.2	29.1	28.9	28.6	29.2	29.4	29.4	29.3	29.1	29.0	28.8
st. dev. In occ.	15.4	15.3	15.3	15.3	15.3	15.3	15.4	15.4	14.8	15.0	15.1	15.3	15.2	15.3	15.4	15.4	14.8	14.9	15.1	15.3	15.3	15.3	15.4	15.4
	[%]	[%]	[%]	[%]	[%]	[%]	[%]	[%]	[%]	[%]	[%]	[%]	[%]	[%]	[%]	[%]	[%]	[%]	[%]	[%]	[%]	[%]	[%]	[%]
RSD [%]	58	57	57	57	56	56	56	56	52	51	51	52	52	52	53	53	52	51	51	52	52	53	53	54
% of occ. Δp>0Pa	100.0	100.0	100.0	100.0	100.0	100.0	100.0	100.0	100.0	100.0	100.0	100.0	100.0	100.0	100.0	100.0	100.0	100.0	100.0	100.0	100.0	100.0	100.0	100.0
% of occ. Δp>5Pa	99.2	99.5	99.5	99.6	99.6	99.6	99.6	99.6	99.8	99.9	99.9	99.8	99.8	99.7	99.6	99.5	99.8	99.9	99.8	99.8	99.8	99.8	99.7	99.6
% of occ. Δp>10Pa	91.7	92.2	92.6	93.0	93.2	93.4	93.6	93.8	97.2	97.6	97.5	97.2	96.8	96.5	96.0	95.5	97.1	97.6	97.4	97.1	96.8	96.4	95.9	95.4
% of occ. Δp>20Pa	61.9	62.4	62.9	63.3	63.9	64.5	65.0	65.6	70.8	72.4	72.4	72.0	71.2	71.1	70.5	69.7	70.6	72.0	72.0	71.7	71.4	70.9	70.1	69.5
	Fan energy consumption																							
	[kWh]	[kWh]	[kWh]	[kWh]	[kWh]	[kWh]	[kWh]	[kWh]	[kWh]	[kWh]	[kWh]	[kWh]	[kWh]	[kWh]	[kWh]	[kWh]	[kWh]	[kWh]	[kWh]	[kWh]	[kWh]	[kWh]	[kWh]	[kWh]
Fan energy per floor 100% mechanical	30.0	30.5	30.8	31.0	31.2	31.4	31.5	31.5	30.0	30.5	30.8	31.0	31.2	31.4	31.5	31.5	30.0	30.5	30.8	31.0	31.2	31.4	31.5	31.5
Fan energy per floor natural	0.70	0.80	0.95	1.26	0.36	0.43	0.58	1.07	0.69	0.79	0.92	1.19	0.36	0.27	0.37	0.74	0.71	0.80	0.93	1.15	0.48	0.31	0.34	0.51
fan energy per wing	6.16								5.32								5.22							
Fan energy consumption for building case	16.70																							

[case-1B] - results in office occupation

	Volume flow North office wing								South-East office wing								South-West office wing							
office floor	0th	1st	2nd	3rd	4th	5th	6th	7th	0th	1st	2nd	3rd	4th	5th	6th	7th	0th	1st	2nd	3rd	4th	5th	6th	7th
	[m3/s]	[m3/s]	[m3/s]	[m3/s]	[m3/s]	[m3/s]	[m3/s]	[m3/s]	[m3/s]	[m3/s]	[m3/s]	[m3/s]	[m3/s]	[m3/s]	[m3/s]	[m3/s]	[m3/s]	[m3/s]	[m3/s]	[m3/s]	[m3/s]	[m3/s]	[m3/s]	[m3/s]
maximum in occ.	2.13	2.27	2.42	2.52	2.99	2.79	2.89	3.06	2.26	2.43	2.59	2.70	3.23	3.02	3.14	3.34	2.06	2.20	2.35	2.44	2.93	2.72	2.83	3.02
minimum in occ.	-0.23	-0.18	-0.06	-0.18	-0.34	-1.03	-1.10	-1.22	-0.62	-0.63	-0.62	-0.62	-0.81	-1.10	-1.18	-1.30	-0.62	-0.63	-0.62	-0.59	-0.63	-0.82	-0.88	-0.98
average in occ.	0.89	0.91	0.93	0.93	1.03	0.90	0.86	0.81	0.83	0.85	0.87	0.87	0.96	0.86	0.81	0.74	0.84	0.87	0.89	0.89	0.99	0.89	0.84	0.79
st. dev. In occ.	0.30	0.31	0.31	0.31	0.36	0.36	0.36	0.39	0.31	0.32	0.31	0.29	0.33	0.34	0.33	0.34	0.32	0.32	0.32	0.29	0.32	0.35	0.33	0.34
	[%]	[%]	[%]	[%]	[%]	[%]	[%]	[%]	[%]	[%]	[%]	[%]	[%]	[%]	[%]	[%]	[%]	[%]	[%]	[%]	[%]	[%]	[%]	[%]
RSD [%] in occ.	34	34	33	33	35	40	42	48	38	37	36	34	34	40	41	46	38	37	36	33	33	39	39	43
Qv>0,5m3/s [%]	93.8	94.0	94.1	93.7	94.5	91.3	88.9	84.3	92.1	92.5	92.5	91.9	92.9	91.2	88.0	81.1	92.8	93.1	93.2	92.8	93.6	92.2	89.9	85.2
	Total driving pressure																							
	[Pa]	[Pa]	[Pa]	[Pa]	[Pa]	[Pa]	[Pa]	[Pa]	[Pa]	[Pa]	[Pa]	[Pa]	[Pa]	[Pa]	[Pa]	[Pa]	[Pa]	[Pa]	[Pa]	[Pa]	[Pa]	[Pa]	[Pa]	[Pa]
maximum in occ.	186.4	184.3	180.7	177.1	173.6	169.2	165.8	162.5	183.2	179.3	175.5	171.7	167.8	164.2	160.3	156.4	169.4	165.2	161.4	157.6	153.8	150.7	146.7	142.7
minimum in occ.	-9.9	1.2	1.2	1.3	1.1	-0.3	-0.2	-1.5	-9.9	-8.5	-7.3	-6.0	-4.8	-0.4	-0.2	-0.7	-6.1	-1.8	-1.4	-1.0	-0.6	0.4	0.5	0.0
average in occ.	24.6	23.4	21.3	19.3	17.3	15.3	13.3	11.2	25.1	23.2	21.3	19.3	17.4	15.9	13.8	11.8	25.4	23.7	21.7	19.7	17.7	15.8	13.8	11.8
st. dev. In occ.	14.6	14.0	13.6	13.2	12.9	12.6	12.4	12.2	14.9	14.5	14.1	13.7	13.3	13.1	12.8	12.7	14.8	14.3	13.9	13.5	13.2	12.9	12.7	12.5
	[%]	[%]	[%]	[%]	[%]	[%]	[%]	[%]	[%]	[%]	[%]	[%]	[%]	[%]	[%]	[%]	[%]	[%]	[%]	[%]	[%]	[%]	[%]	[%]
RSD [%]	59	60	64	68	75	82	93	109	59	62	66	71	77	82	93	107	58	60	64	69	74	82	92	106
% of occ. Δp>0Pa	99.7	100.0	100.0	100.0	100.0	100.0	100.0	99.7	99.8	99.8	99.8	99.8	99.8	100.0	100.0	99.8	99.8	99.8	99.8	99.8	99.9	100.0	100.0	100.0
% of occ. Δp>5Pa	98.9	99.3	98.8	97.5	95.0	90.5	82.2	66.2	99.1	98.7	98.0	96.2	94.1	91.3	83.5	68.2	99.3	99.3	98.9	97.8	95.4	91.1	83.3	68.4
% of occ. Δp>10Pa	90.7	89.4	85.3	79.9	71.0	60.0	46.2	33.9	91.1	88.3	84.3	78.9	70.4	61.8	47.7	35.7	92.1	89.8	85.3	80.3	71.9	61.9	47.9	35.8
% of occ. Δp>20Pa	56.5	51.5	42.7	34.2	27.0	22.0	18.2	15.3	57.2	49.9	41.5	34.5	27.1	23.5	20.2	17.4	58.3	52.3	43.5	35.2	28.4	23.6	20.1	17.1
	Fan energy consumption																							
	[kWh]	[kWh]	[kWh]	[kWh]	[kWh]	[kWh]	[kWh]	[kWh]	[kWh]	[kWh]	[kWh]	[kWh]	[kWh]	[kWh]	[kWh]	[kWh]	[kWh]	[kWh]	[kWh]	[kWh]	[kWh]	[kWh]	[kWh]	[kWh]
Fan energy per floor 100% mechanical	38.2	37.0	35.9	35.0	32.9	31.7	31.9	31.8	38.2	37.0	35.9	35.0	32.9	31.7	31.9	31.8	38.2	37.0	35.9	35.0	32.9	31.7	31.9	31.8
Fan energy per floor natural	0.53	0.51	0.85	1.17	0.91	0.79	1.69	1.96	0.51	0.47	0.49	1.31	0.79	0.57	1.50	2.33	0.32	0.28	0.26	1.34	0.79	0.47	1.10	1.99
fan energy per wing	8.41								7.98								6.56							
Fan energy consumption for building case	22.95																							

[case-2A] - results in office occupation

	Volume flow North office wing								South-East office wing								South-West office wing							
office floor	0th	1st	2nd	3rd	4th	5th	6th	7th	0th	1st	2nd	3rd	4th	5th	6th	7th	0th	1st	2nd	3rd	4th	5th	6th	7th
	[m3/s]	[m3/s]	[m3/s]	[m3/s]	[m3/s]	[m3/s]	[m3/s]	[m3/s]	[m3/s]	[m3/s]	[m3/s]	[m3/s]	[m3/s]	[m3/s]	[m3/s]	[m3/s]	[m3/s]	[m3/s]	[m3/s]	[m3/s]	[m3/s]	[m3/s]	[m3/s]	[m3/s]	[m3/s]
maximum in occ..	3.19	3.03	2.79	2.59	2.91	3.15	3.22	3.29	3.19	3.03	2.79	2.59	2.92	3.15	3.22	3.29	3.19	3.03	2.79	2.59	2.91	3.15	3.22	3.29
minimum in occ.	-0.46	-0.44	-0.39	-0.36	-0.41	-0.50	-0.54	-0.59	-0.17	-0.23	-0.26	-0.28	-0.36	-0.45	-0.50	-0.56	0.19	0.14	0.07	-0.08	-0.16	-0.24	-0.31	-0.38
average in occ.	1.24	1.14	1.01	0.90	0.97	0.98	0.93	0.85	1.27	1.16	1.04	0.92	0.99	1.01	0.96	0.89	1.27	1.16	1.04	0.92	0.99	1.01	0.96	0.89
st. dev. In occ.	0.36	0.34	0.32	0.29	0.34	0.37	0.40	0.45	0.35	0.33	0.30	0.28	0.32	0.36	0.38	0.43	0.35	0.33	0.30	0.28	0.32	0.36	0.38	0.43
	[%]	[%]	[%]	[%]	[%]	[%]	[%]	[%]	[%]	[%]	[%]	[%]	[%]	[%]	[%]	[%]	[%]	[%]	[%]	[%]	[%]	[%]	[%]	[%]
RSD [%]	29	30	31	33	35	38	43	53	28	29	29	31	33	35	40	48	28	28	29	31	33	35	40	48
Qv>0,5m3/s [%]	99.3	99.1	98.3	96.8	97.8	97.7	93.5	78.1	99.5	99.3	98.8	97.7	98.6	98.7	97.0	86.7	99.5	99.4	98.8	97.8	98.6	98.8	97.0	86.4
	Total driving pressure																							
	[Pa]	[Pa]	[Pa]	[Pa]	[Pa]	[Pa]	[Pa]	[Pa]	[Pa]	[Pa]	[Pa]	[Pa]	[Pa]	[Pa]	[Pa]	[Pa]	[Pa]	[Pa]	[Pa]	[Pa]	[Pa]	[Pa]	[Pa]	[Pa]
maximum in occ.	4.0	3.9	3.8	3.7	3.6	3.4	3.0	2.7	4.3	4.3	4.3	4.4	4.3	4.2	4.1	4.0	3.5	4.3	4.4	4.4	4.4	4.4	4.3	4.3
minimum in occ.	329.6	329.4	330.0	330.9	330.5	329.8	329.6	328.0	329.5	329.4	329.9	330.9	330.4	329.8	329.5	328.1	329.1	329.0	329.5	330.5	330.0	329.4	329.1	327.6
average in occ.	39.6	39.7	39.8	39.9	40.0	40.1	40.2	40.2	39.6	39.7	39.8	39.9	40.0	40.0	40.1	40.1	39.3	39.3	39.5	39.6	39.6	39.7	39.8	39.8
st. dev. In occ.	27.3	27.3	27.3	27.4	27.4	27.4	27.4	27.3	27.3	27.3	27.3	27.4	27.4	27.4	27.4	27.3	27.3	27.3	27.4	27.4	27.4	27.4	27.4	27.3
	[%]	[%]	[%]	[%]	[%]	[%]	[%]	[%]	[%]	[%]	[%]	[%]	[%]	[%]	[%]	[%]	[%]	[%]	[%]	[%]	[%]	[%]	[%]	[%]
RSD [%]	69	69	69	69	68	68	68	68	69	69	69	69	68	68	68	68	70	69	69	69	69	69	69	69
% of occ. Δp>0Pa	100.0	100.0	100.0	100.0	100.0	100.0	100.0	100.0	100.0	100.0	100.0	100.0	100.0	100.0	100.0	100.0	100.0	100.0	100.0	100.0	100.0	100.0	100.0	100.0
% of occ. Δp>5Pa	100.0	100.0	100.0	99.9	99.9	99.9	99.9	99.9	100.0	100.0	100.0	100.0	100.0	99.9	99.9	99.9	99.9	100.0	99.9	99.9	99.9	99.9	99.9	99.9
% of occ. Δp>10Pa	97.9	97.9	97.9	97.9	97.9	98.0	98.1	98.2	97.9	97.9	97.9	97.9	97.9	98.0	98.1	98.2	98.0	98.0	98.0	98.0	98.0	98.0	98.1	98.0
% of occ. Δp>20Pa	80.6	80.8	81.0	81.2	81.3	81.4	81.6	81.6	80.6	80.7	80.9	81.1	81.3	81.4	81.5	81.6	79.4	79.6	79.8	80.0	80.2	80.3	80.5	80.5
	Fan energy consumption																							
	[kWh]	[kWh]	[kWh]	[kWh]	[kWh]	[kWh]	[kWh]	[kWh]	[kWh]	[kWh]	[kWh]	[kWh]	[kWh]	[kWh]	[kWh]	[kWh]	[kWh]	[kWh]	[kWh]	[kWh]	[kWh]	[kWh]	[kWh]	[kWh]
Fan energy per floor 100% mechanical	37.7	38.1	38.4	38.7	38.9	39.0	39.1	39.2	37.7	38.1	38.4	38.7	38.9	39.0	39.1	39.2	37.7	38.1	38.4	38.7	38.9	39.0	39.1	39.2
Fan energy per floor natural	0.07	0.08	0.17	0.33	0.22	0.24	0.66	3.01	0.06	0.07	0.14	0.26	0.16	0.17	0.30	1.74	0.05	0.07	0.14	0.26	0.17	0.17	0.30	1.77
fan energy per wing	4.79								2.89								2.93							
Fan energy consumption for building case	10.61																							